Plasticity associated with Up/Down states in the mouse barrel cortex



Antonia Langfelder

Christ Church

University of Oxford

A thesis submitted for the degree of

Doctor of Philosophy

Michaelmas 2016

Abstract

Slow wave sleep is characterised by synchronised slow oscillations, which manifest themselves in cortical neurons as depolarised Up states and more hyperpolarised, silent Down states. Up/Down states have been implicated in synaptic plasticity during sleep-associated memory consolidation. However, the underlying mechanism is not well-understood.

I used the mouse somatosensory barrel cortex as a model system to investigate whether Up states and Down states differentially facilitate synaptic plasticity. Initial experiments were carried out *in vitro* in slices of barrel cortex. Here, Up states were evoked by electrical stimulation, making it possible to precisely control onset timing. Perforated patch-clamp recordings were obtained from pyramidal neurons in layer 2/3 to determine whether pairing of inputs with electrically-evoked Up states results in plasticity of the paired input. I found that pairing a train of EPSPs at different frequencies with Up states resulted in synaptic depression. However, there was no significant difference between Up states and Down states in their propensity to mediate plasticity of paired inputs. This lack of state-dependent plasticity could have been due to an insufficient number of pairings, as well as differences between electrically-evoked and spontaneous Up states in their ability to facilitate plasticity of paired inputs in the barrel cortex. To overcome these issues, plasticity was studied using long-term extracellular recordings *in vivo* under anaesthesia. Here, spontaneous Up states were automatically detected and paired with whisker deflections. While persistently pairing inputs with Up states led to long-term depression of the whisker response in the barrel cortex, Down state pairings did not induce any long-term effects. Taken together, results from experiments *in vivo*, but not *in vitro*, suggest that Up states facilitate depression of inputs in an activity-dependent manner.

Acknowledgements

I would first like to thank Prof Ed Mann for supervising this project. I am immensely grateful for all the support and guidance I have received throughout.

I would like to extend my gratitude to all members of the group for their cooperation. Thanks in particular to fellow students Pantelis Antonoudiou, Julian Bartram, and Martin Kahn for making my time in the lab more fun. I am additionally grateful to Pantelis Antonoudiou for invaluable help with the *in vivo* feedback system.

I would also like to thank Dr Louise Upton for being the best teacher of surgical procedures, and for sharing equipment and advice.

I would like to thank the Wellcome Trust for funding this project.

Finally, I would like to thank my friends and family. To my parents, Traude and Thomas, I will always be grateful for their constant love and support. I would not be where I am without it. To my husband Rahul, who has not only provided me with love and encouragement throughout, but always knows how to cheer me up during difficult times. I would also like to acknowledge my grandfather Karl, who greatly valued higher education for his family, even though he himself did not have access to it.

List of abbreviations

aCSF	Artificial cerebrospinal fluid
AMPA	α-amino-3-hydroxy-5-methyl-4-isoxazolepropionic acid
ArchT	Archaerhodopsin T
CamKII	Calcium/calmodulin-dependent protein kinase II
ChR2	Channelrhodopsin-2
CSD	Current-source density
DS	Down state
EPSP	Excitatory postsynaptic potential
GABA	Gamma-aminobutyric acid
L1, L2/3, L4, L5, L6	Cortical layers
LFP	Local field potential
LTD	Long-term depression
LTP	Long-term potentiation
mGluR	Metabotropic glutamate receptor
MUA	Multiunit activity
NMDA	N-Methyl-D-aspartate
PKA	Protein kinase A
POM	Posterior medial nucleus of the thalamus
REM	Rapid-eye-movement
R_i	Input resistance
SEM	Standard error of the mean
SHY	Synaptic homeostasis hypothesis
STDP	Spike-timing-dependent plasticity
STH	Spike-time histogram
SWA	Slow wave activity
SWS	Slow wave sleep
US	Up state
V_m	Membrane potential
VPM	Ventral posterior medial nucleus of the thalamus

Table of figures

Figure 1	Visualisation of spontaneous membrane rupture during perforated patch-clamp	33
Figure 2	Custom-made 64-channel electrode array	39
Figure 3	Up states *in vitro* in slices of barrel cortex	49
Figure 4	Ca^{2+}-dependent decrease of Up state duration	51
Figure 5	Inhibition of NMDA receptors suppresses electrically-evoked Up states	53
Figure 6	Inhibition of mGluRs does not significantly affect electrically-evoked Up states	54
Figure 7	Local application of Acetylcholine (ACh) reversibly inhibits electrically-evoked Up states	56
Figure 8	Setup for plasticity experiments *in vitro*	65
Figure 9	Changes in R_i and V_m over time during whole-cell patch-clamp	66
Figure 10	Up state versus Down state pairings with EPSPs	69
Figure 11	Plasticity after pairing of EPSPs at different frequencies with Up states or Down states	71
Figure 12	Relationship between synaptic depression and Up state properties	74
Figure 13	Suprathreshold pairings with Up states versus Down states	75
Figure 14	Plasticity after pairing of suprathreshold synaptic inputs with Up states and Down states	77
Figure 15	Optogenetic inhibition of Up states *in vitro*	85

Figure 16 Optogenetic inhibition did not suppress Up states *in vivo* 86

Figure 17 Setup for plasticity experiments *in vivo* 88

Figure 18 Up/Down state detection and sham pairing 90

Figure 19 Experimental paradigm for plasticity experiments *in vivo* 91

Figure 20 Identification of 64-channel electrode array recording sites 93

Figure 21 State-dependent plasticity of the whisker response 95

Figure 22 Long-term depression after pairing with Up states, but not Down states 99

Figure 23 Correlation between paired and unpaired whisker responses 101

Figure 24 Relationship between the normalised whisker response at each electrode after Up state pairing and its distance to the principal barrel 103

Figure 25 Identification of cortical layers and 32-channel linear probe recording sites 105

Figure 26 AP5 strongly suppressed responses to whisker deflection in all layers 107

Figure 27 Average Up/Down state duration before and after AP5 application. 108

Figure 28 Normalised whisker response measures before and after Up state pairing across layers 110

Figure 29 Differences in plasticity between layers 113

Figure 30 Example CSD profile before and after Up state pairing 114

Figure 31 CSD current sink peaks in layer 2/3 and layer 4 117

Figure 32 AP5 did not inhibit long-term depression of whisker responses after Up state pairing 118

Table of Contents

Abstract ..... **i**

List of abbreviations ..... **iii**

List of figures ..... **iv**

1 Introduction **1**

1.1 Structure and function of the mouse barrel cortex **1**

1.1.1 What is the barrel cortex? 1

1.1.2 Pathways from whisker to cortex 2

1.1.3 Sensory processing in the barrel cortex 4

1.2 Plasticity of the mouse barrel cortex **8**

1.2.1 General principles of synaptic plasticity 8

1.2.2 Synaptic plasticity in the mouse barrel cortex 11

1.2.3 Experience-dependent plasticity 13

1.3 Up/Down states **17**

1.3.1 What are Up/Down states? 17

1.3.2 Mechanisms of Up/Down state generation 19

1.4 Slow oscillations and the memory function of sleep **20**

1.4.1 Introduction 20

1.4.2 The synaptic homeostasis hypothesis 22

1.4.3 The active system consolidation hypothesis 25

1.5 Thesis objectives **27**

2 Materials and methods 31

2.1 Animals 31

2.2 Preparation of acute slices of mouse barrel cortex 31

2.3 Electrophysiology in acute slices 32

2.3.1 Whole-cell patch-clamp recordings 32

2.3.2 Perforated patch-clamp recordings 33

2.4 Electrical stimulation in slices of barrel cortex 34

2.5 *In vitro* plasticity protocol 35

2.6 Application of drugs to barrel cortex slices 35

2.7 Identification of pyramidal neurons in slices of barrel cortex 35

2.8 Virus injections 36

2.8.1 Injections in neonates 36

2.8.2 Injections in adolescent mice 37

2.9 Extracellular recordings in anaesthetised mice 37

2.9.1 Surgery 37

2.9.2 Electrophysiology 38

2.10 Optical inhibition *in vitro* and *in vivo* 39

2.11 Real-time Up state detection and whisker stimulation 40

2.12 Application of drugs to the barrel cortex *in vivo* 41

2.13 Immunohistochemistry 42

2.14 Histological identification of recording sites 43

2.15 Data analysis 43

2.16 Post hoc Up state detection (*in vitro* and *in vivo*) 44

2.17 Statistics 45

3 Characterisation of Up/Down state dynamics in the barrel cortex *in vitro* 46

3.1 Introduction 46

3.2 Results **48**

3.2.1 Up states can be evoked by electrical stimulation in slices of barrel cortex ... 48

3.2.2 Generation of electrically-evoked Up states is dependent on NMDA receptors 52

3.2.3 Electrically-evoked Up states are not significantly affected by inhibition of metabotropic glutamate receptors 53

3.2.4 Electrically-evoked Up states are reversibly suppressed by Acetylcholine..... 55

3.3 Discussion **57**

3.3.1 Extracellular Ca^{2+} affects Up states in slices of barrel cortex 57

3.3.2 Pharmacological manipulation of Up states *in vitro* by inhibition of glutamate receptors 58

3.3.3 Effects of Acetylcholine on Up/Down states in the barrel cortex *in vitro*..... 60

4 Plasticity associated with Up/Down states in the barrel cortex *in vitro* ..62

4.1 Introduction **62**

4.2 Results **64**

4.2.1 Pairing of electrically-evoked Up states with EPSPs in slices of barrel cortex 64

4.2.2 Change of the input resistance over time in whole-cell mode 65

4.2.3 Pairing of subthreshold inputs with Up states or Down states 68

4.2.4 Pairing of suprathreshold inputs with Up states or Down states..... 74

4.3 Discussion **78**

4.3.1 Practical implications of the experimental protocol 78

4.3.2 No difference in plasticity after pairing of inputs with Up states or Down states..... 79

5 Plasticity associated with Up/Down states in the barrel cortex *in vivo*....81

5.1 Introduction **81**

5.2 Results **84**

5.2.1 Optogenetic inhibition of Up states *in vitro*, but not *in vivo* 84
5.2.2 Detection of Up states and whisker stimulation in real time 87
5.2.3 Experimental design 91
5.2.4 Pairing of whisker stimulation with Up states induces long-lasting depression of sensory responses in the barrel cortex 94
5.2.5 Relationship between the amount of depression after Up state pairing and distance to the principal barrel 102
5.2.6 Experimental design for investigations into the laminar profile and molecular pathway of Up state pairing-dependent depression 104
5.2.7 Effects of the NMDA receptor antagonist AP5 on whisker responses and Up states 106
5.2.8 Laminar profile of plasticity in the barrel cortex after Up state pairing 109
5.2.9 Inhibition of NMDA receptors with AP5 did not significantly affect depression after Up state pairing 118
5.3 Discussion 120
5.3.1 Optogenetic approach to control Up/Down states 120
5.3.2 Up states and Down states differentially modulate plasticity of whisker responses in the barrel cortex after chronic whisker stimulation 122
5.3.3 Laminar profile and locus of plasticity after Up state pairing 125
5.3.4 Potential mechanism of long-term depression after Up state pairing 127
6 General discussion 129
6.1 Summary of findings 129
6.2 Feasibility of the mouse barrel cortex as a model system for evoked Up states and associated plasticity *in vitro* 132
6.3 Feasibility of the mouse barrel cortex as a model system for plasticity during spontaneous network activity under anaesthesia *in vivo* 133
6.4 Comparison between *in vitro* and *in vivo* findings 134

6.5 Conclusions and future directions 136

7 Appendix 138

7.1 General properties of *in vitro* plasticity experiments 138

7.2 General properties of *in vivo* plasticity experiments 141

8 References 144

1 Introduction

1.1 Structure and function of the mouse barrel cortex

1.1.1 What is the barrel cortex?

The barrel cortex is the area of primary somatosensory cortex responding to the whiskers. It was originally identified by Woolsey and Van der Loos in mice (Woolsey and Van der Loos, 1970) and later also found in other whisker-bearing animals (Woolsey et al., 1975). The barrel cortex derives its name from the appearance of prominent barrel-shaped structures in layer 4, which arise due to the clustering of thalamocortical terminals and differences in cell density (Schlaggar and O'Leary, 1994; Woolsey and Van der Loos, 1970). Each barrel predominantly receives input from a single whisker (Armstrong-James and Fox, 1987). Furthermore, barrels are arranged according to the whiskers on the snout, forming a somatotopic map on the contralateral side of the cortex (Feldmeyer et al., 2013; Petersen, 2007). This cortical map is formed during early development, making its overall structure and layout insensitive even to major perturbations after the first postnatal week (Fox, 1992; Woolsey and Wann, 1976). Sensory pathways do remain plastic within the barrel cortex, however, and display experience-dependent plasticity into adulthood (Glazewski, 1998; Glazewski and Fox, 1996). The whiskers are highly sensitive, with their sensory representations occupying a large area of the cortex (Lee and Erzurumlu, 2005). They are also under motor control, such that mice are able to actively use their whiskers to

localise objects in their environment (Feldmeyer et al., 2013; Woolsey et al., 1975). This may be particularly important for nocturnal animals such as mice and rats to compensate for a lack of visual information in the darkness (Petersen, 2007).

Since its discovery in the 1970s, the barrel cortex has been used extensively as a model system to study cortical processing, even though barrels are absent from somatosensory cortex of animals which do not have whiskers. This is partly due to significant practical advantages such as its accessibility for experimental manipulations both *in vivo* and *in vitro*. In addition, studying the functional properties of a well-defined barrel column is thought to provide insight into general information processing capabilities of a cortical column. This can potentially be translated to other areas as a common mechanism, since cortical columns are the proposed building blocks of the whole cortex (Mountcastle, 1997). The fact that a wealth of information is already available about the barrel cortex further contributes to the advantages of this model system (Feldmeyer et al., 2013; Fox, 2008).

1.1.2 Pathways from whisker to cortex

The main anatomical pathway from the whiskers to the barrel cortex is now well-characterised. Deflection of a whisker activates nerve terminals innervating the whisker follicle, which come in a variety of slowly- and rapidly-adapting types (Ebara et al., 2002). From there, the infraorbital nerve of the trigeminal ganglion projects to trigeminal nuclei in the brain stem. A somatotopic whisker map is already present at the level of the trigeminal nuclei, where individual units are

referred to as barrellettes (Ma and Woolsey, 1984). Projections from nucleus principalis terminate in the ventral posterior medial nucleus of the thalamus (VPM), forming the so-called lemniscal pathway, which is the main pathway from a whisker to the cortex (Chiaia et al., 1991). The VPM also contains somatotopically arranged whisker representations, which are referred to as barreloids (Van Der Loos, 1976). From the VPM, axons innervate spiny neurons and inhibitory interneurons in layer 4 of the barrel cortex, where they terminate in clusters and give rise to the prominent anatomically identifiable barrels. Besides layer 4, VPM also projects more weakly to layer 6 (Bernardo and Woolsey, 1987; Feldmeyer et al., 2013; Lu and Lin, 1993). In layer 4, excitatory neurons not only connect to each other for signal amplification (Feldmeyer et al., 1999), but also relay the whisker response to other cortical layers of the same barrel via intracortical connections, most prominently to layer 2/3 (Feldmeyer et al., 2002; Lübke et al., 2000), but also to layer 5 (Feldmeyer, 2012; Feldmeyer et al., 2005; Schubert et al., 2001, 2007). Furthermore, reciprocal connections exist between layer 2/3 and layer 5, and between layer 4 and layer 6 (Feldmeyer, 2012; Schubert et al., 2007). In addition to this lemniscal pathway from nucleus principalis to the barrel cortex, two other pathways exist which originate from the interpolaris nucleus in the brain stem (Jacquin et al., 1989; Pierret et al., 2000). One of these pathways is referred to as the extralemniscal pathway, which gives rise to innervation of secondary somatosensory areas, as well as the septal regions in between barrels via the VPM (Pierret et al., 2000). In the second, paralemniscal pathway, axons are sent to the posterior medial nucleus of the thalamus (POM), which mainly projects to layers 1 and 5 of the barrel cortex (Ohno et al., 2012; Wimmer et al., 2010). However, the contribution of the paralemniscal pathway to

the overall whisker response has been found to depend on the brain state, which regulates the amount of inhibition the POM receives from zona incerta (Trageser et al., 2006). Inhibition in the thalamus is not limited to the POM. The VPM receives feedback inhibition from the reticular nucleus of the thalamus, which restricts the timing of the whisker response transmitted to layer 4 of the barrel cortex (Desîlets-Roy et al., 2002; Hartings et al., 2000). The barrel cortex itself also contains diverse types of inhibitory interneuron. For instance, thalamocortical neurons from the VPM also activate interneurons in layer 4, which form projections within layer 4 and to layer 2/3, to both excitatory neurons and interneurons. Inhibition at this stage is considered to limit the spread of excitation from layer 4 in response to a whisker stimulus (Porter et al., 2001). In addition, it has been found to contribute to direction selectivity (Wilent and Contreras, 2005).

1.1.3 Sensory processing in the barrel cortex

Efforts have been made to describe the whisker-to-barrel pathway with respect to labelled-line and integrated (convergent/divergent) processing of sensory information (Fox, 2008; Schubert et al., 2007). Labelled-line processing refers to a situation in which each cortical column receives very localised input via a specific pathway, which does not converge with inputs from other areas. In the context of the barrel cortex, this would be equivalent to each whisker being represented by a separate pathway, without any overlap between individual whisker representations. Conversely, integrated processing takes place when a pathway contains divergent and convergent connections, such that sensory input from one location overlaps with that from another location. In the context of the

barrel cortex, this situation would be equivalent to integration between individual whisker pathways, leading to overlapping whisker representations. Classically, this has been studied in the barrel cortex using extracellular recordings to assess receptive field properties in response to whisker deflections under anaesthesia (for example: Armstrong-James et al., 1992; De Kock et al., 2007; Petersen and Diamond, 2000; Welker, 1971). Other methods have later complemented these data, including voltage-sensitive dye imaging of subthreshold response properties under anaesthesia or in awake mice (Berger et al., 2007; Ferezou et al., 2006; Petersen et al., 2003a, 2003b). These studies suggest that the whisker system consists of a combination of both labelled-line and integrated processing. Until a whisker response reaches its barrel, the labelled-line organisation seems to be largely preserved. Consistent with this, the earliest whisker response component, which has a latency of 5-10 ms, is restricted to the principal barrel for the stimulated whisker. However, this initial short-latency response is followed by significant lateral spread of excitation to surrounding barrels (Armstrong-James and Fox, 1987; Petersen and Diamond, 2000). Indeed, monitoring subthreshold activity in response to a whisker stimulus with voltage-sensitive dye imaging reveals that, after an initial localised response, the evoked depolarisation spreads across the entire barrel field (Petersen et al., 2003b). Receptive field measurements of single neurons within a barrel indicate that the majority, if not all, neurons in layer 4 respond to more than their principal whisker, albeit with a time delay (Armstrong-James and Fox, 1987; Brecht et al., 2003; Ito, 1985; Moore and Nelson, 1998; Zhu and Connors, 1999). However, the exact size of the receptive field depends on the type of anaesthetic used and on anaesthetic depth,

or on cortical state if no anaesthetic is used (Armstrong-James and George, 1988; Friedberg et al., 1999; Petersen et al., 2003a).

Such convergence of whisker pathways is not only present at the level of the cortex, but also in the thalamus, where it was found that individual neurons in VPM and POM can receive inputs from up to 20 whiskers (Diamond et al., 1992; Friedberg et al., 1999; Nicolelis and Chapin, 1994; Simons and Carvell, 1989). This raised the question to what extent the thalamus contributes to multi-whisker receptive fields in the cortex. Thalamic input to cortical neurons has been found to be only very weak, suggesting that significant temporal summation is required for thalamocortical projections to drive spiking activity in the cortex (Benshalom and White, 1986; Bruno and Sakmann, 2006). Due to the much sharper distribution of response latencies of thalamic neurons to their principal whisker compared to surround whiskers, the principal whisker is much more likely to produce sufficient temporal summation to generate a response in the cortex (Pinto et al., 2003). In addition, it was found that electrolytically lesioning an individual barrel or inactivating it by iontophoresis of muscimol results in the absence of a response to that whisker in surrounding barrels, further suggesting that surround receptive fields in the barrel cortex are mediated by intracortical connections (Armstrong-James et al., 1991; Fox et al., 2003).

Upon activation of layer 4 of the barrel cortex by thalamocortical projections, excitation spreads within 2-4 ms to layer 2/3 directly above, consistent with the notion that the whisker response is initially laterally confined within the principal barrel column. This is followed 1 ms later by activation of the near side of

neighbouring barrels, before propagating to the far side a further 8 ms later, as measured by extracellular spike recordings (Armstrong-James et al., 1992). Several intracortical pathways exist which could account for this pattern of excitatory spread within the barrel cortex. For example, sparse direct innervation has been found from layer 4 and layer 5 to the near side of surrounding barrels, which could contribute to the initial cross-barrel response component (Bernardo et al., 1990; Schubert et al., 2001, 2003). There are also horizontal projections from pyramidal neurons in layers 2/3 and 5 which can reach further into neighbouring barrels (Gottlieb and Keller, 1997). Indeed, a recent study of excitatory axonal projection patterns *in vivo* has found that most excitatory neurons display horizontal projections reaching outside of their principal barrel column, forming distinct horizontal strata in superficial and deep layers (Narayanan et al., 2015).

Taken together, single whisker representations in the barrel cortex result from a combination of labelled-line and convergent/divergent sensory processing, which are temporally segregated. Given that sensory information from touching an object is conveyed to the barrel cortex by several whiskers, such a dual approach could enable integration of information from multiple whiskers while at the same time preserving individual whisker identity (Fox, 2008). Moreover, the information integrated by neurons in the barrel cortex includes specific stimulus parameters, such as direction (Wilent and Contreras, 2005), as well as amplitude and velocity of whisker deflections (Wilent and Contreras, 2004). In addition, sensory processing in the barrel cortex is influenced by top-down connections

during active touch (Krupa et al., 2004). It is thus not surprising that a large number of neurons is required to represent a single whisker in the barrel cortex.

1.2 Plasticity of the mouse barrel cortex

1.2.1 General principles of synaptic plasticity

Synaptic plasticity refers to the cellular process thought to underlie learning and memory, encompassing a long-lasting activity-dependent change in synaptic strength between neurons. Classic experiments in the hippocampus reported long-term potentiation (LTP) of synapses after high-frequency stimulation (Bliss and Lømo, 1973). LTP was later also found in the visual cortex (Artola and Singer, 1987) and in the somatosensory cortex (Bindman et al., 1988). Over the years, a lot of effort has been made to investigate LTP and its underlying mechanism. It was found that LTP can be induced by a variety of protocols other than high-frequency tetanic stimulation. For example, LTP can be induced by theta-burst stimulation, in which a short burst of four spikes at 100 Hz is repeatedly applied at 5 Hz (Larson et al., 1986). Another well-characterised protocol for LTP induction falls under the category of spike timing-dependent plasticity (STDP), and involves pairing of presynaptic activity with a postsynaptic spike (Markram et al., 2011). This is also referred to as t-LTP. In slices, this is done by stimulating the presynaptic pathway before injecting current into the postsynaptic cell to make it spike. Numerous other studies have focussed on investigating LTP induction and expression. LTP was commonly found to be dependent on the activity of NMDA receptors (Bliss and Collingridge, 1993; Malenka and Nicoll,

1999, 1993). Here, activation of NMDA receptors on the postsynaptic neuron mediates an influx of Ca^{2+} into the dendritic spine (Lynch et al., 1983; Malenka et al., 1988), which in turn triggers LTP via a protein signalling cascade. Specifically, calcium/calmodulin-dependent protein kinase II (CamKII) acts as a mediator for changes further downstream (Lisman et al., 2002). CamKII can autophosphorylate and thus maintain its activity over longer time periods beyond the duration of the Ca^{2+} rise (Miller et al., 1988). Other protein kinases which have been implicated in LTP include, most notably, protein kinases A and C (PKA and PKC) (Blitzer et al., 1998; Linden and Routtenberg, 1989; Lisman, 1989). Pathways for LTP expression which are activated by this signalling cascade include changes in AMPA receptor trafficking, leading to increased expression of AMPA receptors in the postsynaptic cell, as well as modifications of AMPA receptor activity by subunit phosphorylation (Benke et al., 1998; Malinow and Malenka, 2002). The AMPA receptor subunit GluR1 has been implicated in particular (Hayashi et al., 2000; Malenka and Bear, 2004). LTP expression also includes long-lasting changes, which are mediated by structural alterations such as growth of new dendritic spines and maturation or enlargement of existing spines, as well as changes in gene expression (Abraham and Williams, 2003; Yuste and Bonhoeffer, 2001). In addition to such postsynaptic mechanisms of LTP expression, presynaptic changes have also been found, which are linked to an increase in neurotransmitter release (Castillo, 2012).

LTP is not the only existing type of synaptic plasticity, since the converse has also been extensively demonstrated. Long-term depression (LTD) refers to the process of decreasing, rather than increasing, the efficacy of synapses in an activity-

dependent manner. LTD was first found in hippocampal slices as a heterosynaptic process, whereby depression occurred in a pathway other than the one which was stimulated to induce plasticity (Barrionuevo et al., 1980). Homosynaptic LTD was later found in the hippocampus (Bramham and Srebro, 1987) and cortex (Artola et al., 1990). Homosynaptic LTD can be induced by different stimulation protocols, the most common ones being low-frequency stimulation, application of NDMA, or spike pairings (Malenka and Bear, 2004). Spike pairings can induce LTD in a form of STDP in which the postsynaptic spike precedes the presynaptic activation, which is the reverse order of t-LTP and is also referred to as t-LTD (Markram et al., 2011). It has been suggested that the sign of plasticity jointly depends on firing rate and timing, as well as the number of active inputs (Sjöström et al., 2001). Different molecular mechanisms have been demonstrated to mediate LTD. One of these, like LTP induction, is dependent on Ca^{2+} entry through NMDA receptors (Mulkey and Malenka, 1992). Since Ca^{2+} entry occurs during both LTP and LTD, the direction of plasticity may be distinguished by differences in Ca^{2+} dynamics (Ismailov et al., 2004). In LTD, this is associated with a downstream pathway involving dephosphorylation of AMPA receptors, particularly its GluR1 subunit, by protein phosphatases (Lee et al., 2000). Such a change in AMPA receptor phosphorylation is not only associated with a decrease in receptor open probability, but also with a reduction in surface expression due to internalisation (Malenka and Bear, 2004). Another form of LTD has been found to be dependent on metabotropic glutamate receptors (mGluRs), which is associated with AMPA receptor internalisation. In addition, a presynaptic mGluR-dependent form of LTD exists in the hippocampus and in the cortex, associated with a reduction in neurotransmitter release (Bellone et al., 2008; Malenka and Bear, 2004). A third

mechanism for LTD induction by changes in presynaptic activity is dependent on postsynaptic release of endocannabinoids, which in turn activate CB1 receptors on the presynaptic cell (Bender et al., 2006; Gerdeman et al., 2002; Sjöström et al., 2003).

1.2.2 Synaptic plasticity in the mouse barrel cortex

LTP and LTD can be induced in different pathways in the barrel cortex, depending on the developmental stage. In layer 4, LTP of the thalamocortical synapse can be induced during barrel development by applying axonal stimulation at 1 Hz while depolarising the postsynaptic cell to -10 to 0 mV (Crair and Malenka, 1995). As alluded to in the previous section, this pathway displays a critical period which ends with the first postnatal week (Crair and Malenka, 1995; Fox, 1992, 1995). LTP at the thalamocortical synapse was found to involve unmasking of silent synapses, presumably by insertion of AMPA receptors (Isaac et al., 1997).

During the first postnatal week, it is also possible to induce LTD in layer 4. This can be done by pairing low-frequency stimulation of the thalamic input with postsynaptic depolarisation to -50 mV, suggesting that induction of LTP versus LTD depends on the amount of postsynaptic depolarisation applied during pairing. LTD in this pathway is dependent on NMDA receptors and has been linked to a decrease in synaptic efficacy rather than silencing of functional synapses (Feldman et al., 1998).

In contrast, potentiation of intracortical pathways is not accompanied by a critical period (Glazewski, 1998). In layer 2/3, LTP can be induced by stimulation of different pathways from neighbouring columns by using different stimulation protocols (for example: Aroniadou-Anderjaska and Keller, 1995; Castro-Alamancos et al., 1995; Glazewski et al., 1998). Here, LTP was found to be dependent on NMDA receptors (Castro-Alamancos et al., 1995a) and CamKII autophosphorylation (Hardingham et al., 2003), as well as GluR1 (Hardingham and Fox, 2006). LTP in layer 2/3 has been suggested to engage a pathway involving an increase in AMPA receptor activity after phosphorylation. It also seems to be associated with a significant presynaptic component which is dependent on nitric oxide (Hardingham and Fox, 2006). In addition to spike-timing-dependent forms of plasticity, an induction mechanism for LTP has been found in layer 2/3 of the barrel cortex *in vivo* which is independent of backpropagating action potentials and is instead associated with dendritic spikes. Here, dendritic spikes were driven by the POM and mediated by activation NMDA receptors (Gambino et al., 2014). Interestingly, NMDA receptor-dependent dendritic spikes in the barrel cortex have not only been implicated in plasticity, but also in sensory processing and perceptual detection of whisker deflections (Lavzin et al., 2012; Takahashi et al., 2016).

LTD can also be induced in the layer 4 to layer 2/3 pathway (for example: Allen et al., 2003; Banerjee et al., 2014; Hardingham et al., 2008). LTD of this pathway is dependent on GluR1 (Wright et al., 2008). As described in the previous section, this has been linked to a decrease in AMPA receptor open probability and surface expression (Malenka and Bear, 2004). In addition to this postsynaptic mechanism,

a presynaptic component has also been described for LTD in layer 2/3, which was found to be mediated by mGluRs and endocannabinoid release (Bender et al., 2006), as well as presynaptic NMDA receptors (Bender et al., 2006; Rodríguez-Moreno and Paulsen, 2008; Rodríguez-Moreno et al., 2011). It has been suggested that mGluRs act as coincidence detectors for post- before presynaptic spike timing sequences to induce t-LTD via endocannabinoid release in layer 2/3, which otherwise displays similar spine Ca^{2+} transients to those associated with t-LTP (Nevian and Sakmann, 2006). Furthermore, astrocytic Ca^{2+} signalling has been implicated in t-LTD at this synapse, in a mechanism which acts via astrocytic glutamate release and activation of NMDA receptors on the presynaptic neuron (Min and Nevian, 2012). However, findings by Carter and Jahr seem to contradict these studies, and instead suggest that t-LTD at synapses between layer 4 and layer 2/3 is dependent on non-ionic signalling by postsynaptic NMDA receptors (Carter and Jahr, 2016).

1.2.3 Experience-dependent plasticity

In addition to studying synaptic plasticity processes on a cellular level, the barrel cortex has also been used extensively as a model system for experience-dependent plasticity *in vivo*. Experience-dependent plasticity in the barrel cortex was first described after lesioning of all but one whisker follicle on one side of the snout, which led to an expansion of the cortical territory responding to the spared whisker (Kossut and Hand, 1984). This effect has also been observed after whisker trimming, suggesting that it is not due to injury (for example: Fox, 1992; Glazewski, 1998). In addition to potentiation of spared responses, whisker

trimming is also accompanied by a decrease in the response to the deprived whisker (Glazewski, 1998). Different deprivation patterns have been used to study varying effects of plasticity. For example, removing all but two adjacent whiskers leads to potentiation of the response in the neighbouring spared barrel (Diamond et al., 1993), whereas removing all but one whisker leads to potentiation in the neighbouring deprived barrels (Fox, 1992; Glazewski and Fox, 1996). Another commonly used deprivation pattern is referred to as the chessboard pattern, in which every other whisker is removed. This pattern causes particularly robust potentiation and depression across a large area of the barrel cortex, suggesting that plasticity is supported by an interaction between spared and deprived columns (Wallace and Fox, 1999). Using the chessboard deprivation pattern, it has also been demonstrated that experience-dependent plasticity is associated with an increased turnover of cortical synapses (Trachtenberg et al., 2002).

While potentiation in deprived barrels seems to take up to 18 days to develop (Glazewski and Fox, 1996), potentiation within the spared barrels has been observed after as little as 15-24 hours in layer 2/3 during environmental enrichment (Rema et al., 2006). Like potentiation, depression is not restricted to the principal barrel, which makes sense since whisker responses in surrounding barrels are intracortically-mediated (Armstrong-James et al., 1991; Fox et al., 2003) (see section 1.1.3). Depression of responses to whisker deflection has also been found after as little as 15 hours when mice were kept in enriched environments (Rema et al., 2006).

Several different studies indicate that experience-dependent plasticity is mediated by intracortical connections. For instance, application of muscimol to inhibit activity in the barrel cortex blocks both experience-dependent potentiation and depression (Wallace et al., 2001). Furthermore, whisker deprivation does not affect whisker responses in the thalamus or brainstem (Glazewski et al., 1998b). Another indication that experience-dependent plasticity is expressed in the cortex comes from studies linking whisker deprivation with LTP and LTD. Here, a period of whisker deprivation was found to increase the amount of LTP induced in layer 2/3 by a spike timing-dependent protocol, whereas LTD was occluded in the same pathway (Hardingham et al., 2008). In addition, these results suggest that experience-dependent plasticity may indeed be mediated by LTP and LTD mechanisms on the cellular level.

Experience-dependent plasticity in the barrel cortex is to some extent developmentally regulated. Experience-dependent plasticity of thalamocortical input to layer 4 is restricted to the first postnatal week, consistent with the critical period observed for this pathway (Fox, 1992; Woolsey and Wann, 1976). During adolescence, which lasts up to approximately two months after birth in the rodent, both potentiation and depression of whisker responses can be observed in layer 2/3 following whisker deprivation. However, while depression of deprived whiskers has not been found at a later stage, potentiation of spared inputs does not seem to undergo a critical period, since it has also been demonstrated in adult animals (Fox, 2002; Glazewski and Fox, 1996).

Investigations into the molecular mechanisms underlying experience-dependent plasticity have been carried out using pharmacological and knockout studies. Establishing a role for NMDA receptors in experience-dependent plasticity using pharmacological methods has been proven difficult. This is because normal synaptic transmission *in vivo* includes a large NMDA receptor-dependent component (Armstrong-James et al., 1993), which means that application of antagonists strongly suppresses whisker responses in the barrel cortex. During a period of whisker deprivation, application of the NMDA receptor antagonist AP5 affected plasticity in layer 4 of surrounding barrels, but not in layer 2/3 (Rema et al., 1998). However, using knockout studies, it was found that CamKII, which is the proposed downstream effector of NMDA receptor-dependent plasticity, is required for experience-dependent plasticity (Glazewski et al., 1996, 2000). Furthermore, depression after whisker deprivation was found to be impaired in GluR1 knockout mice, suggesting that experience-dependent depression is expressed via a pathway involving the AMPA receptor subunit GluR1 (Wright et al., 2008). In addition to this, another pathway has been suggested for experience-depression in a recent study, which involves mGluR signalling and a change in presynaptic release probability (Kubota et al., 2016).

In addition to experience-dependent plasticity after whisker deprivation, another type of long-lasting plasticity has been found in the barrel cortex that is dependent on whisker stimulation. Here, a period of rhythmic whisker deflections applied at a certain frequency can alter the response to the stimulated whisker in the barrel cortex. For instance, a 24-hour period of whisker stimulation applied as 50 Hz bursts led to depression of the response to the stimulated whisker (Quairiaux et

al., 2007). In another study, potentiation of the whisker response was found in anaesthetised mice after 10 minutes of whisker stimulation at 8 Hz (Mégevand et al., 2009). It has further been suggested that the direction of plasticity depends on the stimulation frequency, and that this type of plasticity is cortically-mediated (Han et al., 2015). Whisker stimulation in anaesthetised mice also provides scope to investigate how plasticity is modulated by ongoing network activity. There is one study in the rat in which it was found that stimulation of two adjacent whiskers for one hour led to increased cross-correlation between responses in infragranular layers of the stimulated barrel columns. Cross-correlation measurements were performed on recordings of whisker-evoked spiking activity using a Utah electrode array covering a large area of the barrel cortex. Interestingly, increased cross-correlation only occurred when stimulation was applied during Up states (referred to here as bursts), but not Down states (referred to here as interburst intervals). Up/Down state pairings were achieved by triggering deflection of the two whiskers upon detection of a spike in a selected channel. A delay of 1 ms between each spike and whisker deflection was applied to achieve pairings with Up states, and a delay of 300 ms was used for pairings with Down states (Erchova and Diamond, 2004).

1.3 Up/Down states

1.3.1 What are Up/Down states?

Up/Down states represent the cellular manifestation of slow oscillations in the cortex (Steriade et al., 1993a). They are comprised of alternating phases of

membrane depolarisation associated with neuronal activity (Up states) and membrane hyperpolarisation associated with neuronal silence (Down states). Slow oscillations arise from the highly synchronised activity of cortical and thalamocortical networks of neurons undergoing Up/Down states at a frequency of < 1 Hz (Steriade, 2006; Steriade et al., 1993a, 1993b). Up/Down states occur all over the cortex, in both excitatory and inhibitory neurons (Steriade et al., 2001; Volgushev et al., 2006). Slow oscillations are the defining feature of slow wave sleep (SWS), the predominant sleep phase during the first half of sleep (Diekelmann and Born, 2010; Rasch and Born, 2013). They also occur under anaesthesia, albeit with varying Up/Down state dynamics depending on the anaesthetic used (Crunelli and Hughes, 2010; Steriade et al., 1993a). During SWS, this low frequency rhythmic activity, which is also referred to as slow wave activity (SWA), can be observed by EEG in humans due to the large-scale nature of synchronisation across the cortex (Achermann and Borbély, 1997). SWS alternates with rapid-eye-movement (REM) sleep, which becomes more prevalent during the second half of sleep and is characterised by fast oscillations (such as those also observed during Up states) and the absence of silent Down states (Compte et al., 2008; Diekelmann and Born, 2010; Rasch and Born, 2013; Steriade et al., 1993c). SWS, which is also referred to as non-REM sleep, can also be distinguished from REM sleep by differences in the levels of neuromodulators such as Acetylcholine (ACh), which is at a minimum during SWS but high during REM sleep and waking (Marrosu et al., 1995, 1995; Steriade, 2004). Sleep itself is a homeostatic process, meaning that the need to sleep increases proportionally with time spent awake and then decreases again during subsequent sleep. Interestingly, the marker for this homeostatic process is indeed SWA, which not

only undergoes rebound after sleep deprivation, but also increases in cortical areas which were more heavily used during preceding waking experience (Borbély, 2001; Riedner et al., 2007; Vyazovskiy et al., 2007). For instance, SWA was enhanced in the barrel cortex of the rat after unilateral whisker stimulation specifically in the cortical hemisphere responding to the stimulated whiskers (Vyazovskiy et al., 2000).

1.3.2 Mechanisms of Up/Down state generation

The precise mechanism of how slow oscillations are generated and regulated on the level of individual neurons and neuronal networks is an active area of research. Up/Down states can be observed not only in the intact brain, but also in reduced preparations such as isolated cortical slices, and it has been suggested that the generation of slow oscillations is not dependent on subcortical activity (Sanchez-Vives and McCormick, 2000; Steriade et al., 1993c; Timofeev et al., 2000). However, it is currently understood that slow oscillations in the intact brain are the result of an interplay between the thalamus and the cortex (Crunelli and Hughes, 2010). Indeed, spontaneous Up states occur much less frequently in cortical slices, where they can be induced by electrical stimulation targeted to the cortex or thalamus (MacLean et al., 2005; Mann et al., 2009; Rigas and Castro-Alamancos, 2007; Shu et al., 2003). At least in the cortex, layer 5 seems to be particularly important for Up state generation (Beltramo et al., 2013; Chauvette et al., 2010; Sanchez-Vives and McCormick, 2000). For instance, Up states still occurred in layer 5, but not layer 2/3, of slices in which superficial and deep layers were disconnected from each other (Sanchez-Vives and McCormick, 2000). In

particular, it has been suggested that Up states are generated by the summation of spontaneous subthreshold synaptic activity and that they are sustained by a balance between recurrent excitation and inhibition within neuronal networks (Compte et al., 2003; Sanchez-Vives and McCormick, 2000; Timofeev et al., 2000). It has also been suggested that Up states are triggered by intrinsically bursting pyramidal neurons in layer 5 (Lorincz et al., 2015). It is currently not fully understood how the network returns to a Down state by terminating this persistent activity. Possible mechanisms for the generation of Down states include activation of K^+ conductances and disfacilitation (Compte et al., 2003; Contreras et al., 1996; Sanchez-Vives and McCormick, 2000; Timofeev et al., 2001), as well as active inhibition by interneurons (Chen et al., 2012; Mann et al., 2009; Sanchez-Vives et al., 2010).

Taken together, a comprehensive understanding of precisely how slow oscillations are generated and maintained on a cellular and network level remains elusive. This is further complicated by the fact that Up/Down states in the intact brain are likely to be the result of a complex interplay of different processes which have the ability to modulate Up/Down state dynamics.

1.4 Slow oscillations and the memory function of sleep

1.4.1 Introduction

Awake behaviour is associated with acute processing of stimuli and activity-dependent plasticity during learning. Conversely, sleep appears to be involved in

the integration of newly formed memories into long-term storage, a process which is referred to as memory consolidation (Diekelmann and Born, 2010; Rasch and Born, 2013; Tononi and Cirelli, 2014). Indeed, numerous behavioural studies have established that sleep not only improves performance in memory tasks, but also that it is actively involved in memory consolidation (Diekelmann and Born, 2010; Rasch and Born, 2013). For instance, there are behavioural studies suggesting that a period of sleep improved subjects' performance in tasks requiring some form of insight about an underlying sequence which they were not previously aware of (Wagner et al., 2004). Furthermore, the beneficial effects of sleep are not restricted to a particular memory system, but apply to declarative, procedural and emotional memories (Gais et al., 2006; Smith, 2001; Wagner et al., 2001; Walker et al., 2002).

There is evidence to suggest that SWS plays a role in sleep-dependent memory consolidation. For instance, it was found that inducing slow oscillations during early sleep by transcranial stimulation can enhance memory consolidation (Marshall et al., 2006) and that disruption of slow oscillations can impair it (Garside et al., 2015). However, both SWS and REM sleep have been implicated in memory consolidation during sleep. For example, a combination of SWS and REM sleep seems to be more beneficial for performance in a visual discrimination task than a nap consisting only of SWS, when daytime naps with and without REM sleep were compared (Mednick et al., 2003). Given the different electrical and neuromodulatory activity during SWS and REM sleep, it has been suggested that the two sleep phases may support different functions during memory consolidation (Diekelmann and Born, 2010; Rasch and Born, 2013). However,

what these functions are is currently a subject of debate. In particular, two somewhat competing hypotheses have been proposed which support a large number of experimental findings: the synaptic homeostasis hypothesis and the active system consolidation hypothesis.

1.4.2 The synaptic homeostasis hypothesis

The synaptic homeostasis hypothesis (SHY) states that synapses undergo global downscaling in the cortex during SWS (Tononi and Cirelli, 2003). The rationale behind this is that potentiation of synapses should happen when an organism is awake and interacting with the environment, whereas during sleep this process could be harmful. This is because learning and formation of new memories without feedback from the environment could lead to strengthening of false connections. However, if synapses were to be continually potentiated during wake, this would not only become energetically unsustainable, but also lead to a loss of selectivity, which would impair the ability of the brain to extract relevant information from the environment (Tononi and Cirelli, 2006, 2014). The SHY provides a framework which allows for restoration of net synaptic strength during sleep. Different scenarios have been proposed for synaptic depression which are compatible with this idea. Firstly, all synapses may undergo synaptic depression in a uniform manner (Hill et al., 2008). Another possibility is that synapses which are stronger are subjected to less downscaling than weak synapses (Olcese et al., 2010), or that strong synapses are protected from depression while weak synapses are downscaled (Nere et al., 2013). All three possibilities are consistent

with the idea that synaptic depression during sleep leads to renormalisation of synaptic weights, while simultaneously increasing the signal-to-noise ratio.

The SHY is consistent with findings from molecular, structural, and electrophysiological studies. For instance, it was found that AMPA receptors are differentially expressed after sleep and wakefulness. Specifically, expression of the AMPA receptor subunit GluR1was higher in the cortex of the rat at the end of a period spent awake than at the end of sleep (Vyazovskiy et al., 2008). Other findings include changes in AMPA receptor trafficking leading to a decreased expression after sleep (Lanté et al., 2011) and phosphorylation/ dephosphorylation of subunits linked to an increase in activity after wake and decrease after sleep (Hinard et al., 2012; Vyazovskiy et al., 2008). Given that a higher density of AMPA receptors is associated with synaptic strength, these findings are consistent with the idea that synapses get potentiated during wake and depressed during sleep. Recent findings in mice by Diering *et al.* suggest that cortical synapses undergo a loss of GluR1 and concomitant decrease in size during sleep, in a mechanism involving group I mGluR signalling and the scaffolding protein Homer1a (Diering et al., 2017). Further structural studies in support of the SHY include observations indicating an increase in the number of synapses after wake and a decrease after sleep, both in fruit flies (Bushey et al., 2011; Donlea et al., 2009; Gilestro et al., 2009) and in adolescent mice (Maret et al., 2011; Yang and Gan, 2012). A recent study in the motor cortex and barrel cortex of adolescent mice suggests that sleep is associated with a decrease in the size of synapses. Interestingly, this decrease in size does not seem to occur in large synapses, suggesting that stronger synapses may be protected from downscaling (Vivo et al.,

2017). Finally, there is also some evidence for the SHY from electrophysiological studies. It was found that the response to electrical stimulation in the frontal cortex of rats increased over time during wakefulness and decreased during SWS (Vyazovskiy et al., 2008). A similar trend was also found in human frontal cortex for the response to transcranial magnetic simulation (TMS) (Huber et al., 2013). Other electrophysiological observations include changes in the amplitude and frequency of miniature excitatory postsynaptic currents measured in cortical slices, which appear to be higher after wake than sleep (Liu et al., 2010), and an increase in cortical firing after long periods of wakefulness (Vyazovskiy et al., 2009). However, the SHY does not come without criticism, since there is also some evidence which seems to challenge its core idea (Frank, 2012). For instance, a recent finding in the motor cortex of mice points towards the possibility that SWS supports synaptic potentiation, rather than depression. In this study, learning of motor tasks was associated with sleep-dependent formation of new spines on layer 5 pyramidal neurons, which was not affected by REM sleep deprivation (Yang et al., 2014).

Under the SHY framework, it is thought that SWA directly regulates synaptic renormalisation. This is because the SHY ties in with observations that SWA is homeostatically regulated and increases locally in the cortex after periods of high waking activity (Borbély, 2001; Riedner et al., 2007; Vyazovskiy et al., 2007) (see section 1.3.1). The build-up of synaptic weights during wakefulness has been linked to increased synchronisation of neurons and thus increased SWA (Rodriguez et al., 2016; Tononi and Cirelli, 2014; Vyazovskiy and Faraguna, 2014). It has been proposed that global synaptic downscaling would in turn serve to

decrease synchronisation and SWA over the course of SWS (Tononi and Cirelli, 2014; Vyazovskiy and Faraguna, 2014).

1.4.3 The active system consolidation hypothesis

The active system consolidation hypothesis is based on the idea that memory consolidation involves an interplay between the hippocampus and the cortex. In this model, the hippocampus and the cortex represent two memory systems, whereby the first acts as a fast-learning temporary store and the latter as a slow-learning long-term store (Frankland and Bontempi, 2005). It is thought that, during SWS, newly formed memories are reactivated in both memory systems, which ultimately drives their integration into pre-existing cortical networks for long-term storage (Diekelmann and Born, 2010; Rasch and Born, 2007, 2013). This concept is based on findings in the hippocampus demonstrating a replay during SWS of neuronal firing patterns which were observed during tasks learned in the preceding waking period (Kudrimoti et al., 1999; Lee and Wilson, 2002; Nádasdy et al., 1999; Skaggs and McNaughton, 1996; Wilson and McNaughton, 1994). This has been associated with sharp-wave ripple oscillations, which occur in the hippocampus during SWS (Diekelmann and Born, 2010; Kudrimoti et al., 1999; Wilson and McNaughton, 1994). Sharp-wave ripples have recently been found to promote LTP during replay (Sadowski et al., 2016). Replay was later also found in the cortex (Euston et al., 2007; Ji and Wilson, 2007), where it seems to be associated with Up states (Johnson et al., 2010). Indeed, it has been suggested that hippocampus and cortex interact during slow wave sleep, such that sharp-wave ripples directly promote replay and activity-dependent synaptic plasticity during

cortical Up states (Wei et al., 2016). This may not be mutually exclusive with the idea proposed by the SHY that synaptic weights undergo global downscaling during SWS. In an attempt to combine the two ideas, it has been suggested that replay may prime synapses for potentiation on a background of global synaptic downscaling throughout the cortex. The idea behind this is that global downscaling would prevent eventual saturation of synapses (Diekelmann and Born, 2010; Rasch and Born, 2013). In addition, the active system consolidation hypothesis proposes a role for REM sleep in memory consolidation. This is based on the premise that, to fully integrate memories into long-term storage networks, they must be further strengthened after replay (Diekelmann and Born, 2010). Long-term potentiation of synapses after replay is thought to occur during REM sleep, since there is some evidence linking REM sleep and ACh release with potentiation (Rasmusson, 2000b; Ribeiro et al., 2002, 2007). Of note, REM sleep has been found to underlie ocular dominance plasticity in the visual system (Dumoulin Bridi et al., 2015). Ocular dominance plasticity refers to a form of experience-dependent plasticity, whereby monocular deprivation during a critical period results in plasticity leading to a shift of the receptive field from the closed eye to the open eye (Hubel and Wiesel, 1970). Interestingly, the increase in the response to the undeprived eye appears to be dependent on REM sleep (Dumoulin Bridi et al., 2015). Another recent study in the motor cortex of adolescent mice suggests that REM sleep plays a role in synaptic pruning and selective strengthening of new spines after a motor learning task, in a process which seems to be dependent on dendritic spikes (Li et al., 2017).

The active system consolidation hypothesis has also been criticised. In particular, questions have been raised about the replay of newly acquired memories. The occurrence of replay does not appear to be restricted to sleep, since replay of spike sequences has also been found in awake animals during exploration and learning (Davidson et al., 2009; Diba and Buzsáki, 2007; Foster and Wilson, 2006; Karlsson and Frank, 2009), and in anaesthetised animals (Bermudez Contreras et al., 2013). It is therefore unclear whether replay serves an essential function in learning and memory consolidation during sleep (Tononi and Cirelli, 2014). Furthermore, the role of REM sleep in memory consolidation is not unequivocal. It has even been questioned whether REM sleep plays a role in memory consolidation at all (Siegel, 2001). For example, suppression of REM sleep by antidepressants does not seem to affect memory (Rasch et al., 2009). Further studies are therefore needed to resolve the role of REM sleep in memory consolidation.

1.5 Thesis objectives

The two hypotheses described above for memory consolidation during SWS provide interesting ideas about how slow waves can support plasticity. However, there is currently only very little evidence directly implicating slow oscillations in synaptic plasticity. In slices of barrel cortex, LTP was found after 9-29 single spike-timing dependent pairings applied during Up states, but not during Down states (Kruskal et al., 2013). Conversely, recent experiments carried out in slices of entorhinal cortex suggest that pairing of subthreshold inputs with Up states results in depression of the paired input, and that this effect is dependent on postsynaptic NMDA receptors (Bartram et al., in review). Furthermore, as

mentioned briefly in section 1.2.3, one study in the barrel cortex of anaesthetised mice showed that repeated deflections of a whisker pair led to increased cross-correlation between the two whisker responses only when the whisker deflections were applied during Up states, but not during Down states (Erchova and Diamond, 2004).

Potential mechanisms which may support changes in synaptic strength during Up states include plasticity after pairing of inputs with mild postsynaptic depolarisation (Feldman, 2000; Sjöström and Häusser, 2006; Sjöström et al., 2004), and plasticity associated with high-frequency bursts (Aroniadou-Anderjaska and Keller, 1995; Castro-Alamancos et al., 1995b; Czarnecki et al., 2007). Furthermore, it has been suggested that random timing between postsynaptic activity and Up state spiking could lead to depression via spike-timing-dependent mechanisms, since t-LTD is associated with a longer time window compared to t-LTP in the barrel cortex (Feldman, 2000). In any case, whether Up states directly facilitate plasticity is still largely unresolved.

In my study, I chose the mouse barrel cortex as a model system to investigate whether Up/Down states can mediate synaptic plasticity. This is partly due to the wealth of information that is already available about synaptic plasticity in this system, but also because of its accessibility for experiments *in vitro* and *in vivo*. Plasticity in the barrel cortex can be studied in slices, in anaesthetised mice by rhythmic whisker stimulation, and in awake mice by whisker deprivation. Furthermore, certain forms of intracortical plasticity do not seem to be accompanied by a critical period and are present even in adult animals (Fox, 2002;

Glazewski and Fox, 1996). All experiments described in this thesis were carried out in adolescent mice. In the barrel cortex, both potentiation and depression can be induced in layer 2/3 during adolescence (Fox, 2002; Glazewski and Fox, 1996). Furthermore, studying plasticity *in vitro* during adolescence has practical advantages related to the quality of slice preparations. Adolescent mice can also be readily used for *in vivo* recordings and display normal Up/Down state activity under anaesthesia and during natural sleep (Nelson et al., 2013).

Under this premise, experiments were carried out to address the following aims:

1. Establish an *in vitro* model of electrically-evoked Up states in slices of the barrel cortex.

2. Investigate whether electrically-evoked Up states mediate plasticity of paired subthreshold and suprathreshold inputs in layer 2/3 *in vitro*.

3. Investigate whether spontaneous Up states and Down states differentially induce plasticity of the response to a single whisker after pairing deflections of that whisker *in vivo* in anaesthetised mice.

4. If plasticity is found after Up state pairings, investigate the underlying pathway and mechanism.

These aims were addressed as follows: Initial experiments were carried out to assess the conditions which allow for generation of Up states by electrical

stimulation in slices of barrel cortex. In addition, I pharmacologically tested whether different molecular pathways of plasticity also influence electrically-evoked Up states. However, these experiments were only preliminary, with the intention of carrying out further characterisation after evaluating the effects of Up/Down states on paired inputs *in vitro*. Finally, the effect of Up/Down states on plasticity was assessed in anaesthetised mice *in vivo*.

2 Materials and methods

2.1 Animals

Experimental procedures were carried out in accordance with the UK Animals (Scientific Procedures) Act of 1986. Male and female mice of the strain C57BL/6J (Harlan Laboratories) were used for all experiments. Mice were kept in a 12 h light, 12 h dark cycle. Experimental procedures started in the morning, after 3-4 h of light exposure.

2.2 Preparation of acute slices of mouse barrel cortex

Experiments were carried out on mice on postnatal day 15-21 (P15-P21). Mice were deeply anaesthetised with isoflurane and decapitated. The brain was removed and placed in ice-cold artificial cerebrospinal fluid (aCSF) containing 10 mM glucose, 1 mM $MgSO_4$, 3.5 mM KCl, 126 mM NaCl, 1.25 mM NaH_2PO_4, 24 mM $NaHCO_3$, and either 1.2 mM, 1.6 mM, or 2 mM $CaCl_2$ saturated with 95 % O_2/5 % CO_2, pH 7.2-7.4. Coronal slices were prepared at a thickness of 350 µm using a VT 1200S vibratome (Leica). Slices were maintained at room temperature in an interface storage chamber containing aCSF, saturated with 95% O_2/5% CO_2, for at least 1h before recording. Slices containing barrel cortex were identified by the appearance of barrel structures in layer 4.

2.3 Electrophysiology in acute slices

Recordings from barrel cortex pyramidal neurons were made in aCSF at room temperature (25-30 °C) in a submerged recording chamber. Current-clamp recordings in either the whole-cell or perforated-patch configuration were low-pass filtered at 2 kHz and acquired at 10 kHz using a Multiclamp 700B amplifier (Molecular Devices) and custom Igor Pro software (Wavemetrics). The input resistance (R_i) of the patched cell was determined throughout the recording by applying a short hyperpolarising current step of 20 pA at the start of each recording sweep. In the whole-cell configuration, changes in R_i of more than 30% and concomitant decreases in the membrane potential (V_m) were frequent after the first 10 minutes of recording. Experiments were excluded following such changes. Due to plasticity experiments requiring recording durations of at least 45 minutes, experiments used for further analysis were carried out in the perforated patch configuration to avoid changes in R_i and V_m.

2.3.1 Whole-cell patch-clamp recordings

Whole-cell recordings were obtained using glass micropipettes with a resistance of 6-10 MΩ, pulled from standard borosilicate glass, filled with internal solution containing 110 mM potassium gluconate, 40 mM HEPES, 2 mM ATP-Mg, 0.3 mM GTP-NaCl, 4 mM NaCl (pH 7.2-7.3; osmolarity 270-290 mosmol l^{-1}. 4 mg/ml biocytin (Sigma) was added for post-hoc cell visualisation.

2.3.2 Perforated patch-clamp recordings

Perforated patch-clamp recordings were made using borosilicate glass micropipettes with a resistance of 8-10 MΩ. These micropipettes were first tip-filled with a solution containing 150 mM KCl and 10 mM HEPES (pH 7.2-7.3; osmolarity 280 mosmol l^{-1}) and then back-filled with the same solution containing an additional 5 μM gramicidin-A (Sigma). Gramicidin-A was first dissolved in DMSO to create a stock solution of 5 mM. Gramicidin-A was added from this stock to the KCl and HEPES solution at a 1:1000 dilution. A final concentration of 5 μM Gramicidin-A was low enough for it to dissolve completely after mixing using a vortex mixer. 10 μM Alexa Fluor 594 (Life Technologies) was added to the gramicidin-containing solution to be able to visualise any spontaneous rupture of the membrane patch (Fig. 1).

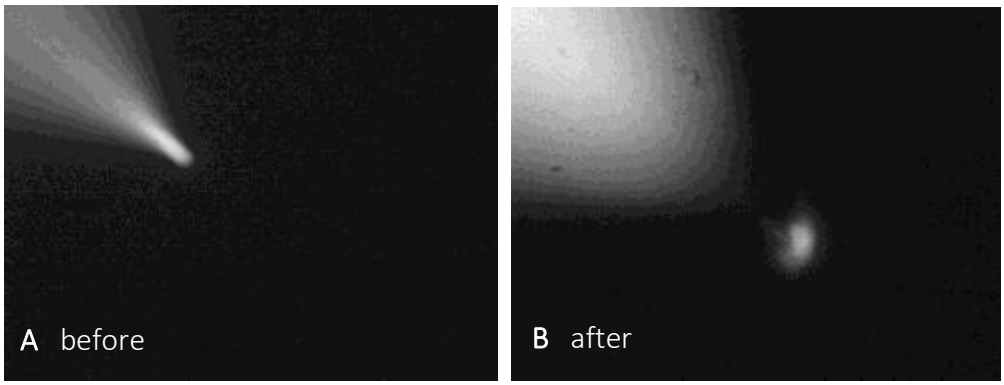


Figure 1. Visualisation of spontaneous membrane rupture during perforated patch-clamp. (**A**) During a successful perforated patch, the fluorescent dye is contained within the electrode and does not pass through the gramicidin pores. (**B**) Fluorescent dye fills the cell body upon spontaneous rupture of the membrane patch.

After formation of a gigaohm seal with the cell of interest, the progress of gramicidin perforation was assessed by monitoring the response to brief hyperpolarising 10 mV step pulses in voltage-clamp mode. Recording was started once a stable access resistance of less than 80 MΩ was reached (typically 20-45 minutes after seal formation).

2.4 Electrical stimulation in slices of barrel cortex

Stainless steel microelectrodes (FHC, Inc.) with <1 μm tip diameter were placed onto the surface of a slice to evoke EPSPs and Up states by brief electrical pulses (100 μs, 50-250 μA). For evoked Up states, the stimulation amplitude was set by incrementally increasing it from 0 until Up states were observed. The amplitude was kept at this value throughout the experiment. For EPSPs, a stimulation amplitude was used which induced small EPSPs of 2-4 mV. Electrical pulses were triggered by a Master-8 stimulator (AMPI) via an Iso-Flex stimulus isolator (AMPI). Single Up states were evoked most effectively by placing the electrode close to the boundary between layers 4 and 5 of the barrel below the patched layer 2/3 pyramidal neuron. EPSPs were evoked by placing the electrode close to the patched cell in layer 2/3, thereby decreasing the probability of the electrical pulse to induce an Up state instead of an EPSP.

2.5 *In vitro* plasticity protocol

Plasticity experiments were carried out in 1.6 mM extracellular $CaCl_2$. Plasticity was induced by pairing trains of 10 consecutive EPSPs every 15 seconds for 5 minutes, giving a total number of 200 pairings with Up or Down states. The inter-stimulus interval between EPSPs was 100 ms, 50 ms, or 25 ms for 10 Hz, 20 Hz, and 40 Hz pairings, respectively. Before and after pairing, single EPSPs were evoked every 15 seconds, followed by single Up states after a delay of 2 seconds. Before pairing, recording periods were at least 10 minutes to establish a stable baseline. In the case of spontaneous rupture of the perforated patch, any cells with a post-pairing recording duration of less than 20 minutes were excluded from the analysis.

2.6 Application of drugs to barrel cortex slices

(S)-MCPG (Sigma) was bath-applied at 500 µM. (R)-CPP (Tocris) was bath-applied at 10 µM. Acetylcholine (Sigma) was applied at 1 mM and 10 mM using a Picospritzer III (Parker) at 5-10 psi.

2.7 Identification of pyramidal neurons in slices of barrel cortex

The identity of cells was assessed based on electrophysiological characteristics by applying a current step protocol. After recording, slices were fixed in 4 % paraformaldehyde and cell identity was confirmed histologically by fluorescent

detection of biocytin. For this, slices were first washed 2x 10 min in PBS, then 1x 10 minutes in 0.3 % Triton X-100 (Sigma) in PBS to permeabilise the cell membranes. This was followed by incubation in a 1:100 dilution of avidin conjugated with either Texas Red or Fluorescein (Vector Laboratories) in PBS with Triton for 1-2 h. After this, slices were washed 3x 10 min in PBS and then mounted on microscope slides with Vectashield Hard Set mounting medium with DAPI (Vector Laboratories) under a coverslip.

2.8 Virus injections

Intracerebral stereotaxic injections of AAV5-CaMKIIa-eArchT3.0-EYFP (UNC Vector Core) were carried out on neonatal mice on P0-P2 and on adolescent mice aged 4-6 weeks.

2.8.1 Injections in neonates

New-born pups were deeply anaesthetised by ~3 min of hypothermia before placing them on a stereotaxic apparatus (Stoelting Co.) using a custom-made plastic mould for head fixation. ArchT3 virus was injected using a Nanoject II Nanoliter Injector (Harvard Apparatus) with a bevelled glass micropipette, mounted on the frame of the stereotaxic apparatus. Bevelled micropipettes were sufficiently sharp to penetrate the skull without prior incision. Injections were targeted to the barrel cortex in the right hemisphere at three different sites, with the following coordinates from lambda: 0.9 mm anterior and 1.65 mm lateral, 0.9 mm anterior and 1.85 mm lateral, and 1.1 mm anterior and 1.75 mm lateral. A

volume of 28 nl was injected each at three depths (0.8 mm, 0.6 mm and 0.4 mm) to achieve infection across layers. After surgery, pups were revitalised at room temperature and returned to the dam.

2.8.2 Injections in adolescent mice

Mice were deeply anaesthetised using 2 % isoflurane and placed on a stereotaxic apparatus (Stoelting Co.). Body temperature was maintained at 37 °C during surgery via a homeothermic blanket and rectal probe (Harvard Apparatus). Marcain was injected under the scalp and a small incision was made to expose the skull. Three small holes were drilled over the right hemisphere around the stereotaxic coordinates corresponding to the D1 barrel (1.5 mm posterior and 3 mm lateral to bregma). A volume of 150 nl of virus was injected at each of two depths (0.8 mm and 0.5 mm) per injection site, amounting to a total volume of 900 nl. This was to enable it to spread across all layers in a large area of the barrel cortex. Injections were made in steps of 50 nl over a period of ~10 min per site via a glass micropipette connected to a Nanoject II Nanoliter Injector (Harvard Apparatus), which was mounted to the stereotaxic frame. Following this, the skin was sutured and mice were placed into a heated chamber for recovery before being returned to their home cage.

2.9 Extracellular recordings in anaesthetised mice

2.9.1 Surgery

Mice were deeply anaesthetised with 2 % isoflurane before being placed on a stereotaxic apparatus (Stoelting Co.) for surgery. Anaesthetic depth was monitored throughout the experiment and anaesthetic strength was adjusted as necessary. Body temperature was maintained at 37 °C for the duration of the experiment via a homeothermic blanket and rectal probe (Harvard Apparatus). Marcain was injected under the scalp before an incision was made to expose the skull. A square craniotomy was drilled over the right hemisphere, taking care not to rupture any blood vessels. The craniotomy was centred around the stereotaxic coordinates of the D1 barrel (1.5 mm posterior and 3 mm lateral to bregma), with its size large enough to accommodate the electrode used (0.8 x 0.8 mm – 2.5 x 2.5 mm). Saline was added to the surface of the brain at regular intervals to prevent it from drying out. Medetomidine was introduced as a second anaesthetic before electrode insertion. This was done by first injecting a bolus of 1 mg/kg medetomidine and then, 5 min later, starting a continuous injection of 2 mg/kg/h medetomidine via a syringe pump (World Precision Instruments) while reducing the isoflurane concentration to approximately 0.5 %.

2.9.2 Electrophysiology

One of three different recording electrodes was coated with DiI for later identification of the recording site, mounted on the stereotaxic frame and inserted into the barrel cortex perpendicular to the cortical surface. For optogenetic experiments, a 32-channel linear probe was used with 4 shanks and 8 sites per shank (50 μm spacing between sites, 200 μm spacing between shanks) (NeuroNexus), inserted at a depth of 0.5 mm to record from layers 2/3 and 4. To

record from several barrels during plasticity experiments, a custom-made 8 x 8 64-channel microelectrode array was used with a spacing of 200 μm between electrodes (Microprobes), which was inserted into layer 2/3 at a depth of 0.2 mm (Fig. 2). To record from all layers during plasticity experiments, a single-shank 32-channel linear probe with a spacing of 50 μm between electrode sites (NeuroNexus) was inserted at the stereotaxic coordinates for the D1 whisker at a depth of 1.2 mm. Continuous recordings of the raw extracellular voltage traces were acquired at 30 kHz using an RHD2164 64-channel amplifier board connected to an RHD2000 amplifier evaluation system (Intan Technologies), controlled by open-source RHD2000 interface software (Intan Technologies).

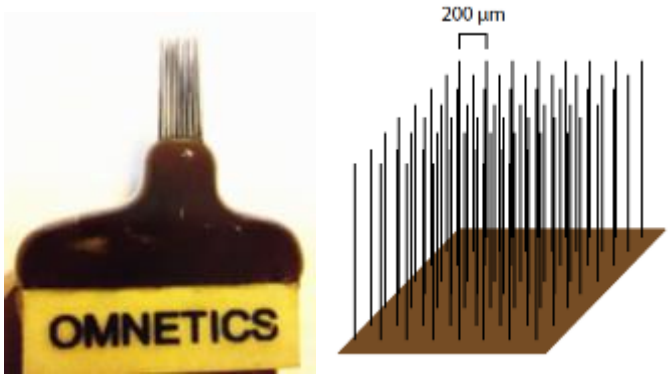


Figure 2. Custom-made 64-channel electrode array. Electrodes are arranged in an 8 x 8 matrix with a spacing of 200 μm between neighbouring electrode sites.

2.10 Optical inhibition *in vitro* and *in vivo*

Optical stimulation *in vitro* was applied to the whole slice by an LED, with the light being passed through the objective. The LED was filtered at 530 nm to achieve

activation of ArchT3. Light pulses were triggered by a Master-8 stimulator (AMPI). Optical inhibition *in vivo* was achieved by a 530 nm fibre-coupled LED (Thorlabs) connected to a T-Cube LED driver (Thorlabs). The LED driver was connected to an Arduino Mega board (Arduino), controlled by custom Arduino software. The LED was switched on by a TTL signal sent via the Arduino board, with a duration and inter-stimulus interval set using the Arduino software. A time stamp was recorded by simultaneously sending a TTL signal from the Arduino board to the RHD2000 amplifier evaluation system. An optic fibre (Thorlabs) was used to deliver the light pulses from the LED to the brain. The fibre was either placed directly on the surface of the brain close to the recording electrode, or inserted into the cortex via a fibre-optic cannula (Thorlabs). Light was presented at an intensity of approximately 5 mW.

2.11 Real-time Up state detection and whisker stimulation

A closed-loop feedback system to initiate whisker deflections upon detection of an Up state was implemented using an Arduino Mega board (Arduino) connected to the RHD2000 amplifier evaluation system (Intan Technologies), controlled by custom Arduino software and open-source RHD2000 interface software (Intan Technologies). Up states were detected when the LFP signal from a selected electrode channel crossed a negative voltage-threshold specified using the RHD interface software (-50-200 μV). The electrode channel was selected by visual inspection of the LFP and the threshold was set at a level which was approximately one-third of the estimated average Up state amplitude. The false positive rate was

determined by applying 5 min of sham pairing, in which the Arduino board output was uncoupled from the whisker stimulator. Whenever the LFP was below threshold, a digital signal was sent from the RHD2000 amplifier evaluation system to the Arduino board, which in turn triggered a train of 5 whisker stimuli with an inter-stimulus interval of 100 ms. For Down state pairings, the Arduino board triggered a train of 5 whisker stimuli when the LFP did not cross the threshold for 200 ms. Single-whisker deflection was achieved by placing the D1 whisker on the contralateral side into a narrow tube attached to a piezoelectric wafer connected to a piezo amplifier (Physik Instrumente), driven by sine wave pulses (40 ms, 12 V) delivered by the Arduino board. Before and after whisker pairing, baseline periods of 5 min were recorded every 10 min in which a single whisker deflection was presented every 5 s. In some Up state pairing experiments, deflections of a second whisker were presented but not paired with Up states. This was achieved by alternating 5 min baseline periods of either D1 or B2 whisker deflections, but only using one of the whiskers for Up state pairings. To get a time stamp for whisker deflections, a digital signal was sent from the Arduino board to the RHD2000 amplifier evaluation system simultaneously to every sine wave pulse and recorded using the RHD interface software.

2.12 Application of drugs to the barrel cortex *in vivo*

D-AP5 was used at a concentration of 100 μM, diluted in sterile saline. This was applied to the surface of the brain, making sure to cover the whole area of the barrel cortex exposed by the craniotomy. First, any excess saline was aspirated before applying the solution containing the drug, which was then topped up

approximately every 10-15 min.

2.13 Immunohistochemistry

At the end of the experiment, mice were injected with a terminal dose of pentobarbital before undergoing cardiac perfusion, first with PBS and then with 4 % paraformaldehyde in PBS. For 32-channel linear probe recordings, the brain was extracted and post-fixed in 4 % paraformaldehyde in PBS at 4 °C. For 64-channel array recordings, the cortex was removed and placed between microscope slides for post-fixation in 4 % paraformaldehyde in PBS at 4 °C. Brains and cortices were incubated in 30 % sucrose in PBS at 4 °C for cryoprotection 24 h before re-sectioning. Thin sections were cut at 50-60 μm thickness on a freezing-stage microtome (Leica). Whole brains were cut coronally to reveal linear probe position and cortices were cut tangentially to reveal electrode array position with respect to the barrel map. Coronal sections were mounted on microscope slides using Vectashield Hard Set with DAPI (Vector Laboratories) under a coverslip directly after cutting. Tangential sections were subjected to antibody staining after cutting to reveal the barrel map. First, they were incubated in a blocking solution containing 10 % normal donkey serum (Sigma) in PBS for approximately 1 h. Sections were then incubated for 24-28 h at 4 °C in a 1:100 or 1:200 dilution of anti-Tenascin C [MTn-12] rat monoclonal antibody (Insight Biotechnology) in blocking solution. Following this, sections were washed 3 x 10 min in PBS at room temperature and incubated in a 1:300 dilution of donkey anti-rat Alexa 488 antibody (Invitrogen) in blocking solution at 4 °C overnight in the dark. After 3 x

20 min washing steps in PBS, they were mounted on microscope slides using Vectashield Hard Set mounting medium with DAPI (Vector Laboratories) under a coverslip.

2.14 Histological identification of recording sites

Coronal and tangential sections were imaged under a fluorescence microscope (Leica) and images acquired with a CCD camera (QImaging). In both cases, the recording site was identified using DiI staining. Individual overlapping images were then taken of the whole slice and merged using Photoshop (Adobe Systems). In tangential sections, electrode array placement was assessed with respect to the barrel map, which was made visible by tenascin-c staining. In coronal sections, electrode placement was evaluated with respect to the cortical layers. The boundaries between layers were identified by differences in the density of cell bodies, as visualised by DAPI staining, in order to measure the thickness of individual layers.

2.15 Data analysis

Data were analysed using custom software written in Igor Pro (Wavemetrics). For *in vitro* plasticity experiments, EPSP slopes after pairing were normalised to the baseline period before pairing and these normalised values were then averaged across experiments. For *in vivo* data, LFP and multiunit responses to whisker deflections were averaged over 5 min for each of the baseline recordings from each electrode. Responses were normalised to the average of three pre-pairing

baseline recordings. Multiunit activity was extracted by high-pass filtering the raw voltage trace at 300 Hz. Spikes were defined as events crossing a threshold of 5 standard deviations of the noise and were each given a value of 1. Spike-time histograms were created with 1 ms bins around the whisker stimulus. For 64-channel array experiments, further analysis was carried out only on those electrode channels which showed responses to whisker deflection. Responding channels were selected by creating z-scores for peak STH responses and defining a threshold for the resulting z-scores. This was done by calculating the mean and standard deviation for the STH during 100 ms before stimulus onset, subtracting the mean from the peak of the whisker response and dividing the resulting value by the standard deviation. Responding channels were then defined as channels with a z-score > 5. Experiments carried out with a 32-channel linear electrode probe were analysed channel-by-channel from layer 2/3 to layer 5. To compare differences between layers, responses were averaged across channels for each layer. The one-dimensional CSD was calculated by taking the second spatial derivative of the LFP waveforms along the electrode to reveal the location of current sinks and sources, according to the following formula: $CSD = [\Phi (z + \Delta z,t) - 2\Phi (z,t) + \Phi (z - \Delta z,t)]/ \Delta z^2$, where Φ is the field potential, z is the recording depth, Δz is the sampling interval (in this case, 50 μm), and t is time (Mitzdorf, 1985; Nicholson and Freeman, 1975).

2.16 Post hoc Up state detection (*in vitro* and *in vivo*)

Custom software written in Igor Pro (Wavemetrics) was used to detect Up states in intracellular recordings and LFP recordings to measure characteristics such as

duration and probability. First, the recording was median filtered and the running standard deviation was calculated over a 400 ms window as a measure of noise. Up states were defined as periods of at least 400 ms (the minimum Up state duration) in which this noise was equal to or exceeded 5 times the standard deviation of the baseline mean. The point at which the noise decreased back to within 1 standard deviation of the baseline mean was defined as the end of the Up state. In intracellular recordings, in which Up states were evoked by electrical stimulation, the stimulus time was defined as the start of the Up state. In continuous LFP recordings, where Up states occurred spontaneously, Up state start was defined as the point of initial increase in noise to 1 standard deviation of the baseline mean. An option was provided which allowed for manual adjustment of Up state start and end.

2.17 Statistics

Statistical analysis was done using IBM SPSS Statistics (IBM). Numbers of observations (*n*) given in results sections correspond to numbers of slices *in vitro* and numbers of mice *in vivo*. The total number was 41 slices from 36 mice for plasticity experiments *in vitro* and 20 mice for plasticity experiments *in vivo*. Results are shown as mean ± SEM. Student's *t*-tests, analyses of variance (ANOVA), Pearson's correlations, and regression analyses were performed as appropriate, as described in each results section. Effects were considered significant at values of $p < 0.05$. Calculations of statistical power were carried out using G*Power (Faul et al., 2007, 2009).

3 Characterisation of Up/Down state dynamics in the barrel cortex *in vitro*

3.1 Introduction

As described previously, slow oscillations can be observed in different cortical areas as spontaneously occurring Up and Down states both *in vivo* and *in vitro*. Spontaneous Up states occur intrinsically within the cortex (Sanchez-Vives and McCormick, 2000; Timofeev et al., 2000). They can also be observed *in vivo* in response to sensory input (Anderson et al., 2000; Petersen et al., 2003a) and can be turned on and off by synaptic stimulation *in vitro* (MacLean et al., 2005; Mann et al., 2009; Rigas and Castro-Alamancos, 2007; Shu et al., 2003).

Here, I sought to establish suitable experimental conditions for reliable generation of Up states *in vitro* in acute slice preparations. This was to lay the groundwork for the next set of experiments investigating synaptic plasticity during Up/Down states in the barrel cortex *in vitro*. Experiments included applying brief electrical pulses to slices of barrel cortex to induce network activity, and measuring how extracellular Ca^{2+} affects the duration and probability of such electrically-evoked Up states. Furthermore, I carried out experiments to pharmacologically investigate different pathways which have previously been shown to affect LTP and LTD that may also impact Up/Down state activity. Specifically, I measured the effect of NMDA receptors, mGluRs, as well as cholinergic activation on electrically-evoked Up states. However, pharmacological experiments were only preliminary,

with the idea that these pathways could be investigated in more detail once an effect of Up/Down states was found on synaptic plasticity *in vitro*.

3.2 Results

3.2.1 Up states can be evoked by electrical stimulation in slices of barrel cortex

Original reports of slow oscillations *in vitro* suggest that reducing extracellular ionic concentrations from 2 mM Ca^{2+} and 2 mM Mg^{2+} to 1.2 mM Ca^{2+} and 1 mM Mg^{2+} supports the generation of Up states in cortical slices (Sanchez-Vives and McCormick, 2000). Based on these findings, I first tested whether similar conditions enable Up state generation in my barrel cortex preparation. Here, Up states were recorded in single cells using whole-cell current-clamp experiments in slices of barrel cortex from adolescent mice (P15-21). Recordings were targeted to layer 2/3 pyramidal neurons in acute slices of barrel cortex (Fig. 3A, B). Neurons were generally in a Down state under the conditions used here. However, Up state transitions could be evoked by synaptic stimulation in the corresponding layer 4 barrel (Fig. 3A, C). Electrical stimulation in layer 4 evoked Up states on the highest proportion of trials, compared to stimulation in other layers (n = 3) (Fig. 3D). One-way repeated-measures ANOVA showed that this difference was significant at low electrical stimulation amplitudes (6.1 ± 3.0 % in layer 2/3, 60.6 ± 3.0 % in layer 4, 3.0 ± 3.0 % in layer 5): $F(2, 4) = 343.00$, $p < 0.001$. Bonferroni post-hoc tests revealed significant differences between layer 4 and layers 2/3 and 5 ($p < 0.001$ between layer 4 and layer 2/3, $p = 0.008$ between layer 4 and layer 5, $p = 1.00$ between layer 2/3 and layer 5). No significant differences in the Up state probability were found between layers at medium (0.0 ± 0.0 % in layer 2/3, 31.2

± 13.1 % in layer 4, 6.1 ± 6.1 % in layer 5; $F(2, 4) = 5.93$, $p = 0.064$) and high (9.1 ± 5.1 % in layer 2/3, 21.2 ± 16.9 % in layer 4, 9.1 ± 5.2 % in layer 5; $F(2, 4) = 0.43$, $p = 0.676$) stimulation amplitudes.

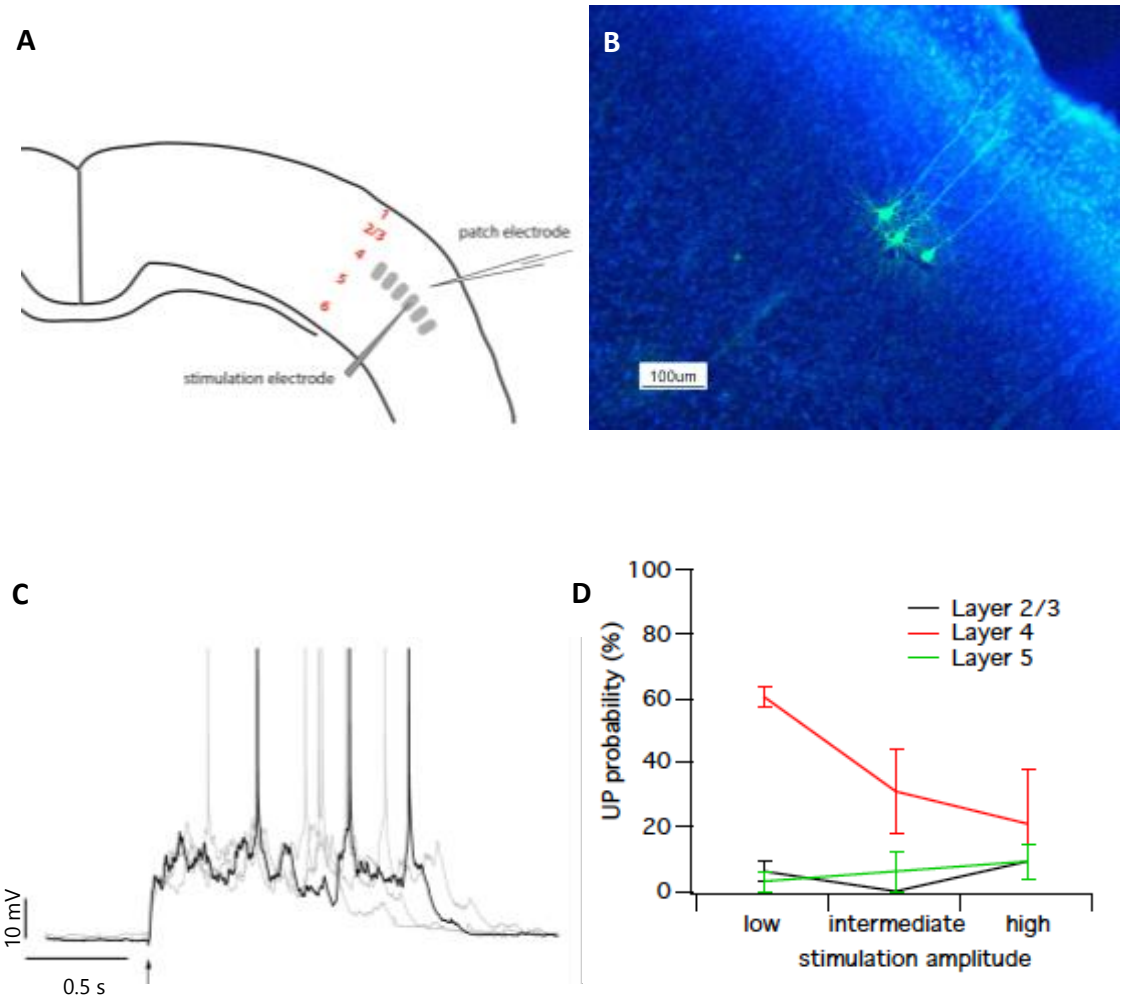


Figure 3. Up states *in vitro* in slices of barrel cortex. (**A**) Experimental setup. Whole-cell patch-clamp recordings were obtained from layer 2/3 pyramidal neurons in acute coronal slices of barrel cortex. Up states were evoked by electrical stimulation in the corresponding layer 4 barrel. (**B**) Patched neurons (green) were identified by fluorescent detection of biocytin. DAPI was used to visualise cell bodies (blue). (**C**) Example current-clamp recordings. Up states were evoked every 20 s by brief 100 µs pulses of electrical

stimulation at a stimulation strength between 5-50 μA (arrow). Action potentials are truncated at 0 mV. (**D**) Up state probability at low, intermediate, and high electrical stimulation strengths compared between electrode placement in layer 2/3 (black), layer 4 (red), and layer 5 (green). Error bars show SEM.

While these data demonstrate that neocortical Up states can be reliably evoked from layer 4 using aCSF containing 1.2 mM Ca^{2+} and 1 mM Mg^{2+}, higher concentrations of extracellular Ca^{2+} are typically used for plasticity experiments *in vitro* (see, for example: Banerjee et al., 2014; Hardingham et al., 2003). In order to test extracellular Ca^{2+} concentration on Up state generation and stability, slices were equilibrated with aCSF solutions containing different Ca^{2+} concentrations (1.2, 1.6 or 2 mM), the responses to layer 4 stimulation monitored every 10 s. With 1.2 mM Ca^{2+}, Up states remained stable over periods of 20 minutes (Fig. 4A). Interestingly, with higher concentrations of extracellular Ca^{2+} the duration of evoked responses gradually decreased over time (Fig. 4B, C). Examining the initial properties of successfully-evoked Up states observed during the first 5 minutes of recording revealed a significant effect of extracellular Ca^{2+} concentration on Up state duration, from 1.43 ± 0.09 s in 1.2 mM Ca^{2+} (n = 11) to 0.92 ± 0.08 s in 1.6 mM Ca^{2+} (n = 14) and 0.86 ± 0.09 s in 2 mM Ca^{2+} (n = 11) (Fig. 2D, E; $F(2, 33) = 13.73$, $p < 0.001$, One-way independent ANOVA). Gabriel's post hoc test further revealed that Up states were significantly shorter in 1.6 mM Ca^{2+} and 2 mM Ca^{2+} compared to 1.2 mM Ca^{2+} ($p < 0.001$ in both cases), whereas there was no significant difference between the 1.6 mM Ca^{2+} and 2 mM Ca^{2+} condition ($p = 0.934$). In addition, the probability of the electrical stimulus to evoke an Up state was lower with increasing concentrations of extracellular Ca^{2+}. During the first 5

minutes of recording, an Up state probability of 67.9 ± 9.4 % was measured in 1.2 mM Ca^{2+} (n = 11), while it was only 53.8 ± 8.3 % in 1.6 mM Ca^{2+} (n = 14), and even lower at 45.3 ± 9.4 % in 2 mM Ca^{2+} (n = 11). However, this reduction in the Up state probability was not significant ($F(2, 33) = 1.48$, $p = 0.242$, one-way independent ANOVA). These analyses only included experiments in which at least one Up state could be evoked by electrical stimulation. In 2 mM Ca^{2+}, I only managed to evoke Up states in approximately 40 % of recordings, whereas the success rate was much higher at approximately 80 % in 1.2 mM Ca^{2+}. Taken together, this suggests that the extracellular solution typically used for plasticity experiments should be adjusted for experiments addressing synaptic plasticity during Up/Down states in the barrel cortex.

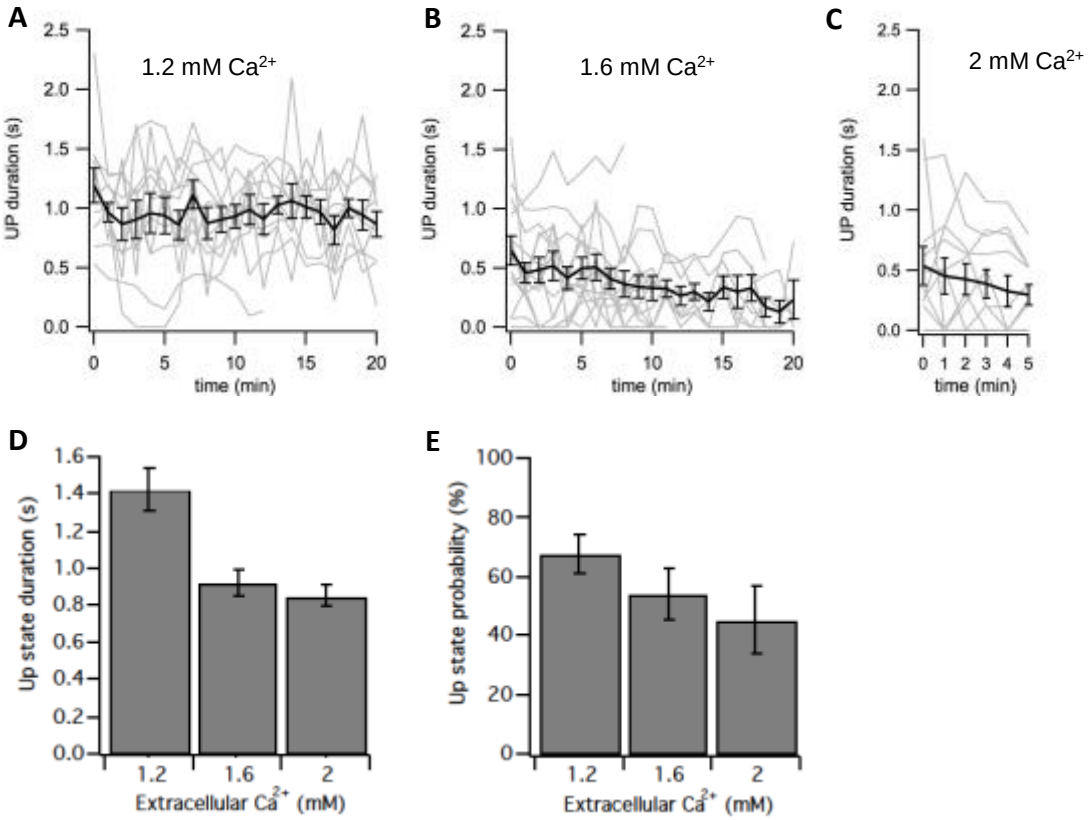


Figure 4. Ca^{2+}-dependent decrease of Up state duration. Up states were evoked every 10 s. Failures to evoke an Up state were counted as 0. Error bars represent SEM. (**A-C**) Mean Up state duration over time at the different Ca^{2+} concentrations. (**D**) Mean Up state duration over the first 5 min of recording at different Ca^{2+} concentrations, excluding failures. (**E**) Mean Up state probability over the first 5 min of recording at different Ca^{2+} concentrations.

3.2.2 Generation of electrically-evoked Up states is dependent on NMDA receptors

To test whether inhibition of NMDA receptors can be used to study the mechanisms underlying plasticity during Up/Down state activity *in vitro*, the antagonist (R)-CPP was applied to slices of barrel cortex during evoked Up states (Fig. 5). However, inhibition of NMDA receptors with 10 µM (R)-CPP completely suppressed Up states. While the probability of inducing Up states by electrical stimulation was 85.0 ± 5.2 % before (R)-CPP was applied, Up states were abolished to a probability of 0.0 ± 0.0 when (R)-CPP was present (n = 3). Similarly, the duration of Up states was reduced from 1.78 ± 0.05 to 0.00 ± 0.00 after application of the drug (n = 3). In both cases, two-tailed paired-samples t-tests showed a significant difference between control and drug conditions: $t(2) = 16.33$, $p = 0.004$, and $t(2) = 39.27$, $p = 0.001$, respectively, for Up state probability and duration.

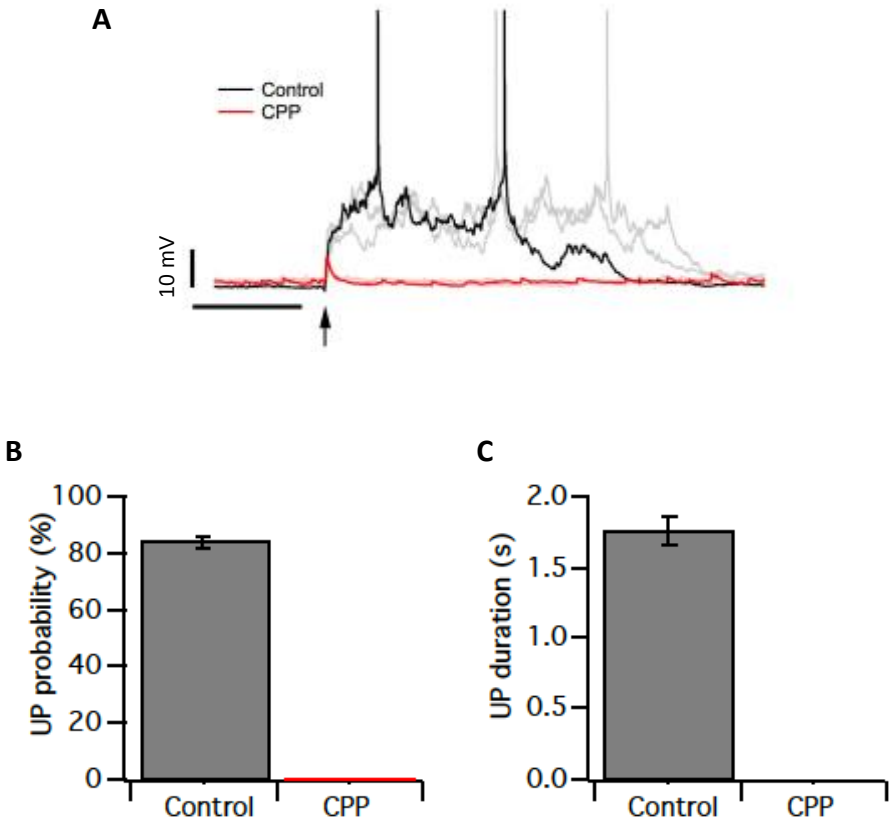


Figure 5. Inhibition of NMDA receptors suppresses electrically-evoked Up states. (**A**) Example current-clamp recordings. Up states were evoked every 20 s (arrow). Experiments were carried out at a concentration of extracellular Ca^{2+} of 1.2 mM. Action potentials are truncated at 0 mV. (**B**) Mean Up state probability. (**C**) Mean Up state duration. (**B, C**) Up states were evoked every 20 s for 5 min (control). (R)-CPP was applied at 10 µM. Error bars represent SEM.

3.2.3 Electrically-evoked Up states are not significantly affected by inhibition of metabotropic glutamate receptors

In a similar way to the experiment described above, the mGluR antagonist (S)-MCPG was applied to slices of barrel cortex during evoked Up states (Fig. 6). Here,

application of 500 µM of the antagonist resulted in a small reduction of the probability of electrical stimulation to evoke Up states, from 90.7 ± 9.3 % to 69.0 ± 14.5 % (n = 3). However, this effect was not statistically significant ($t(2) = 4.19$, $p = 0.052$, two-tailed paired-samples t-test). Similarly, the duration of Up states decreased slightly from 1.38 ± 0.13 s to 0.98 ± 0.13 s after application of the drug (n = 3). Again, the difference between conditions was not found to be significant ($t(2) = 1.70$, $p = 0.231$, two-tailed paired-samples t-test).

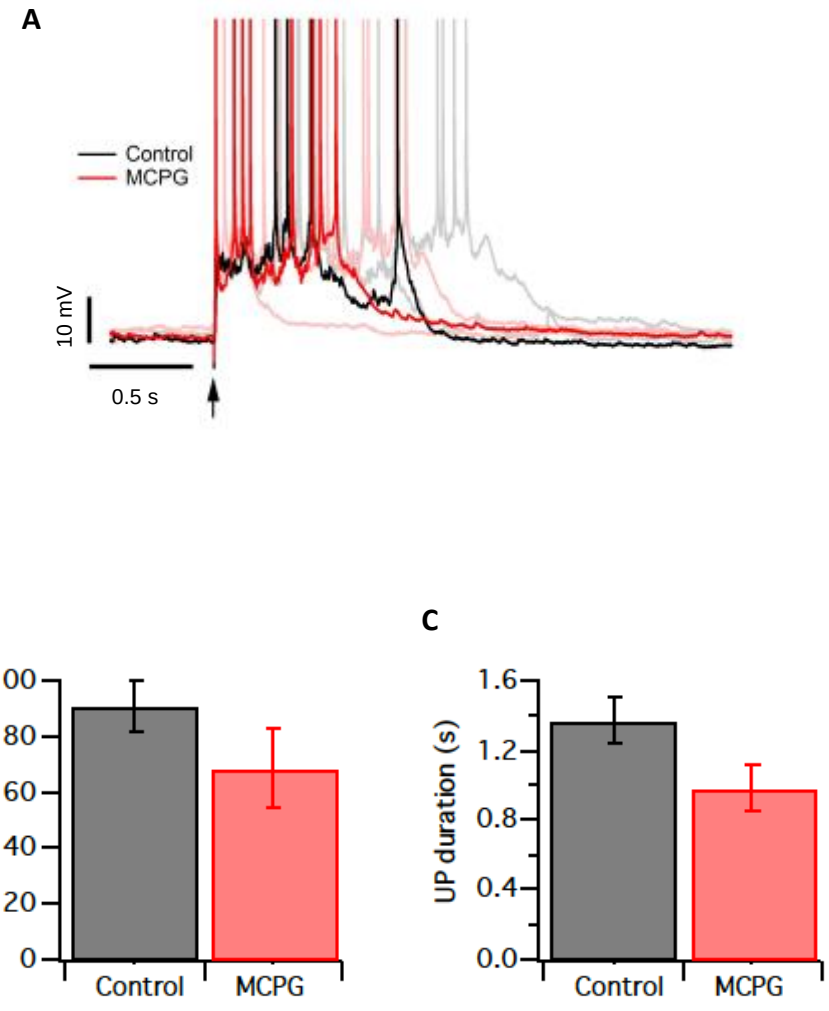


Figure 6. Inhibition of mGluRs does not significantly affect electrically-evoked Up states. (**A**) Example current-clamp recordings. Up states were evoked every 20 s (arrow). Experiments were carried out at a concentration of extracellular Ca^{2+} of 1.2 mM. Action potentials are truncated at 0 mV. (**B**) Mean Up state probability. (**C**) Mean Up state duration. (**B, C**) Up states were evoked every 20 s for 5 min (control). (S)-MCPG was applied at 500 μM. Error bars represent SEM.

3.2.4 Electrically-evoked Up states are reversibly suppressed by Acetylcholine

Acetylcholine (ACh) release in the cortex is high during arousal and REM sleep (Marrosu et al., 1995). It has been found to induce a sustained depolarisation of cortical neurons, which appears similar to the depolarising phase of the slow oscillation, but without any silent off-periods (Steriade, 2004; Steriade et al., 1993d). This raised the possibility that ACh may be used in experiments to study plasticity during associated periods of sustained excitation in the absence of Down states. Here, ACh was applied to slices of barrel cortex in order to test its effect on electrically-evoked Up states. Local application of 1 mM ACh to layer 2/3 did not lead to sustained depolarisation of the resting membrane potential, but resulted in a reversible reduction of the duration of Up states (n = 2 cells) (Fig. 7A). A similar, but delayed reduction in Up state duration was observed when 10 mM ACh was applied in layer 5 (n = 1 cell) (Fig. 7B). These results suggest that local application of ACh may not be used to induce persistent activity.

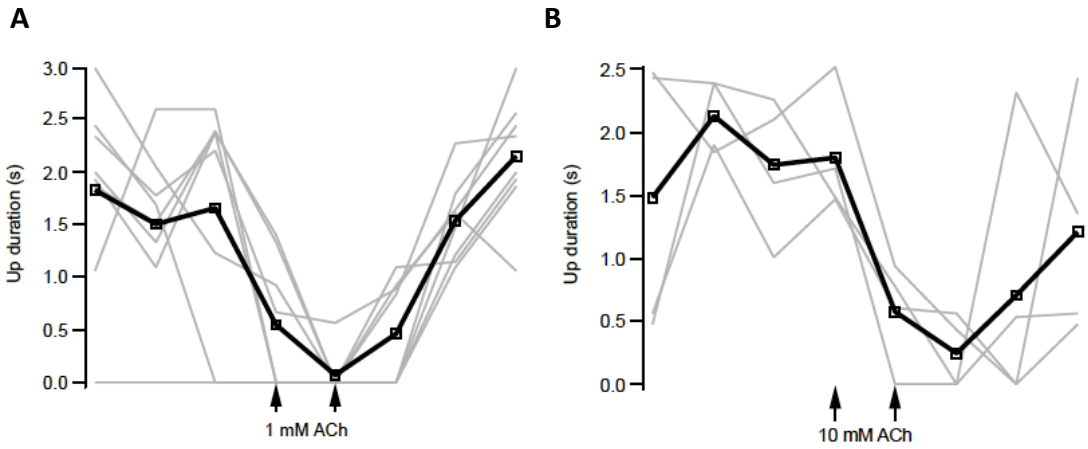


Figure 7. Local application of Acetylcholine (ACh) reversibly inhibits electrically-evoked Up states. Up states were evoked every 20 s. Graphs show mean Up state duration across trials. ACh was applied 0.5 s before each of two consecutive Up states for 1 s (arrows). (**A**) 1 mM ACh was applied in layer 2/3. (**B**) 10 mM ACh was applied in layer 5.

3.3 Discussion

3.3.1 Extracellular Ca^{2+} affects Up states in slices of barrel cortex

Experiments described in this chapter were aimed at investigating Up/Down states in the barrel cortex *in vitro*. Firstly, this involved establishing the conditions supporting generation of Up states in slices of barrel cortex. Whole-cell current-clamp recordings from layer 2/3 pyramidal cells revealed that Up states can be evoked by electrical stimulation in the corresponding layer 4 barrel. Interestingly, recordings of Up states over longer time periods suggest that increasing the concentration of extracellular Ca^{2+} may negatively modulate Up states in the barrel cortex, possibly due to a change in neuronal excitability affecting the generation and propagation of recurrent network activity. This contrasts with slices of entorhinal cortex, where it is still possible to reliably evoke Up states at an extracellular Ca^{2+} concentration of 2 mM. In this system, lower Ca^{2+} levels are associated with more spontaneous activity (Sheroziya et al., 2009). A concentration of 2 mM has already been used to study plasticity associated with Up/Down states in the entorhinal cortex *in vitro* (Bartram et al., in review). In this study, LTD was induced by pairing electrically-evoked Up states with electrically-evoked EPSPs. However, the negative effect of extracellular Ca^{2+} on Up states that I found here meant that I had to adjust the Ca^{2+} concentration to 1.6 mM to carry out similar plasticity experiments in the barrel cortex (described in Chapter 4), which require reliable generation of Up states by electrical stimulation. This is also in contrast to previous studies, where 2 mM Ca^{2+} seems to be the most commonly used concentration to study LTP and LTD mechanisms in the barrel cortex (for

example: Banerjee et al., 2014; Hardingham and Fox, 2006; Hardingham et al., 2003). Given that LTP and LTD are Ca^{2+}-dependent processes (Fox, 2002; Malenka and Bear, 2004), and that changes in Ca^{2+} also affect the resting membrane potential via changes in charge screening (Frankenhaeuser and Hodgkin, 1957), lowering the extracellular concentration may make comparisons with previous studies more difficult. However, it has also been suggested that lower extracellular ionic concentrations more closely resemble actual physiological concentrations in the brain *in situ* (Neske, 2016; Zhang et al., 1990)

3.3.2 Pharmacological manipulation of Up states *in vitro* by inhibition of glutamate receptors

It has previously been found that, in slices of visual cortex, inhibition of AMPA and NMDA receptors with CNQX and AP5 results in attenuation of spontaneous slow oscillations, suggesting that recurrent excitatory connections are necessary for the generation and propagation of Up states (Sanchez-Vives and McCormick, 2000; Shu et al., 2003). Consistent with this, I found that application of the NMDA receptor antagonist (R)-CPP completely abolished evoked Up states in slices of barrel cortex. This finding also has implications for studying plasticity mechanisms associated with Up/Down states. NMDA receptors have been shown to play a role in the induction of LTP and LTD in the barrel cortex (Banerjee et al., 2014; Hardingham and Fox, 2006; Hardingham et al., 2003; Malenka and Bear, 2004). However, studying the effects of NMDA receptors on plasticity during Up/Down states requires a different approach to bath-application of NMDA receptor antagonists due to the requirement of NMDA receptors for Up state

generation. For instance, this can be achieved by applying antagonists intracellularly via the patch pipette or using drugs which are specific to NMDA receptor subunits.

Several studies have also linked *in vitro* forms of plasticity in the cortex to the activity of metabotropic glutamate receptors (mGluRs) (Anwyl, 2009; Malenka and Bear, 2004). However, whether mGluRs have a role in generating Up/Down states has not been extensively studied. I found one publication which suggests that mGluRs may be involved in the regulation of Up state duration (Hays et al., 2011). Here, application of antagonists of mGluR1 and mGluR5 subtypes to thalamocortical slices reduced the duration of spontaneous Up states. When I applied the unspecific mGluR antagonist MCPG to slices of barrel cortex, I found a small reduction in the probability and duration of electrically-evoked Up states, which was not statistically significant. However, it is possible that the lack of significance was due to the low sample size. These data nevertheless suggest that, while mGluRs may play a role in regulating Up/Down states, they do not seem to be essential for Up state generation. Furthermore, this leaves open the possibility to investigate whether plasticity mechanisms related to Up/Down states are linked to mGluR activity.

3.3.3 Effects of Acetylcholine on Up/Down states in the barrel cortex *in vitro*

Up/Down states during slow wave sleep are suppressed by the activity of ACh-releasing subcortical nuclei which form widespread connections to the thalamus and cortex (Steriade, 2004). Release of ACh from subcortical cholinergic nuclei, which is associated with arousal and REM sleep (Jasper and Tessier, 1971; Marrosu et al., 1995), results in activation of thalamocortical and cortical neurons, making them more depolarised and bringing them closer to their firing threshold. On a larger scale, the sustained depolarisation of cortical and thalamocortical neurons is accompanied by fast oscillations between 20 and 60 Hz such as those which also occur during Up states (Steriade, 2004). The final part of this chapter was aimed at investigating whether ACh affects Up/Down states in a similar way *in vitro*. Experiments were carried out to test if ACh can provide a way to induce persistent network activity in slices of barrel cortex. Here, ACh was applied locally while Up states were evoked by electrical stimulation. I found that application of ACh to layer 2/3 or layer 5 reversibly suppressed electrically-evoked Up states. However, ACh did not bring about this effect by inducing large-scale depolarization and high-frequency activity such as that found *in vivo*. The lack of high-frequency activity is not altogether surprising, given that ACh was applied locally under conditions which do not seem to support spontaneous network activity (for instance, hardly any spontaneous Up states were observed in barrel cortex slices under the experimental conditions used here). In summary, while

preliminary data suggests that electrically-evoked Up states *in vitro* are regulated by neuromodulators, it was not possible to induce persistent activity. For this reason, effects of ACh were not explored systematically.

ACh has also been implicated in long-term plasticity in the cortex. For instance, application of ACh or stimulation of its release has been shown to result in long-lasting enhancement of responses to peripheral stimulation in the barrel cortex (Rasmusson, 2000a) and to visual stimulation in V1 (Golmayo et al., 2003). In addition, it has been found that, in V1, ACh mediates LTP at synapses *in vitro* (Bröcher et al., 1992; Kojic et al., 2001) and *in vivo* (Dringenberg et al., 2007). It would be interesting to investigate *in vitro* whether plasticity is differentially expressed during ACh application compared to during Up/Down state activity, since neuromodulatory activity has already been found to influence the polarity of spike-timing-dependent plasticity (Seol et al., 2007).

4 Plasticity associated with Up/Down states in the barrel cortex *in vitro*

4.1 Introduction

Slow oscillations have been widely implicated in memory consolidation (Diekelmann and Born, 2010; Rasch and Born, 2013; Tononi and Cirelli, 2003, 2014). However, a mechanism by which Up/Down states can mediate synaptic plasticity remains elusive. In particular, there is insufficient evidence demonstrating a direct link between on-going network activity and the plasticity of coincident synaptic inputs. A recent study conducted in slices of entorhinal cortex suggests that subthreshold inputs undergo LTD if they arrive during an Up state, but not during a Down state (Bartram et al., in review). In another study in the barrel cortex, pairing of a suprathreshold input with spontaneous Up states resulted in LTP (Kruskal et al., 2013). Both studies implicate activity during Up states in synaptic plasticity *in vitro*. Further studies are needed to establish whether these are ubiquitous mechanisms, or if they are restricted to certain synaptic pathways and experimental conditions.

Here, I investigated whether synaptic activity can be modified by pairing with Up states or Down states. Specifically, I wanted to find out whether Up states can facilitate plasticity of paired inputs. As described in the previous chapter, it is possible to evoke Up states in slices of barrel cortex by electrical stimulation in layer 4. This was reasonably reliable at a concentration of extracellular Ca^{2+} of 1.6

mM, which I went on to use for plasticity experiments described here. Being able to evoke Up states by brief current pulses under conditions which otherwise restrict spontaneous network activity allowed for precise control over the timing of Up states. It was therefore possible to pair layer 2/3 inputs with Up states or Down states by electrical stimulation and measure any changes in synaptic strength by monitoring the size of the EPSP before and after pairing. As cortical plasticity is dependent on rate, timing and cooperativity (Sjöström et al., 2001), I also examined the effect of afferent stimulation frequency on plasticity during Up/Down states by pairing EPSP trains at a 10, 20, and 40 Hz. Different stimulation frequencies have previously been shown to influence the direction of plasticity in the barrel cortex *in vivo* after chronic whisker stimulation (Han et al., 2015). In addition to EPSP pairings, I also assessed the effect of Up/Down states on suprathreshold synaptic inputs.

4.2 Results

4.2.1 Pairing of electrically-evoked Up states with EPSPs in slices of barrel cortex

After establishing conditions that allow for reliable generation of electrically-evoked Up states in slices of barrel cortex, experiments were carried out to test whether activity during an Up state is sufficient to induce plasticity of synapses which are simultaneously active. This was done by pairing excitatory postsynaptic potentials (EPSPs) resulting from stimulation of pathways within layer 2/3 with evoked Up states (Fig. 8). The size of the EPSP was measured before and after pairing to quantify any changes in synaptic strength. Before pairing, baseline recordings were made for at least 10 minutes during which the size of the EPSP remained stable. After pairing, the EPSP was again recorded for at least 20 minutes. Up states were monitored throughout the experiment with a delay of one to two seconds after each EPSP. Data presented in the previous chapter indicated that, at an exctracellular Ca^{2+} concentration of 1.6 mM, electrical stimulation was not always successful at evoking an Up state and that electrically-evoked Up states may become increasingly sparse over time. By monitoring Up states, I could ensure that Up states were sufficiently stable for pairing experiments.

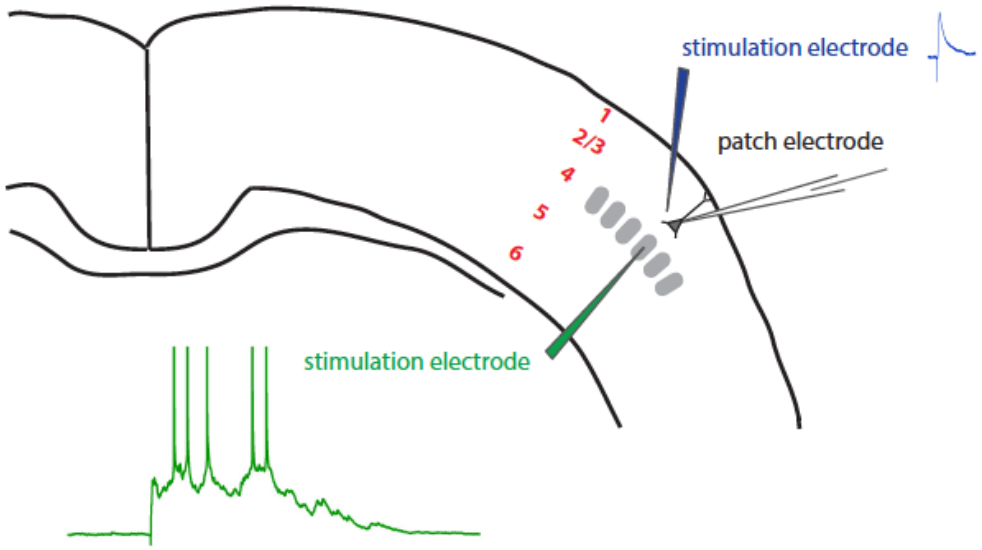
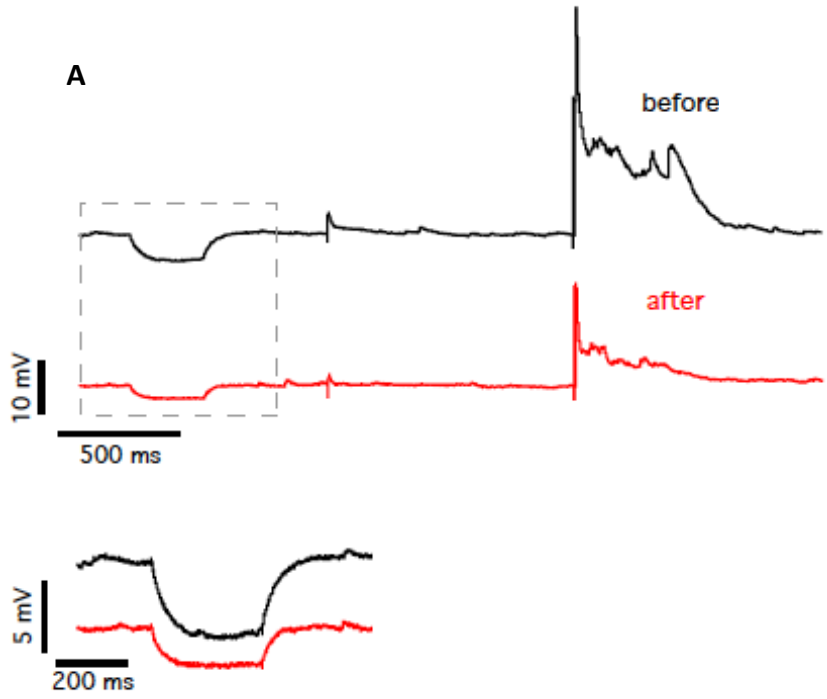


Figure 8. Setup for plasticity experiments *in vitro*. Whole-cell and perforated patch-clamp recordings were made from pyramidal neurons in layer 2/3 of acute slices of barrel cortex. Two stimulation electrodes were placed on the surface of the slice to administer brief pulses of electrical stimulation: One electrode was placed in layer 4 to evoke Up states (green), and another electrode was placed in layer 2/3, near the patched cell, to evoke EPSPs (blue).

4.2.2 Change of the input resistance over time in whole-cell mode

First, patch-clamp experiments were carried out in whole-cell mode. Electrophysiological parameters such as the input resistance (R_i) and membrane potential (V_m) were monitored throughout the recording. This was done with the intention of excluding any experiments from the analysis which showed large changes in R_i and V_m over the course of the recording. Any potential confounds which may arise due to changes unrelated to the experimental manipulation would thus be removed. I found that a large decrease of R_i occurred over time

(usually more than 50 %), accompanied by hyperpolarisation of the neuron (Fig. 9). This happened in 45 out of 61 preliminary experiments (74 %), not counting any recordings in which R_i changed at the start before pairing. R_i was calculated using Ohm's law after applying a brief hyperpolarising current step before each EPSP and measuring the resulting voltage change (Fig. 9A). Changes in R_i occurred within the first 30 minutes of recording, often during or after pairing (Fig. 9B). However, they also frequently occurred in the beginning of the experiment (Fig. 9C), suggesting that the effect was not a consequence of the pairing protocol. To ensure that the R_i measurement was not affected by any changes in access resistance (which would otherwise lead to changes in the voltage response resulting from current injection according to Ohm's law), bridge balance was applied and monitored at least at the start and end of the recording. Rare recordings with >30 % changes were excluded.



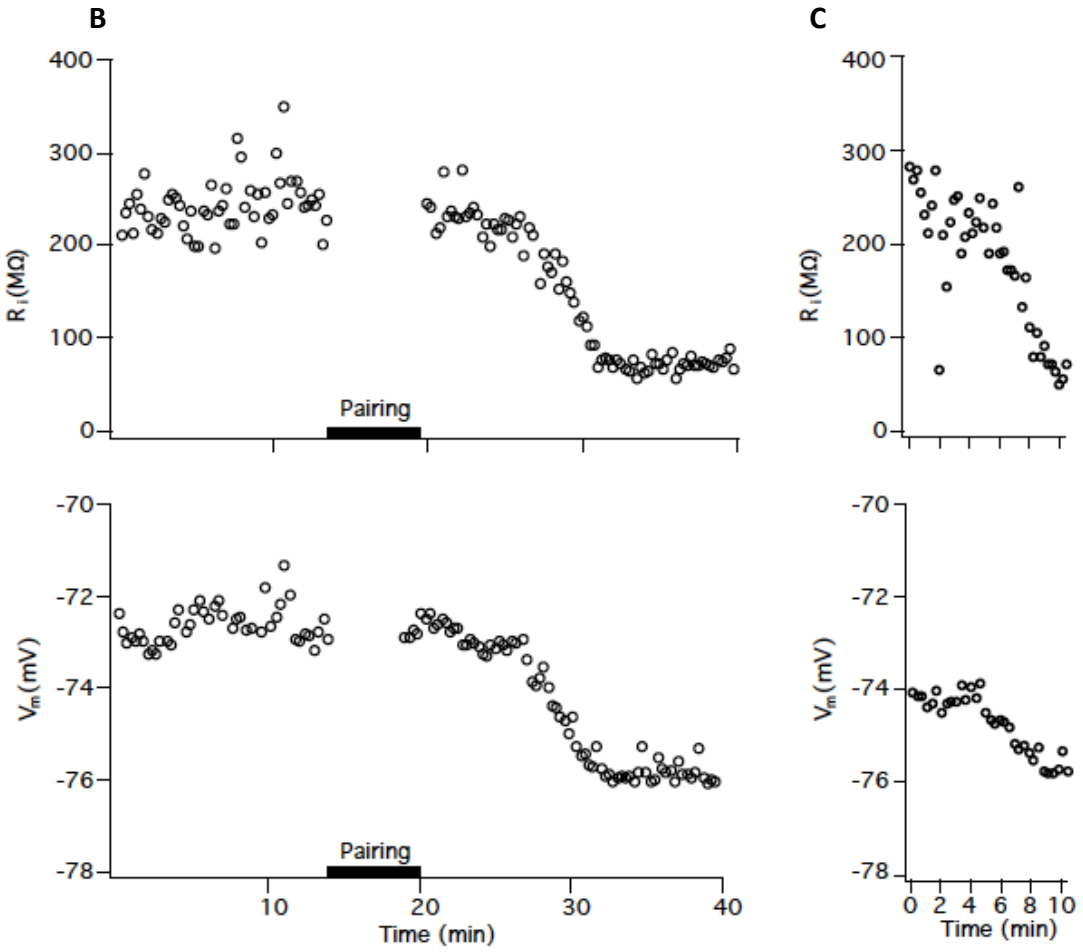


Figure 9. Changes in R_i and V_m over time during whole-cell patch-clamp. (**A**) A 20 pA hyperpolarising current step lasting 300 ms was applied in the beginning of each recording sweep. The input resistance (R_i) of the patched neuron was calculated by dividing the resulting voltage change by the current step according to Ohm's law. (**B, C**) R_i and membrane potential (V_m) plotted over time, each circle representing measurements from one recording sweep. (**B**) Example experiment in which R_i and V_m changed after pairing, approximately 25 minutes after the start of the recording. (**C**)

Example experiment showing a change in R_i and V_m at the beginning of the recording, before any pairing had occurred.

The change in R_i was observed particularly at low access resistances (less than 50 MΩ) such as those normally required for whole-cell recordings, implying that it may have been due to the dilution of the cytosol by the internal solution in the patch pipette. To test this, I went on to establish a suitable protocol for long-term perforated patch-clamp recordings. Indeed, no changes were found in R_i or V_m over long time periods using this method. All plasticity experiments described in the next section were carried out in the perforated patch configuration.

4.2.3 Pairing of subthreshold inputs with Up states or Down states

To determine whether repeated activation of subthreshold inputs during Up states can induce synaptic plasticity, trains of EPSPs were applied at different frequencies (10, 20, and 40 Hz) during evoked Up states (Fig. 10A). Complementary experiments were carried out in which EPSPs were paired with Down states to test whether any changes in synaptic strength are specific to the phase of the slow wave (Fig. 10B). A train of 10 EPSPs was applied during each recording sweep, which allowed for a maximum number of EPSPs to coincide with Up states, even at lower interstimulus intervals such as during 10 Hz EPSP trains. Twenty such pairings were carried out in each experiment, amounting to a total of 200 EPSPs applied during each pairing session. This was to achieve a high number of Up state pairings despite the probability of generating Up states by

electrical stimulation in the barrel cortex being less than 1 (see Chapter 3). Up state duration and probability were measured post-hoc for each experiment (see Appendix). While there appeared to be some differences in the average Up state duration and probability for each condition, all experiments used in the analysis had Up state probabilities above 0.

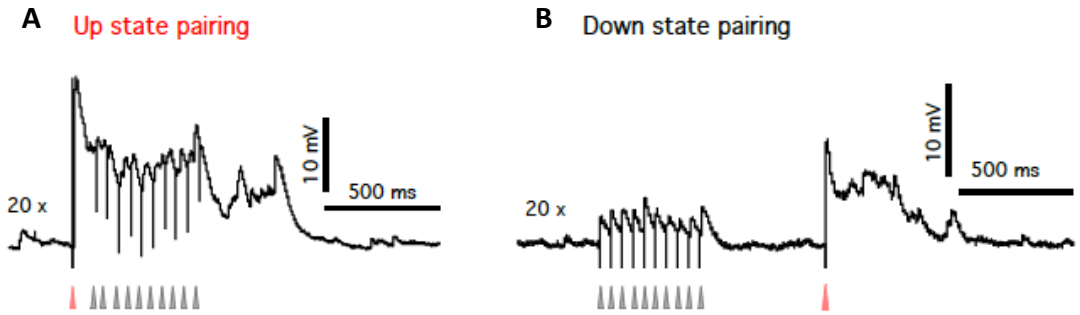
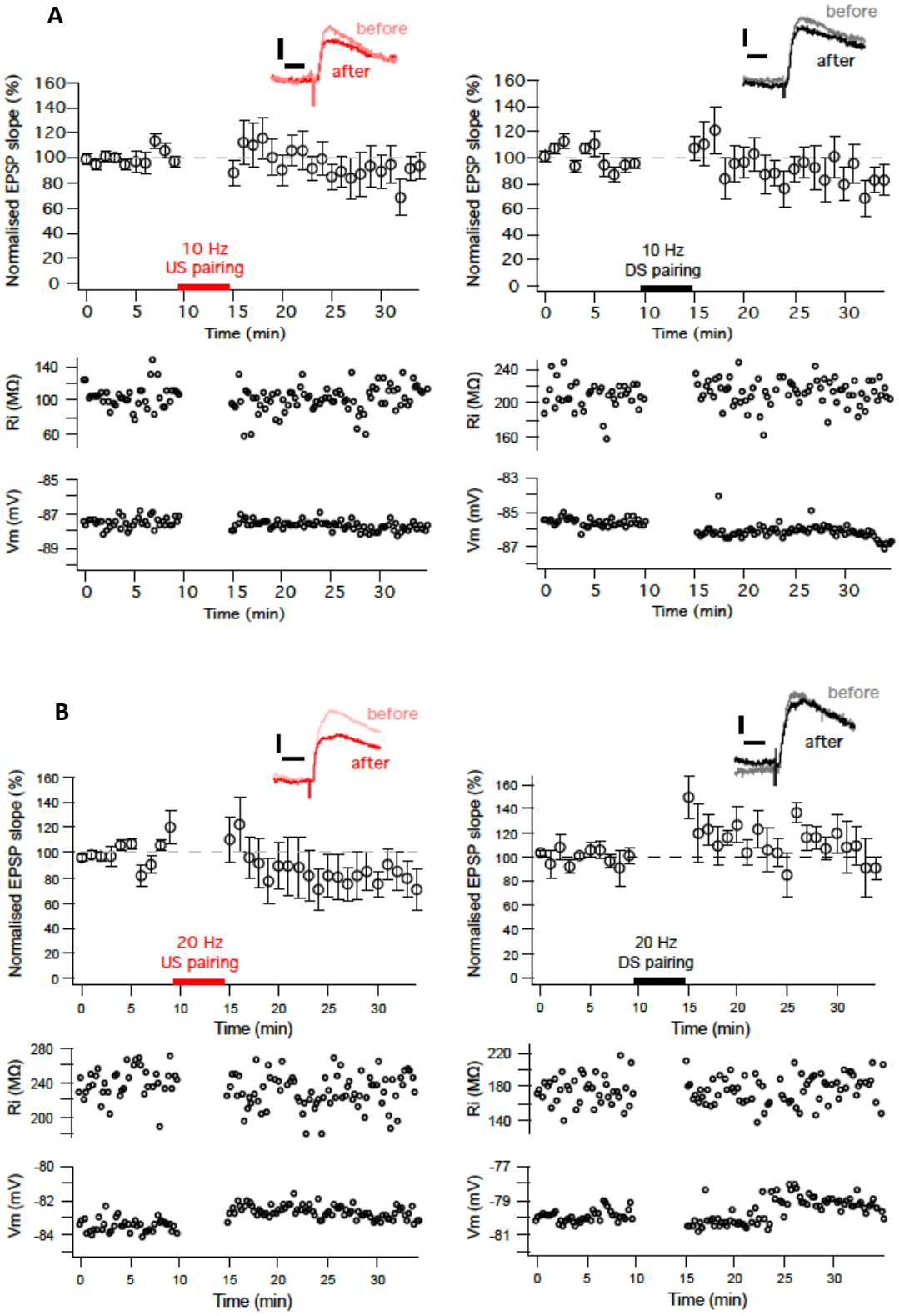


Figure 10. Up state versus Down state pairings with EPSPs. In both conditions, a train of 10 EPSPs was applied during each recording sweep. This was repeated 20 times for each experiment. (**A**) Up state pairings were achieved by applying a brief current pulse to layer 4 to evoke an Up state (red arrow), followed with a delay of 100 ms by 10 brief current pulses in layer 2/3 to evoke consecutive EPSPs (grey arrows). (**B**) Down state pairings were achieved by applying current pulses in layer 2/3 to evoke 10 consecutive EPSPs (grey arrows), followed by stimulation in layer 4 to evoke an Up state 2-3 s after the first EPSP (red arrow).

At an EPSP frequency of 10 Hz, the normalised EPSP slope was reduced to 74.93 ± 12.49 % (n = 6 slices from 6 mice) in the last 5 minutes of the recording. The EPSP slope was also very slightly reduced after pairings with Down states, in this case to 84.01 ± 15.42 % (n = 5 slices from 5 mice) (Fig. 11A, D). However, normalised EPSP slopes were not significantly different compared to pre-pairing baseline

($t(5) = -2.01$, $p = 0.101$ for Up state pairings, $t(4) = -1.04$, $p = 0.358$ for Down state pairings, one-sample two-tailed *t*-tests). Unsurprisingly, no significant difference was found in the normalised EPSP slope between pairing conditions ($t(9) = -0.46$, $p = 0.654$, two-tailed independent *t*-test). At an EPSP frequency of 20 Hz, a marginal reduction in the normalised EPSP slope to 84.53 ± 12.78 % ($n = 5$ slices from 5 mice) was found after Up state pairings, similar to the 10 Hz condition, which was again not significant compared to baseline ($t(4) = -1.21$, $p = 0.293$, two-tailed one-sample *t*-test). Pairings of EPSPs at 20 Hz with Down states did not seem to result in synaptic plasticity. Here, the normalised EPSP slope was 106.88 ± 15.57 % ($n = 5$ slices from 5 mice), which was not significantly different from the baseline ($t(4) = 0.44$, $p = 0.681$, two-tailed one-sample *t*-test) (Fig. 11B, E). There was no significant difference in the normalised EPSP slope after Up state and Down state pairings ($t(8) = -1.11$, $p = 0.300$, two-tailed independent *t*-test). Finally, pairings of 40 Hz EPSP trains led to slightly stronger depression. The normalised EPSP slope was reduced to 69.72 ± 15.53 % ($n = 5$ slices from 5 mice) and 76.86 ± 7.68 % ($n = 5$ slices from 5 mice), after Up state and Down state pairings, respectively (Fig. 11C, F). However, this was only significant from baseline in a two-tailed one-sample t-test for Down state pairings ($t(4) = -3.01$, $p = 0.039$), but not Up state pairings ($t(4) = -1.95$, $p = 0.123$). Again, no significant difference was found in the normalised EPSP slope between the two pairing conditions ($t(8) = -0.41$, $p = 0.691$, two-tailed independent *t*-test). Post-hoc calculations of statistical power revealed that sample sizes were not enough to achieve statistical power ($1 - \beta$) at the 0.8 level (see table 1).


A
before
after
Normalised EPSP slope (%)
10 Hz
US pairing
Time (min)
Ri (MΩ)
Vm (mV)
before
after
10 Hz
DS pairing
Time (min)
B
before
after
20 Hz
US pairing
Time (min)
before
after
20 Hz
DS pairing
Time (min)

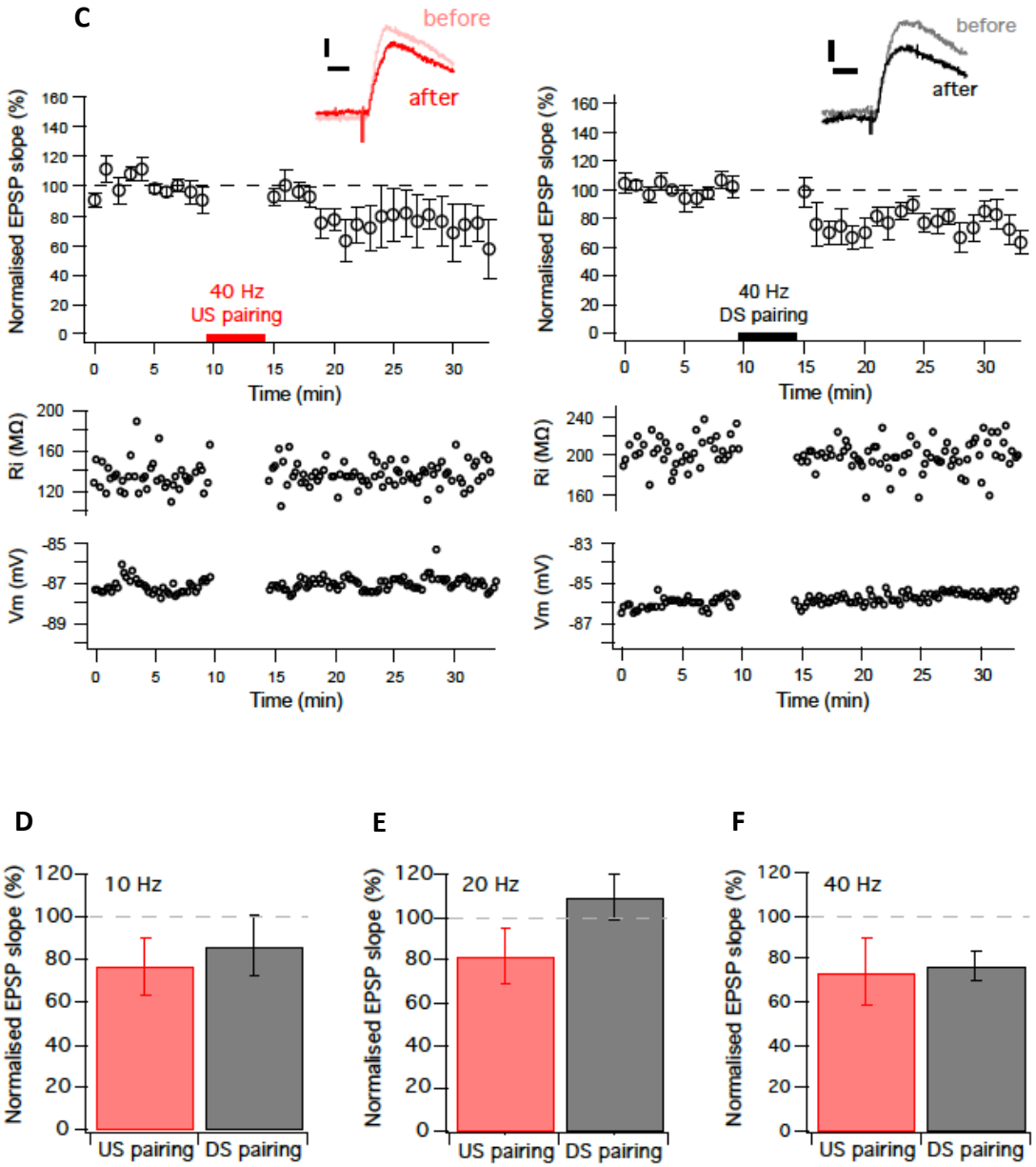


Figure 11. Plasticity after pairing of EPSPs at different frequencies with Up states or Down states. (**A-C**) EPSP slope over time, normalised to pre-pairing baseline and averaged across experiments. Error bars are SEM. R_i and V_m measurements from an example recording are shown below. Traces show example EPSPs before and after pairing, with scale bars showing 10 ms and 1 mV. EPSP trains were applied at 10 Hz (**A**), 20 Hz (**B**), and 40 Hz (**C**) and paired with Up states (red) or Down states (black). (**D-F**) Comparison between the normalised EPSP slope after Up state and Down state pairings,

averaged across experiments over the last 5 min of recording. Error bars are SEM. EPSP trains were applied at 10 Hz (**D**), 20 Hz (**E**), and 40 Hz (**F**).

Pairing frequency	Effect size d	Achieved power ($1 - \beta$)	Required total sample size to achieve $1 - \beta = 0.8$
10 Hz	0.279	0.070	404
20 Hz	0.705	0.166	66
40 Hz	0.275	0.067	418

Table 1. Results from statistical power tests between Up state and Down state pairing groups. The α-level was set at 0.05.

Up states were also evoked in Down state pairing experiments, albeit with a short delay of 2-3 seconds after the first EPSP, to ensure that no experiments were included in the analysis which did not show any Up state activity. To investigate the possibility that Up states may have influenced synaptic strength after pairing even without coinciding with synaptic activity, synaptic strength after pairing was plotted against the probability and duration of electrically-evoked Up states for each experiment (Fig. 12). If synaptic depression was influenced by Up state activity alone, I would expect more depression in experiments with a higher Up state duration and probability, as they were accompanied by more Up state activity overall. However, no significant correlation was found between the normalised EPSP slope and Up state probability and duration at 10 Hz (r = 0.085, p = 0.803 and r = 0.354, p = 0.286), 20 Hz (r = -0.423, p = 0.223 and r = 0.295, p = 0.409), and 40 Hz (r = -0.148, p = 0.684 and r = 0.205, p = 0.570) EPSP pairing frequencies. This does not exclude the possibility that depression relates to

spontaneous activation of the stimulated pathway during Up states, which cannot be assessed here.

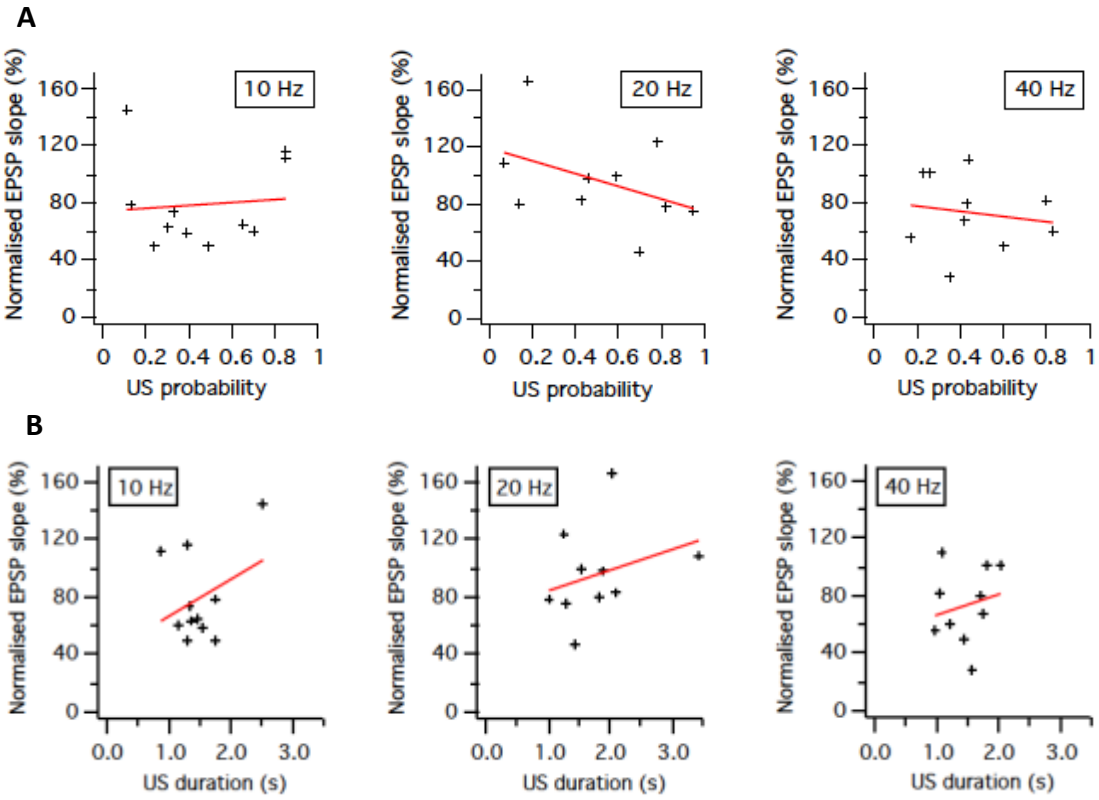


Figure 12. Relationship between synaptic depression and Up state properties. No significant correlation between the normalised EPSP slope in the last 5 min of the experiment and Up state probability (**A**) and duration (**B**) was found after pairings at 10 Hz, 20 Hz, and 40 Hz. Up state and Down state pairing experiments were pooled for each correlation.

4.2.4 Pairing of suprathreshold inputs with Up states or Down states

Experiments were carried out to investigate whether standard spike timing-dependent plasticity (STDP) may be modulated differently by Up states and Down

states. Standard STDP protocols to induce LTD or LTP consist of some form of synaptic stimulation to evoke EPSPs in the postsynaptic neuron, which is preceded or followed by somatic current injection to induce an action potential, respectively (Feldman, 2000; Markram et al., 1997). For vertical inputs to layer 2/3 of the barrel cortex, a time window of 10 ms between an EPSP and subsequent action potential has been found to induce LTP (Feldman, 2000). Such an STDP protocol was paired with Up states or Down states by applying a train of EPSPs as described before, but in addition injecting a brief current pulse into the postsynaptic neuron via the patch pipette to produce a single spike 10 ms after each EPSP (Fig. 13).

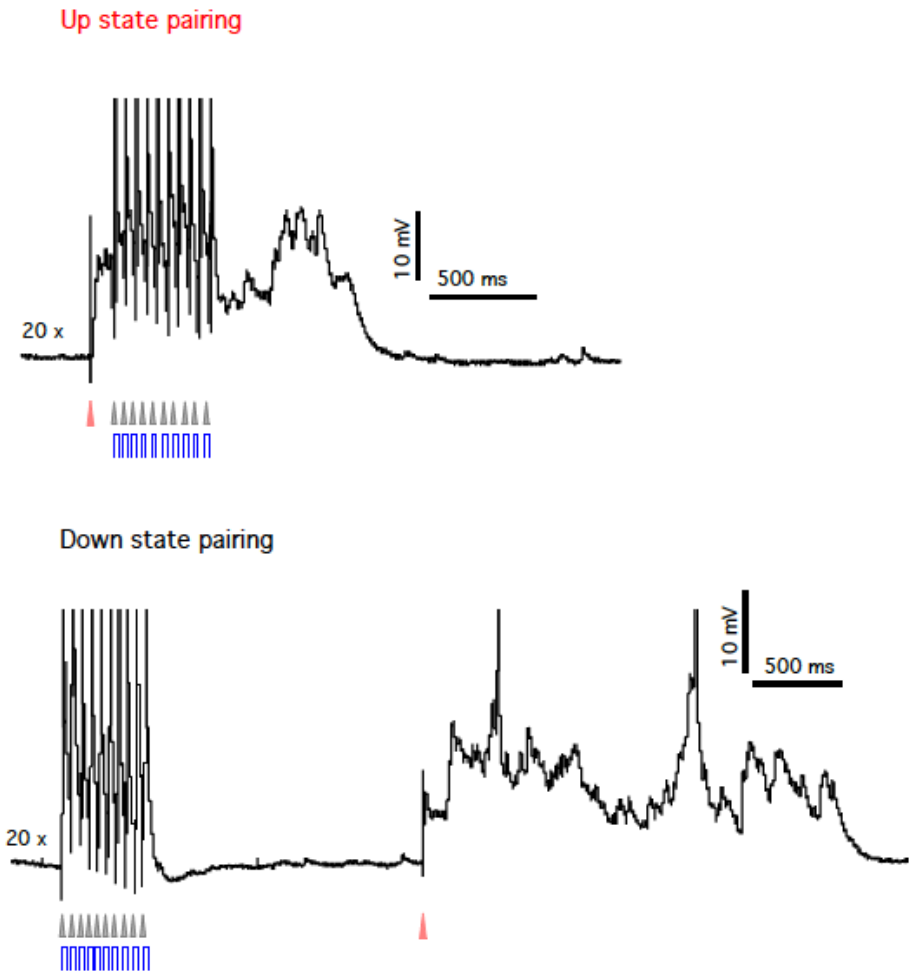


Figure 13. Suprathreshold pairings with Up states versus Down states. Suprathreshold pairings were achieved by applying a 20 Hz train of 10 EPSPs per recording sweep in layer 2/3 as described before, with the addition that current was injected into the postsynaptic cell to make it fire a single action potential after each EPSP. Δt was 10 ms between electrical stimulation and current injection. Again, this was repeated 20 times. (**A**) For Up state pairings, EPSPs (grey arrows) and current injections (blue) were preceded 100 ms by a current pulse in layer 4 to evoke an Up state (red arrow). (**B**) For Down state pairings, an Up state was evoked by stimulation in layer 4 (red arrow) 3 s after the first EPSP of the train of EPSPs (grey arrow) and current injections (blue).

I found that, after suprathreshold pairings with Up states, the size of the EPSP was potentiated, suggesting a reversal of the sign of plasticity compared to subthreshold pairings. However, potentiation was also found after suprathreshold pairings with Down states (Fig. 14). The normalised EPSP slopes were 144.91 $\pm$ 20.06 % (n = 5 slices from 5 mice) and 151.76 $\pm$ 28.97 % (n = 5 slices from 5 mice), respectively, at the end of the experiment. However, this potentiation was not significantly different from baseline in a two-tailed one-sample t-test for Up state pairings ($t(4) = 2.24$, $p = 0.089$) or Down state pairings ($t(4) = 1.79$, $p = 0.149$). No significant difference was found in the normalised EPSP slope between the two pairing conditions ($t(8) = -0.19$, $p = 0.852$, two-tailed independent t-test).

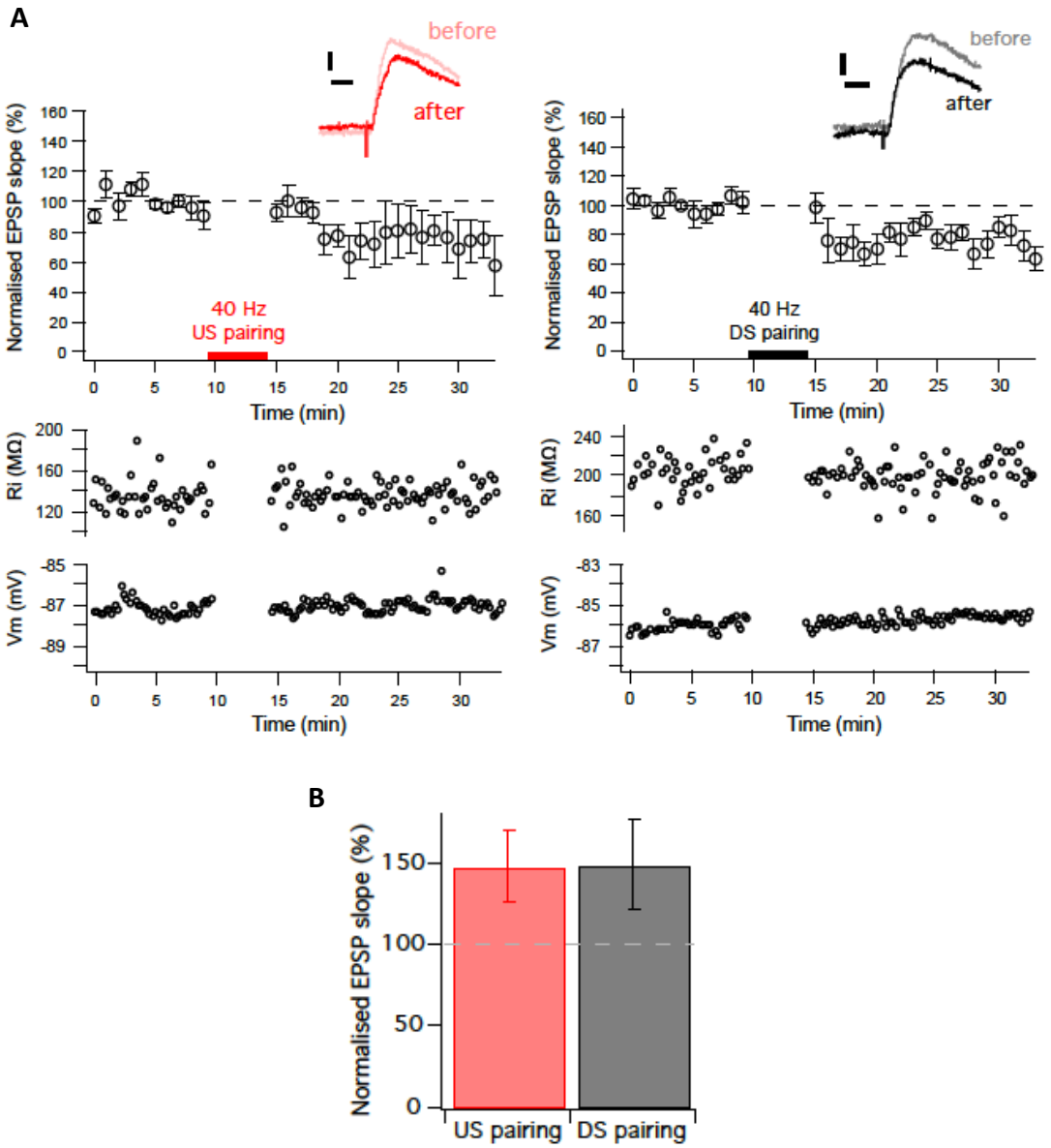


Figure 14. Plasticity after pairing of suprathreshold synaptic inputs with Up states and Down states. (**A**) EPSP slope, normalised to pre-pairing baseline and averaged across experiments. Error bars are SEM. R_i and V_m measurements from an example recording are shown below. Traces show example EPSPs before and after pairing, with scale bars showing 10 ms and 1 mV. EPSP trains and somatic current injections were paired with Up states (red) or Down states (black). (**B**) Comparison between the normalised EPSP slope after Up state and Down state pairings, averaged across experiments over the last 5 min of recording. Error bars are SEM.

4.3 Discussion

4.3.1 Practical implications of the experimental protocol

First recordings of pyramidal neurons in layer 2/3 of the barrel cortex were made in the whole-cell configuration. However, I consistently found a dramatic decrease in the input resistance and concomitant hyperpolarisation of the patched cell, particularly at low access resistances. Furthermore, long-term perforated patch-clamp recordings were not accompanied by any changes in R_i and V_m, suggesting that a dilution of intracellular factors by the pipette solution may have been responsible. Curiously, the phenomenon described here has not been reported before, and indeed the internal solution was made according to a standard recipe which has been widely used. Due to potential implications of changes to normal cellular and electrophysiological properties of the neuron on plasticity measurements, all experiments analysed here were carried out using the perforated patch-clamp method. However, there are some drawbacks to this technique, such as the long perforation time and occasional spontaneous rupture of the membrane patch. More importantly, it does not allow for intracellular application of drugs via the patch pipette, as is often done in pharmacological studies of plasticity mechanisms (for example: Bender et al., 2006; Hardingham et al., 2008; Rodríguez-Moreno et al., 2011).

4.3.2 No difference in plasticity after pairing of inputs with Up states or Down states

Experiments were carried out in the barrel cortex *in vitro* to investigate the hypothesis that synaptic plasticity can be modulated by underlying network activity during Up/Down states. Specifically, it has been proposed that pairing synaptic activity with Up states, but not Down states, induces plasticity of the paired pathway (Kruskal et al., 2013, Bartram et al., in review). Here, I observed a small amount of depression of subthreshold inputs when they were paired with Up states, with a trend towards stronger depression after Up state compared to Down state pairings at all EPSP frequencies. However, there was no significant difference in the size of the EPSP between the two pairing paradigms. There was also no significant difference after suprathreshold pairings, which induced potentiation after both Up state and Down state pairings. Similar to results from subthreshold pairings, this finding suggests that Up states are no more likely than Down states to facilitate plasticity of paired inputs. It is somewhat surprising that network state did not have a strong effect on plasticity, as there are many reports on the effect of membrane depolarisation on plasticity (Feldman, 2000; Sjöström and Häusser, 2006; Sjöström et al., 2004). Nevertheless, my findings do not necessarily imply that Up states do not play a role in plasticity in the barrel cortex, and the discrepancy with other studies may have been the result of other factors. Firstly, there are notable differences between simple depolarisation and Up state activity. In contrast to simple depolarisation, an Up state is maintained by both excitatory and inhibitory activity (Compte et al., 2003; Sanchez-Vives and McCormick, 2000; Timofeev et al., 2000), which is also associated with differences

in the responsiveness to stimuli applied during Up states compared to Down states (Haider et al., 2007; Hasenstaub et al., 2007; Petersen et al., 2003c; Sachdev et al., 2004). For example, it was found that responses to stimuli are diminished during Up states in the barrel cortex, while they are enhanced when a similar level of depolarisation is applied during a Down state (Hasenstaub et al., 2007). Another aspect of note is that, in the model system used here, electrically-evoked Up states were mostly subthreshold and occurred at probabilities of less than 1 (see Appendix). This may have been due to reduced excitability of neurons in barrel cortex slices compared to other systems, such as slices of other brain areas and *in vivo* preparations. For instance, it is possible to evoke suprathreshold Up states in slices of entorhinal cortex at an extracellular Ca^{2+} concentration of 2 mM (Mann et al., 2009). Spontaneous spiking activity during Up states may be conducive to strong synaptic plasticity by spike timing-dependent mechanisms (Feldman, 2000; Markram et al., 1997). Furthermore, the lower Up state probability in my experiments meant that the number of successful pairings was less than 200, which may have simply not been enough to produce a significant effect. Taken together, I propose that it would be preferable to study synaptic plasticity during Up/Down state activity in a different model system which displays much stronger network activity. In the barrel cortex, this can be done *in vivo*, where spontaneous slow oscillations occur naturally during sleep and anaesthesia.

5 Plasticity associated with Up/Down states in the barrel cortex *in vivo*

5.1 Introduction

Up/Down states occur not only during sleep, but also under anaesthesia (Chauvette et al., 2011). Depending on the anaesthetic, they may vary in their duration, amplitude and frequency (Steriade et al., 1993a). Up/Down states are synchronised over large areas of the cortex, such as the barrel cortex (Amzica and Steriade, 1995; Erchova et al., 2002). Testing the hypothesis that Up/Down states differentially affect plasticity in the cortex *in vivo* therefore requires either interfering with or detecting spontaneous activity in a way that allows for control over the timing of plasticity protocols with respect to Up/Down states.

A previous study suggests that it may be possible to evoke or inhibit Up states in the barrel cortex of anaesthetised mice using optogenetics (Beltramo et al., 2013). Inhibiting Up states *in vivo* would make it possible to investigate plasticity paradigms in anaesthetised mice and indeed experience-dependent plasticity in sleeping mice while controlling for the underlying network activity. To test whether it is possible to inhibit Up states using optogenetics, I injected virus containing the optogenetic silencer Archaerhodopsin T3 (ArchT3) into the barrel cortex of mice. ArchT3 was under the control of the CamKII promotor, resulting in expression in pyramidal neurons of all layers over a large area of the barrel cortex.

The effects of ArchT3 silencing were assessed on electrically-evoked Up states *in vitro* and on spontaneous Up states *in vivo* in anaesthetised mice.

Alternatively, the hypothesis that Up/Down states differentially affect plasticity can be investigated in anaesthetised mice by detecting spontaneous Up/Down states and, upon detection, initiate a synaptic stimulation paradigm to induce plasticity. In one study, Up states were detected in the barrel cortex of anaesthetised mice as bursts of spikes in real time. Here, paired whisker stimulation induced changes in connectivity between whiskers only when stimulation was applied during Up states, but not during Down states (Erchova and Diamond, 2004). Plasticity has also been found in the barrel cortex after periods of chronic stimulation of a single whisker, which induced either potentiation or depression of the response to the stimulated whisker, depending on experimental conditions such as stimulation frequency (Han et al., 2015; Mégevand et al., 2009; Quairiaux et al., 2007). However, whether this type of long-term plasticity is differentially modulated by Up states and Down states has not been determined. I investigated this possibility by pairing deflections of a single whisker with either Up states or Down states over a period of 30 minutes and measuring plasticity as the difference in the size of the response to that whisker before and after pairing. Here, Up/Down states were detected in real time by a mechanism involving crossings of a set voltage threshold during Up states. Initial extracellular recordings were made with an 8 x 8 matrix electrode array, which was inserted into layer 2/3 and covered a large area of the barrel cortex. Using this array, effects of pairing were assessed on principal and surrounding barrels.

In another set of experiments, plasticity after Up state pairing was investigated across layers using a linear electrode probe.

5.2 Results

5.2.1 Optogenetic inhibition of Up states *in vitro*, but not *in vivo*

To investigate whether Up/Down states can be controlled by optogenetics, mice were injected with a virus containing the optogenetic silencer ArchT3 into the barrel cortex. ArchT3 was under the control of the CamKII promoter, resulting in expression across all cortical layers, but restricted to pyramidal neurons (Fig. 15A, Fig. 16A). For each mouse, injections were made at three sites around the stereotaxic coordinates of the D1 barrel to cover a large area of the barrel cortex.

First, I tested whether optogenetic inhibition was feasible *in vitro*. For this, mice were injected at P0 and used for whole-cell current-clamp experiments at P14-20. Pyramidal cells were patched in layer 2/3, while optical stimulation was targeted to the whole slice via epi-illumination using an LED light source. I found that pulses of green light suppressed pyramidal cell spiking (Fig. 15B), confirming that optical stimulation was effective at inhibiting ArchT3-expressing neurons. In addition, brief light pulses were sufficient to achieve complete inhibition of electrically-evoked Up states (Fig. 15C, D). Here, Up states were evoked every 15 seconds, while optical stimulation was applied during every second stimulation. However, the probability of generating any Up states at all was much lower in slices from virus-injected mice compared to slices from un-injected mice, suggesting that virus expression had a negative effect on network activity. This may have been due to cellular damage induced by the virus, but was not explored

systematically. Slices from only 2 of a total of 12 mice displayed Up states, but the Up state-inhibiting effect was observed in both these mice.

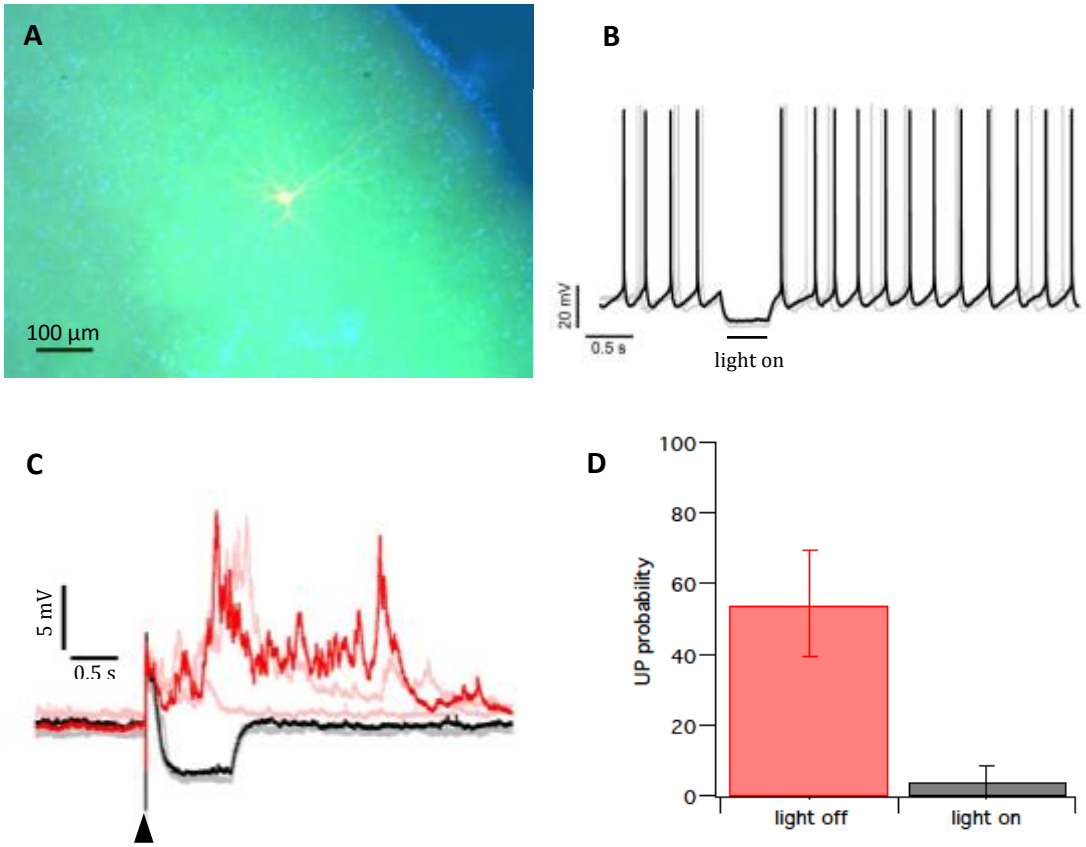


Figure 15. Optogenetic inhibition of Up states *in vitro*. (**A**) Example slice, showing patched cell in layer 2/3 (red) and ArchT3 expression (green) across layers. Cell bodies were stained with DAPI (blue). Mice were injected at P0 and recordings were made at P14-20. (**B**) Example current-clamp recording of a layer 2/3 pyramidal neuron, held above action potential threshold. Activation of ArchT3 by 500 ms light pulses inhibited spiking of the patched neuron. (**C**) Up states were evoked every 15 s by electrical stimulation in layer 4 (arrow) when the light was off (red), but not when the light was on (black). (**D**) Mean Up state probability with (black) and without (red) light stimulation.

I then went on to test whether it is also possible to suppress Up states *in vivo* by optogenetic silencing. For this, virus containing ArchT3 was injected into the barrel cortex of adolescent mice, resulting in expression across a large area (Fig. 16A). Three weeks later, local field potential (LFP) recordings of spontaneous Up states were made from layer 2/3 of the barrel cortex under medetomidine and isoflurane anaesthesia using a 4-shank 32-channel electrode probe. Optical stimulation was applied via an optic fibre connected to a green LED. In contrast to results obtained *in vitro*, preliminary experiments indicate that light stimulation did not lead to suppression of Up states *in vivo* (Fig. 16B). This was true both when the optic fibre was placed on the cortical surface and when it was inserted into deeper layers via a cannula.

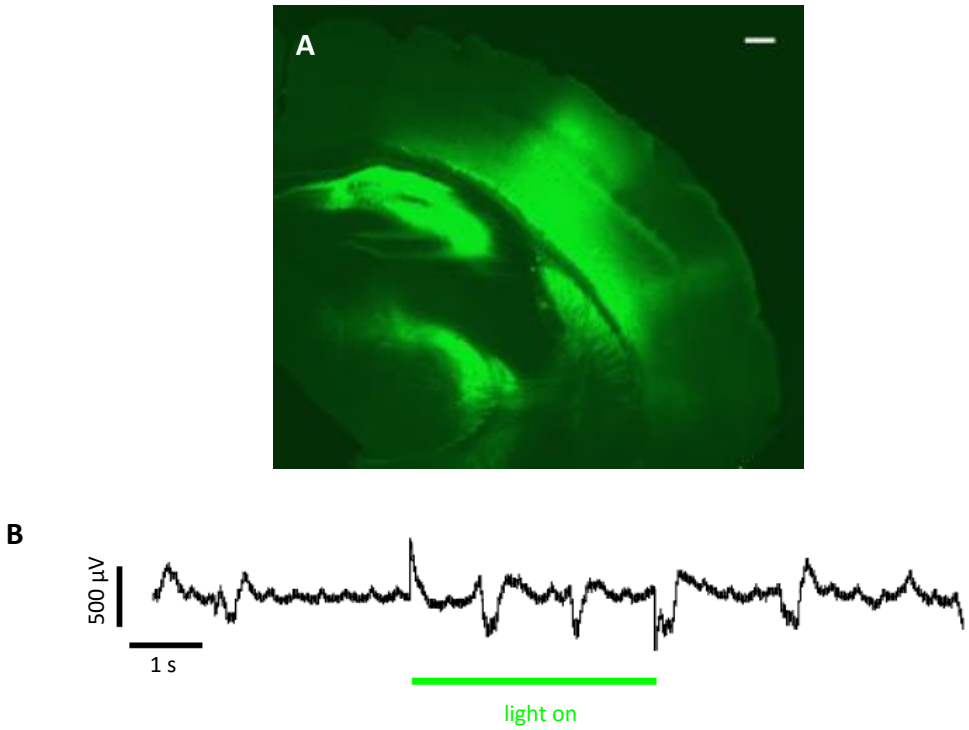


Figure 16. Optogenetic inhibition did not suppress Up states *in vivo*. (**A**) Coronal section showing ArchT3 expression in the barrel cortex (green). Mice were injected at 4-6 weeks and recordings were obtained 3 weeks later. Scale bar shows 200 μm. (**B**) Example LFP trace recorded in layer 2/3. Optical stimulation did not suppress Up states, shown here as negative voltage deflections. Stimulation artefacts are truncated.

5.2.2 Detection of Up states and whisker stimulation in real time

To achieve pairings of somatosensory inputs with spontaneous Up states or Down states *in vivo*, a closed-loop feedback system was developed, consisting of an Intan RHD2000 evaluation system connected to an Arduino board. This system made it possible to perform electrophysiological recordings coupled with detection of Up/Down states in real time and initiation of a train of whisker deflections upon detection (Fig. 17). Recordings were made under medetomidine and isoflurane to maintain a stable anaesthesia, which produced slow oscillations with clear Up/Down state transitions. LFP and multiunit activity (MUA) were collected from the somatosensory barrel cortex by extracellular electrodes. Here, a single channel was selected for Up state detection, which was representative due to Up/Down state activity being synchronised across the cortex (Amzica and Steriade, 1995; Erchova et al., 2002).

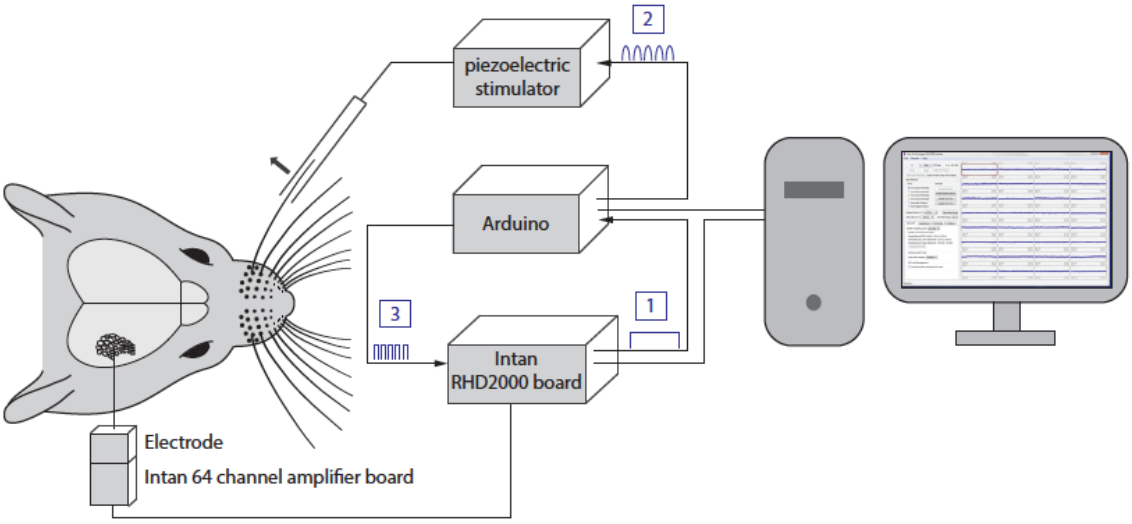


Figure 17. Setup for plasticity experiments *in vivo*. Recordings were made from the barrel cortex using an Intan RHD2000 evaluation system, connected to the recording electrode via a 64-channel amplifier board. The Intan board was controlled by open-source RHD2000 interface software. (**1**) A voltage threshold was set for the LFP from a selected electrode channel based on visual inspection at approximately one-third of the maximum Up state amplitude. Whenever the LFP crossed this voltage threshold during an Up state, a digital pulse was sent from the Intan board to an Arduino board. (**2**) A train of 5 sine wave pulses at 10 Hz was delivered by the Arduino board to a piezoelectric stimulator. Each pulse initiated the deflection of a single whisker inserted into a narrow tube attached to a piezoelectric wafer. (**3**) With each whisker stimulus, digital pulses were sent from the Arduino board back to the Intan board and recorded as a time stamp.

Up/Down states were detected by the LFP of the selected channel crossing a voltage threshold during an Up state (Fig. 18). In the case of Up state pairings, crossing of the threshold instructed the Arduino board to send a train of stimuli to a piezoelectric stimulator to deflect a single whisker. In the case of Down state pairings, a train of whisker stimuli was initiated when the LFP remained below threshold for 200 ms. Each train of stimuli consisted of 5 deflections delivered at

10 Hz. Stimulation frequencies of 8-10 Hz have previously been shown to induce plasticity after periods of continuous whisker stimulation (Han et al., 2015; Knott et al., 2002; Mégevand et al., 2009; Quairiaux et al., 2007), and they are within the range of naturally occurring frequencies of active whisking. The accuracy of Up/Down state detection and pairing protocols were assessed in sham experiments, during which Arduino board output was uncoupled from the piezoelectric stimulator. False positive rates for Up state pairings were on average 8.5 % for 64-channel recordings and 4.6 % for 32-channel recordings, while the average false positive rate for Down state pairings was 33.2 % (see Appendix). The higher false positive rate for Down state pairings was due to unavoidable overlap of whisker deflections with subsequent Up states, rather than misdetection.

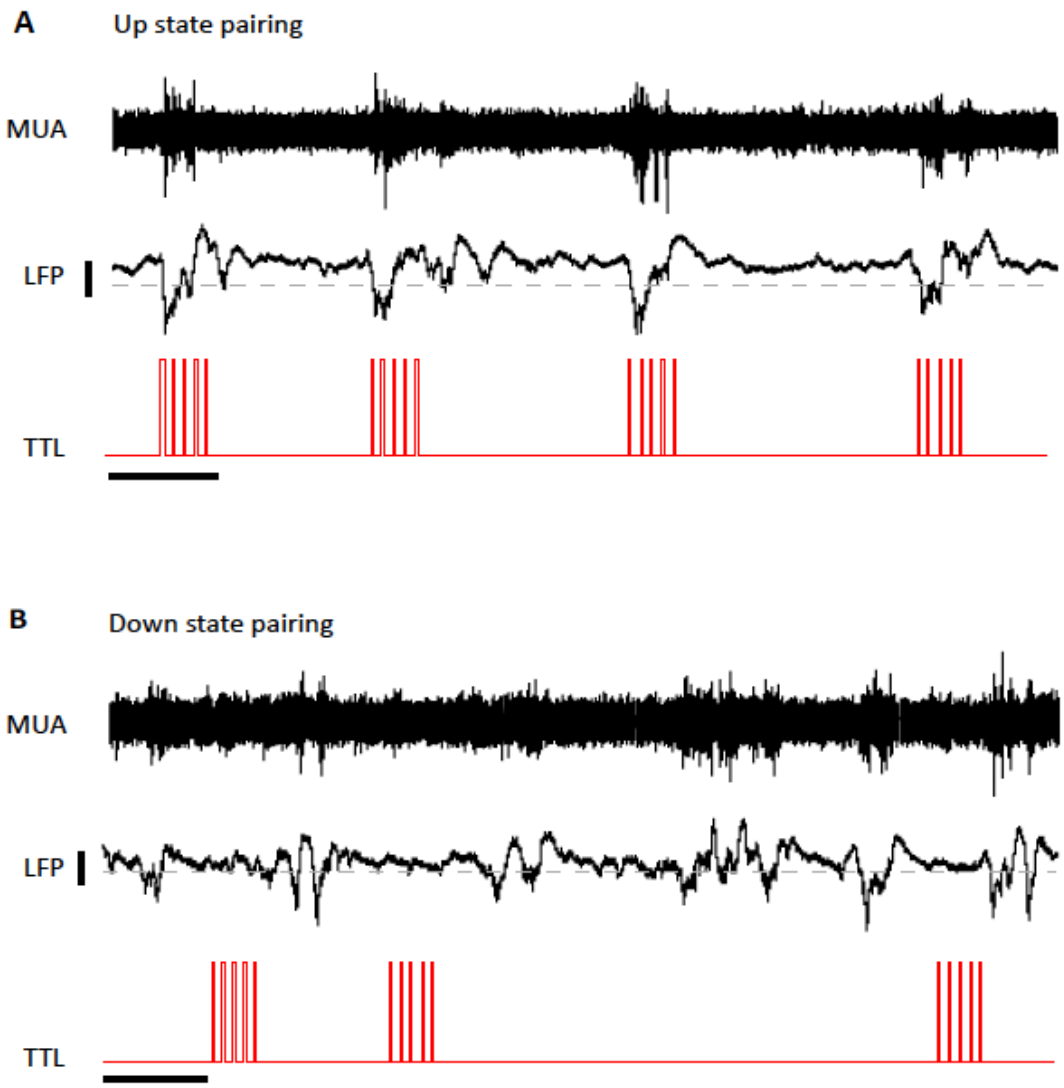


Figure 18. Up/Down state detection and sham pairing. Dashed grey lines indicate the voltage threshold used for Up state detection. It was set at approximately one-third of the maximum Up state amplitude. The MUA and LFP traces are shown in black above the recording of digital pulses time-locked to whisker deflections. Each Up state was associated with a negative deflection of the LFP and associated spiking activity. Horizontal scale bars display 1 s. Vertical scale bars display 200 µV. (**A**) Spontaneous Up states, which caused negative deflections of the LFP crossing the voltage threshold, resulted in a train of 5 whisker stimuli given by the Arduino board. (**B**) Down states were detected when the LFP remained below threshold for 200 ms.

5.2.3 Experimental design

Each experiment consisted of multiple 5 minute sessions of baseline whisker stimulation once every 5 seconds without Up/Down state detection (Fig. 19). These baseline recordings were used to measure the average size of the sensory response over time before and after pairing to determine the amount of plasticity induced by the pairing. This was done by calculating the average LFP response and spike-time histogram (STH) for each 5-minute recording period. In some Up state pairing experiments, responses to deflection of a second, unpaired whisker were measured in parallel to determine whether any effects induced by the pairing were pathway-specific. A total pairing duration of 30 minutes was used in all experiments. This was based on findings from previous studies of chronic whisker stimulation, in which plasticity was observed after 10 min to 1 h (Erchova and Diamond, 2004; Han et al., 2015; Mégevand et al., 2009). The total number of whisker deflections delivered during 30 minutes was similar for Up state and Down state pairing experiments (see Appendix).

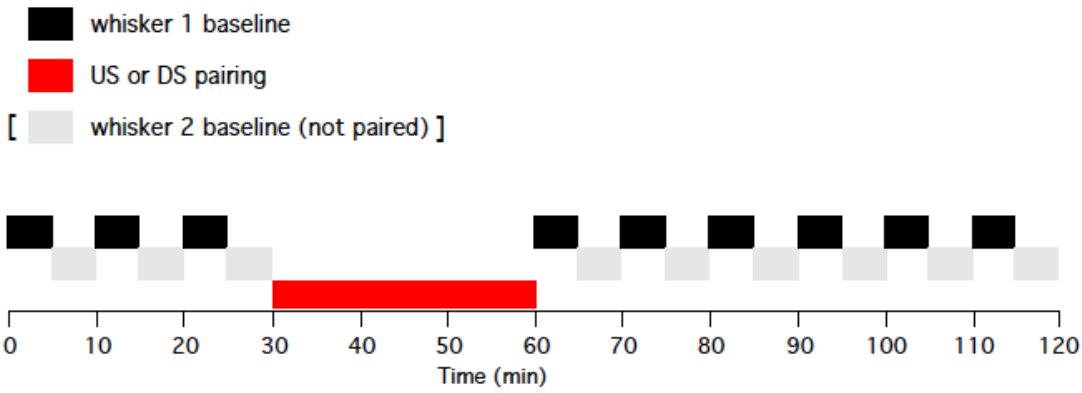


Figure 19. Experimental paradigm for plasticity experiments *in vivo*. 5 min baseline responses, each consisting of 1 whisker deflection every 5 seconds, were recorded every

10 min before and after 30 min of pairing with either Up states or Down states. Average LFP responses and STHs were calculated for each baseline recording period. In some Up state pairing experiments, a second whisker stimulus was presented which was not paired with Up states.

The location of individual recording sites was determined post-hoc by histological methods. This was because stereotaxic insertion of electrodes did not provide complete control over the exact location of each recording site. Electrodes were coated with DiI for visualisation in brain sections. The first set of experiments were carried out with a 64-channel matrix array inserted into layer 2/3 over multiple barrels. Here, the location of individual electrodes was estimated with respect to the barrel map in tangential cortical sections (Fig. 20). As expected, electrodes located in the principal barrel for the stimulated whisker also showed the strongest response to deflection of that whisker in the STH and LFP. As described in previous studies (Armstrong-James and Fox, 1987; Petersen et al., 2003b), the whisker response was not restricted to the principal barrel, but spread across several neighbouring barrels.

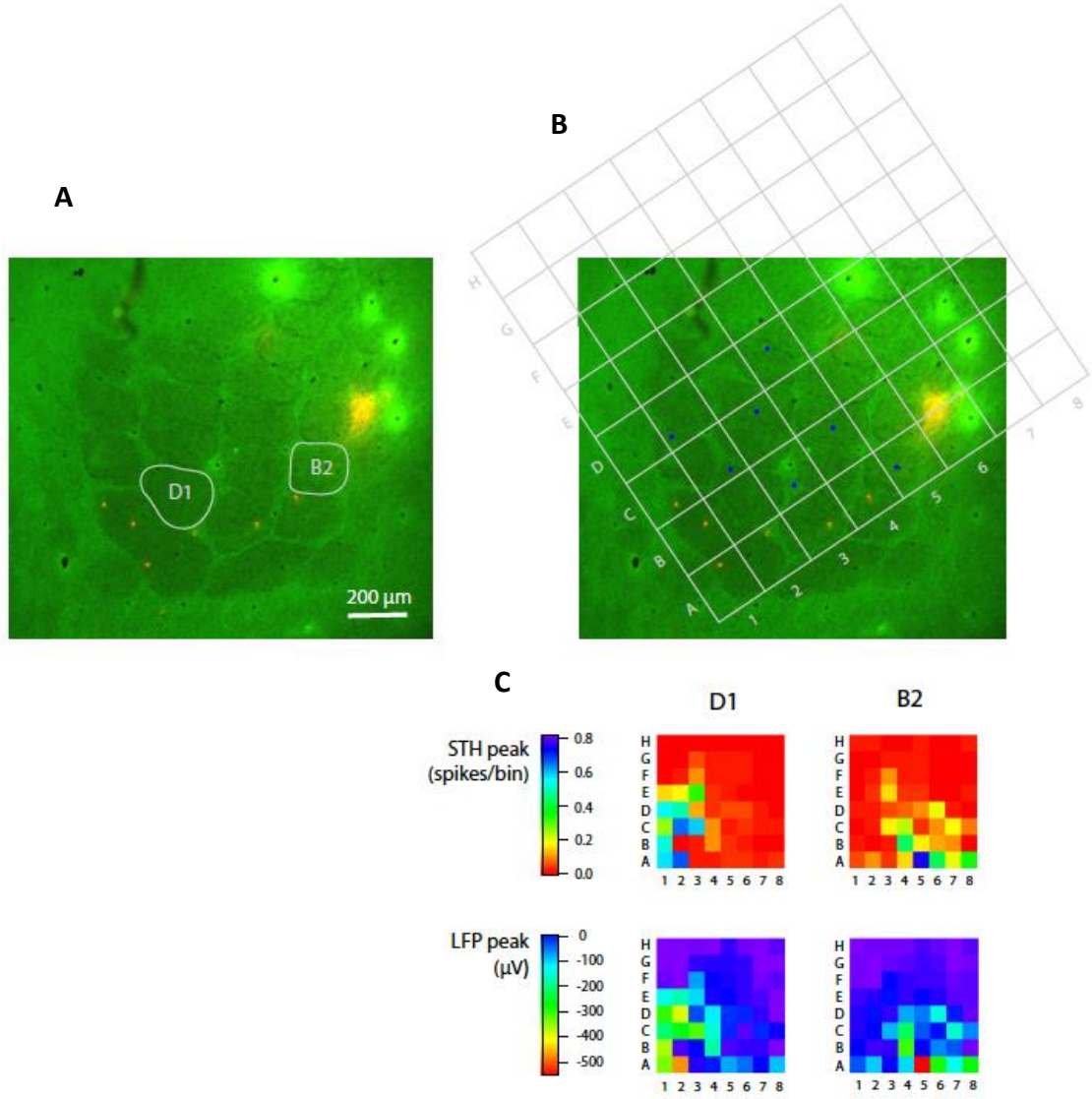


Figure 20. Identification of 64-channel electrode array recording sites. (**A, B**) Horizontal section of the barrel cortex stained with tenascin-c (green). Electrode sites were made visible with DiI. Electrodes contained within the section are shown in orange. Additional sites visible in sections above or below are shown in blue. (**A**) Barrels D1 and B2 are highlighted as the principal barrels responding to the whiskers used in the experiment. Scale bar is 200 µm. (**B**) An 8 x 8 electrode grid with 200 µm spacing was superimposed using the visible electrode points as a reference to estimate approximate locations for the remaining electrodes. (**C**) The strongest responses to deflection of the D1 and B2 whiskers occurred at the electrodes located in the respective principal barrel.

Electrodes A2 and C2 on the grid recorded the strongest responses to D1 whisker deflection. Electrode A5 responded strongest to B2 whisker deflection.

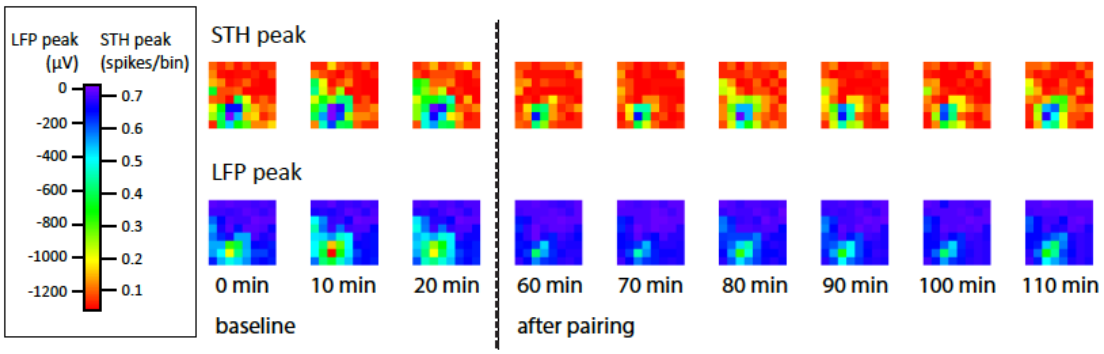
5.2.4 Pairing of whisker stimulation with Up states induces long-lasting depression of sensory responses in the barrel cortex

Initial experiments addressed the possibility that Up states and Down states differentially modulate long-lasting changes in the cortical processing of somatosensory input after 10 Hz whisker stimulation. As described in the previous section, three baseline sessions of whisker responses were recorded over 30 minutes, followed by 30 minutes of pairing with either Up states or Down states. After pairing, the baseline whisker response was again measured over the course of one hour to determine whether pairing induced any long-term plasticity. The response was quantified by measuring the peak of the average LFP and STH, as well as the total number of spikes of the average STH (here referred to as spike count).

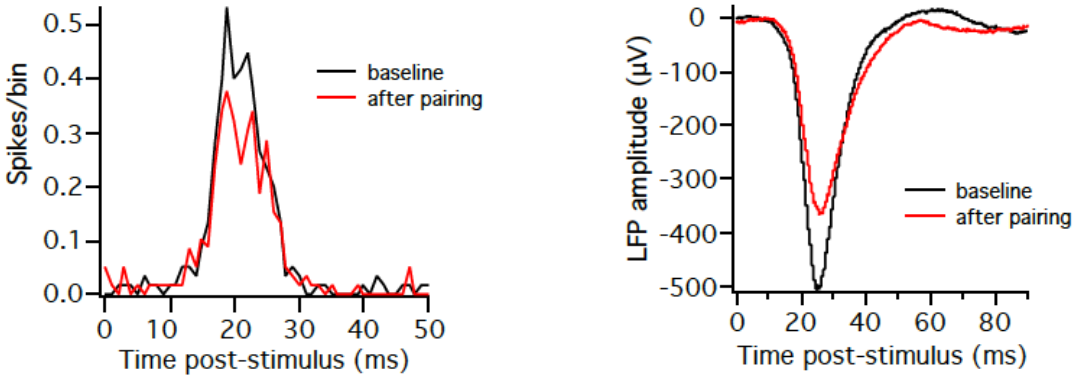
I found that pairing of whisker stimulation with Up states induced long-term depression of LFP and multiunit responses to the paired whisker in all responding channels (Fig. 21A, B, E). Conversely, pairing of whisker stimuli with Down states did not induce long-lasting plasticity (Fig. 21C, D). When the average whisker response was plotted over time after Down state pairing, I found that it was initially transiently depressed and gradually recovered back to its pre-pairing baseline level after 15-30 minutes (Fig. 21 F).

A

Up state pairing

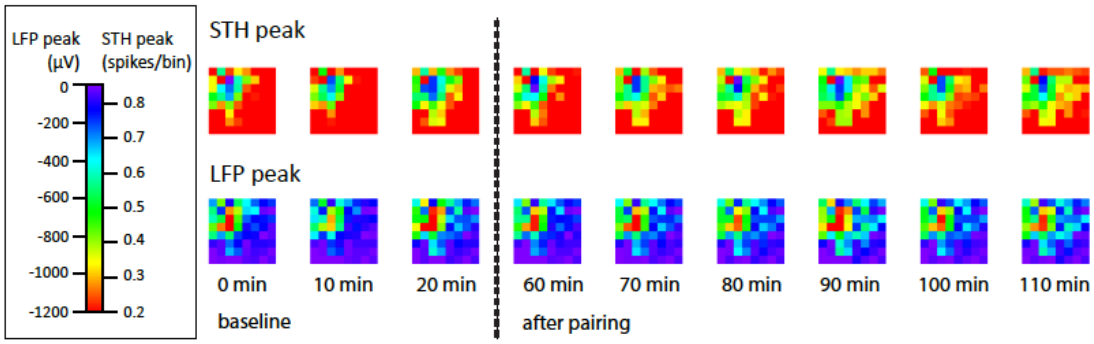


B



Down state pairing

C



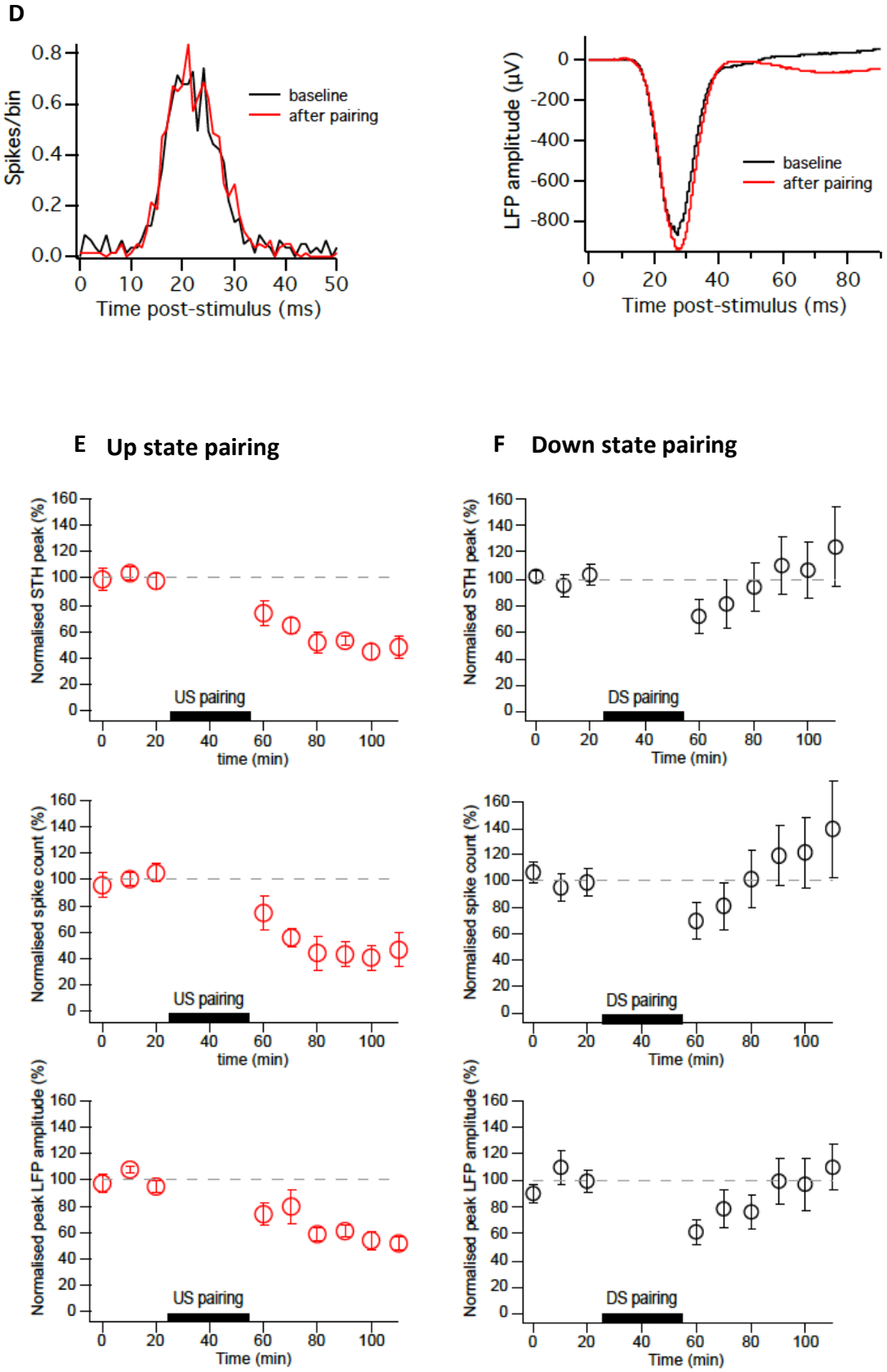


Figure 21. State-dependent plasticity of the whisker response. (**A-D**) Example traces before and after pairing. (**A, C**) 64-channel electrode grid showing

the STH peak and LFP peak amplitude over time. After Up state pairing (**A**), responses to whisker deflection were depressed across all responding channels compared to pre-pairing baseline. Pairing with Down states (**C**) did not induce any long-term changes in the whisker response. (**B, D**) Example STH and LFP of a single channel before (black) and 30 minutes after pairing (red). Bin size for STHs was 1 ms. (**E, F**) Time course of whisker responses before and after pairing, normalised to pre-pairing baseline and averaged across experiments, with error bars showing SEM. Only those channels which responded to whisker deflection were used in the analysis. STH peak and spike count (number of spikes per stimulus) were measured using STHs created around the whisker stimulus with 1 ms bins. Peak LFP amplitude was measured relative to pre-stimulus baseline. (**E**) 30 min of Up state pairing induced long-term depression of whisker responses (n = 6). (**F**) Whisker responses were initially depressed after Down state pairing, but recovered to their initial size within 30 min after pairing (n = 5).

The effect of the pairing condition (Up state versus Down state) on the size of the post-pairing normalised whisker response over time was analysed in a two-way mixed ANOVA. While there was no significant main effect of time on the size of the average STH peak over time after pairing (F(1.8, 16.5) = 0.78, p = 0.463, Greenhouse-Geisser-corrected dF), a significant interaction was found with the type of pairing (F(1.8, 16.5) =5.74, p = 0.014). Similarly, there was no significant main effect of time on the size of the average spike count after pairing (F(1.7, 15.7) = 1.26, p = 0.305, Greenhouse-Geisser-corrected dF), but a significant interaction with the pairing condition (F(1.7, 15.7) = 5.81, p = 0.015). In agreement with results from STH response measures, the main effect of time on the average LFP peak after pairing was not significant (F(2.4, 21.5) = 1.37, p = 0.278, Greenhouse-

Geisser-corrected *dF*), whereas the pairing condition significantly interacted with this response ($F(2.4, 21.5) = 6.86$, $p = 0.003$). Taken together, these results show that Up states and Down states differentially affected whisker responses after pairing.

To quantify the amount of depression, responses were averaged over 0-30 minutes and 30-60 minutes after pairing (Fig. 22). Since the data were normalised to pre-pairing baseline, one-sample two-tailed *t*-tests were carried out to compare the response after pairing with the baseline response of 100 %. After pairing with Up states, whisker responses were significantly depressed compared to baseline both in the first and second half of the post-pairing recording period (see table 2 for results from one-sample two-tailed *t*-tests). Whisker responses were initially depressed after pairing with Down states, but recovered to pre-pairing baseline levels by the end of the recording period. When measured over the first 30 minutes after pairing, this initial depression was not significant in a two-tailed one-sample *t*-test against 100 % (see table 3). Unsurprisingly, the whisker response was also not significantly different to 100 % in the second half after pairing with Down states.

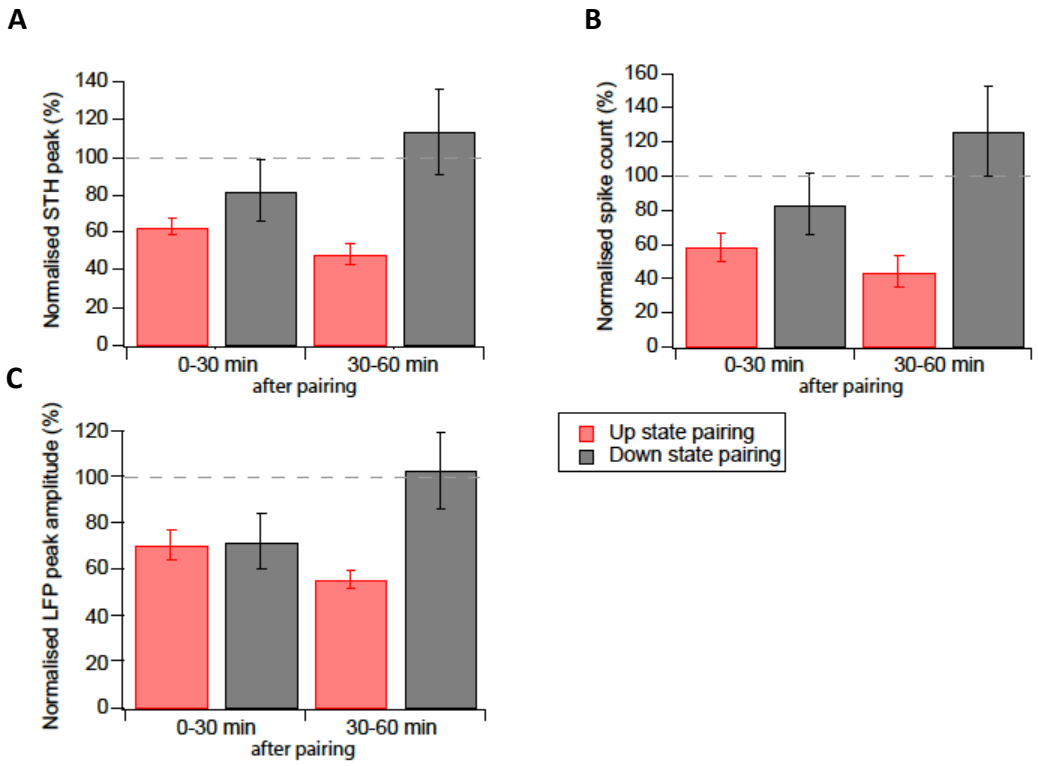


Figure 22. Long-term depression after pairing with Up states, but not Down states. (**A-C**) Average responses 0-30 min and 30-60 min after pairing with Up states (red, n = 6) and Down states (black, n = 5), normalised to pre-pairing baseline. Error bars are SEM. (**A**) Normalised STH peak. (**B**) Normalised spike count. (**C**) Normalised LFP peak.

	Paired with	Time after pairing (min)	Mean ± SEM (%)	t (5)	p
STH peak	Up state	0-30	63.33 ± 4.46	-8.22	< 0.001
STH peak	Up state	30-60	48.13 ± 5.34	-9.72	< 0.001
Spike count	Up state	0-30	58.66 ± 7.91	-5.23	0.003
Spike count	Up state	30-60	43.49 ± 9.53	-5.93	0.002
LFP peak	Up state	0-30	70.68 ± 6.20	-4.73	0.005
LFP peak	Up state	30-60	55.48 ± 4.27	-10.43	< 0.001

Table 2. Results from two-tailed one-sample t-tests versus 100 % for all response measures 0-30 and 30-60 minutes after Up state pairing.

	Paired with	Time after pairing (min)	Mean ± SEM (%)	t (4)	p
STH peak	Down state	0-30	82.03 ± 16.12	-1.12	0.327
STH peak	Down state	30-60	113.57 ± 22.75	0.60	0.583
Spike count	Down state	0-30	83.91 ± 17.47	-0.92	0.409
Spike count	Down state	30-60	126.70 ± 26.53	1.01	0.371
LFP peak	Down state	0-30	72.03 ± 11.68	-2.40	0.075
LFP peak	Down state	30-60	102.53 ± 16.29	0.16	0.884

Table 3. Results from two-tailed one-sample *t*-tests versus 100 % for all response measures 0-30 and 30-60 minutes after Down state pairing.

To investigate whether the changes induced by Up state pairing were specific to the stimulated whisker pathway, baseline recordings were made of responses to a second whisker which was not paired with Up states (see Fig. 19). This was done in a subset of Up state pairing experiments (n = 5). The two whiskers used in these experiments were D1 and B2, and both whiskers were used equally for the Up state pairing and unpaired condition in different experiments. Unpaired whisker responses were plotted against Up state-paired whisker responses to determine whether Up state pairing had an effect on the unpaired whisker pathway (Fig. 23). This indicated that unpaired whisker responses were less depressed than their paired counterparts, since most points were located above the grey dashed line representing perfect correlation. However, statistical analysis revealed a significant relationship between all three paired and unpaired response measures (r = 0.447, p = 0.013 for the normalised STH peak, r = 0.563, p = 0.001 for the normalised spike count, r = 0.403, p = 0.027 for the normalised LFP peak), suggesting that they were not independent. This also implies that depression after Up state pairing was not pathway-specific.

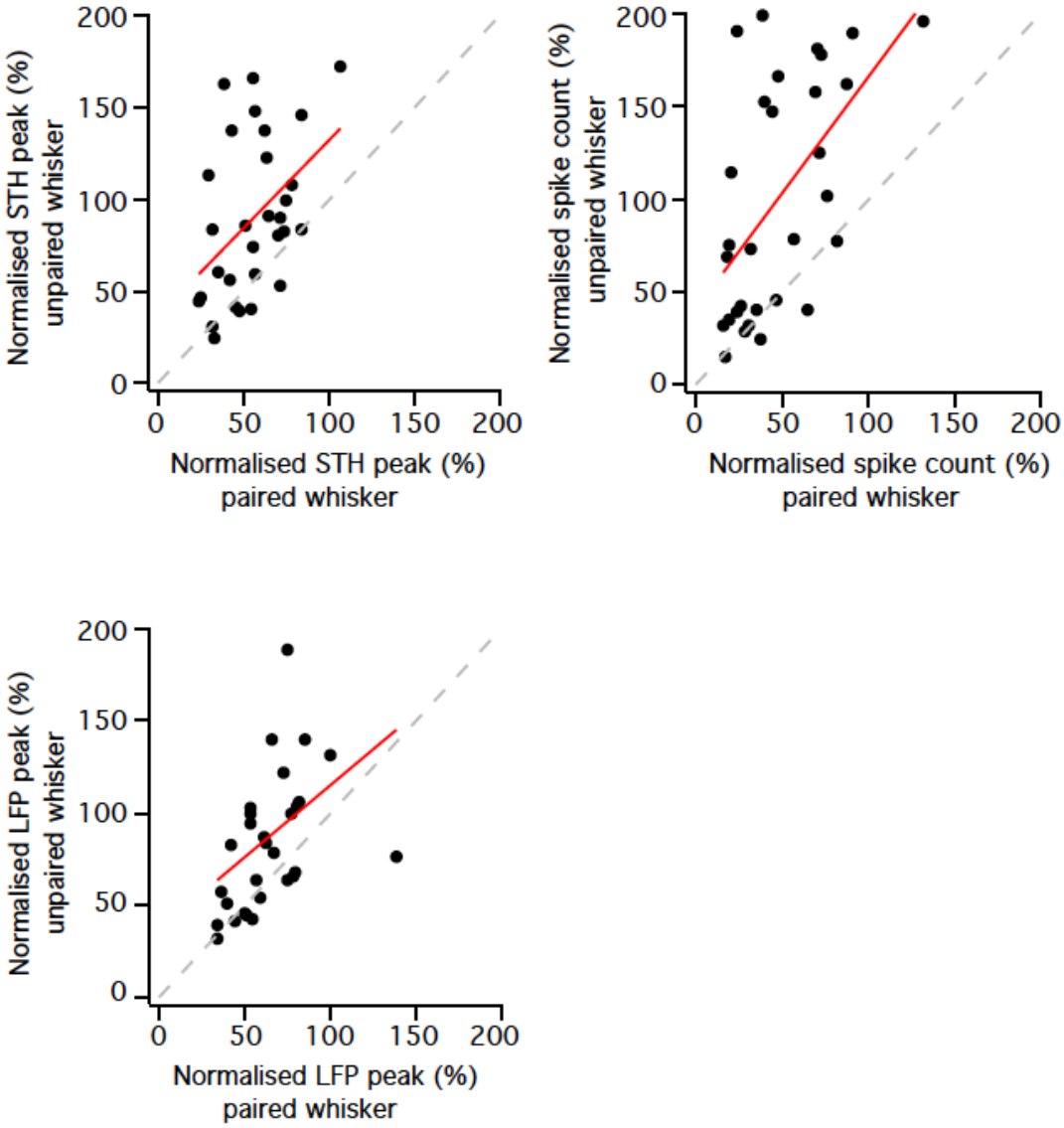


Figure 23. Correlation between paired and unpaired whisker responses. Average normalised responses to deflection of the unpaired whisker were plotted against normalised responses to deflection of the Up state-paired whisker. This includes all responses after pairing (n = 30 responses from 5 mice). Dashed grey lines represent perfect correlation. Points above that line indicate that responses to the unpaired whisker were less depressed than responses to the paired whisker, and vice versa. (**A**) Normalised STH peak. (**B**) Normalised spike count. (**C**) Normalised LFP peak.

5.2.5 Relationship between the amount of depression after Up state pairing and distance to the principal barrel

To investigate whether the amount of plasticity after Up state pairing differs between principal and neighbouring barrels, the normalised response measures for all responding channels showing depression after Up state pairing were plotted against their distance to the principal barrel in the electrode grid (Fig. 24). Linear regression analyses were then conducted on all response measures to investigate whether the amount of depression induced by Up state pairing at a particular channel can be predicted by its distance to the principal barrel. Here, a negative relationship was found for all normalised response measures after pairing, meaning that the whisker response was more depressed after pairing the further away the electrode was from the principal barrel. Distances of over 200 μm are likely to correspond to recording sites in surrounding barrels, given that it is the approximate width of a large barrel (see Fig. 20). This finding suggests that whisker responses after Up state pairing may be more depressed in surrounding barrels compared to the principal barrel. Although values of R^2 were relatively small, implying that less than 10 % of variance of the whisker response can be explained by distance to the principal barrel, a significant relationship was found for both measures of spiking activity (see table 4). The lack of a significant effect in the LFP peak may be due to the LFP signal not being localised, making changes over distance more difficult to interpret.

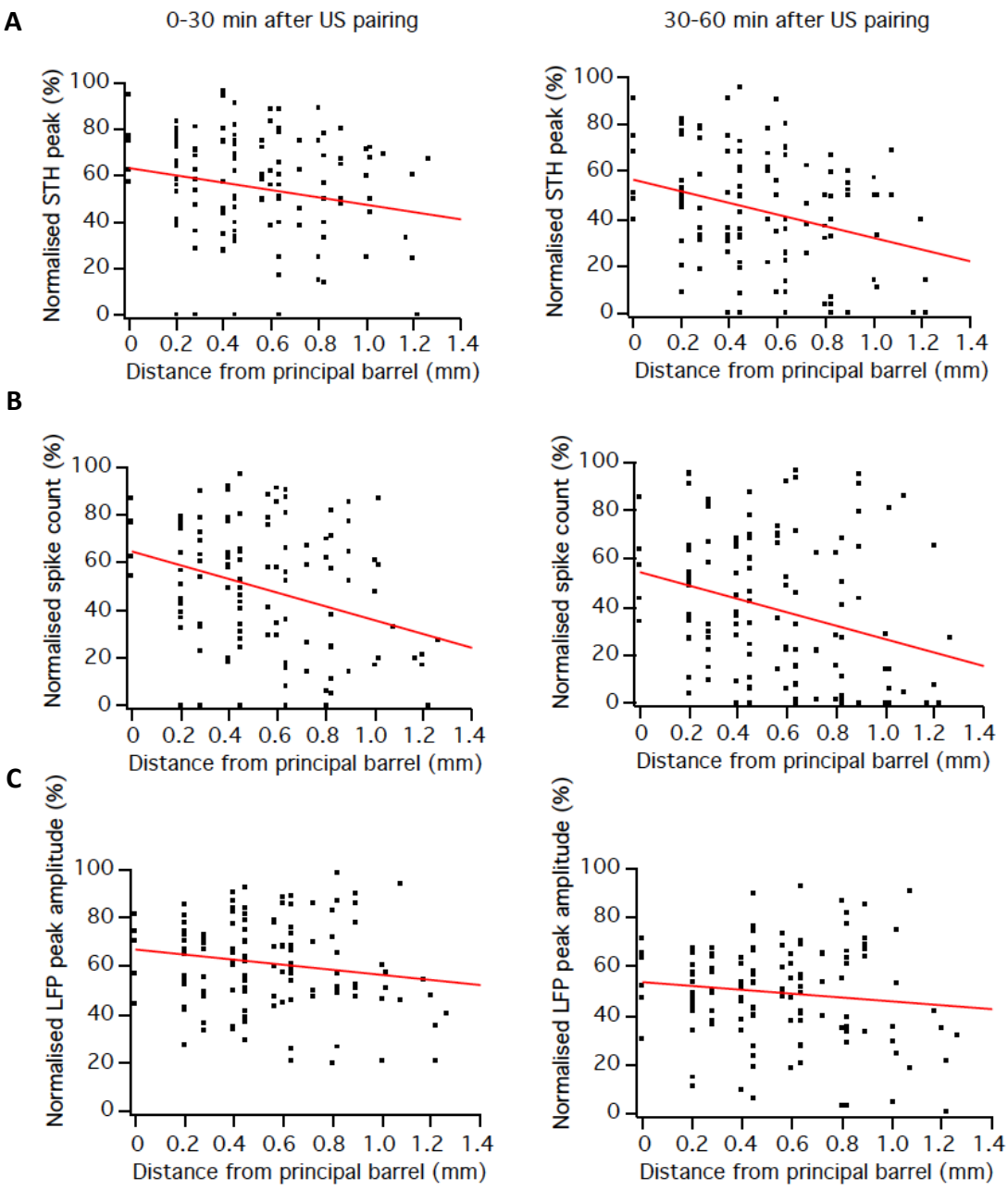


Figure 24. Relationship between the normalised whisker response at each electrode after Up state pairing and its distance to the principal barrel. All channels showing a depressed response to whisker deflection after pairing were plotted against distance, with regression lines displayed in red. (**A**) The prediction of the size of the normalised STH peak from the distance to the principal barrel was significant 0-30 min (n = 125) and 30-60 min (n = 128) after pairing. (**B**) Similar to (**A**), there was a significant relationship between the normalised spike count and the distance from the principal

barrel 0-30 min (n = 119) and 30-60 min (n = 130) after pairing. (**C**) There was no significant relationship between the normalised LFP peak and the distance both 0-30 min (n = 125) and 30-60 min (n = 130) after pairing.

	Time after pairing (min)	F	dF	R^2	β	p
STH peak	0-30	4.80	1, 122	0.038	-0.20	0.030
STH peak	30-60	12.97	1, 126	0.093	-0.31	< 0.001
Spike count	0-30	12.70	1, 117	0.098	-0.31	0.001
Spike count	30-60	10.74	1, 128	0.077	-0.28	0.001
LFP peak	0-30	3.63	1, 123	0.029	-0.17	0.059
LFP peak	30-60	1.79	1, 128	0.014	-0.12	0.183

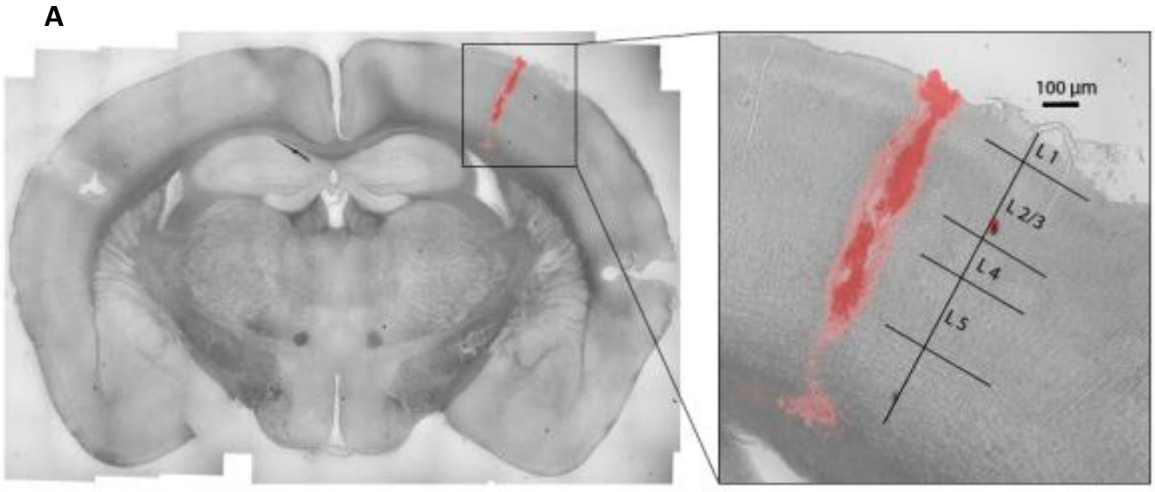
Table 4. Results from linear regression analyses, with distance to the principal barrel predicting the normalised whisker response.

5.2.6 Experimental design for investigations into the laminar profile and molecular pathway of Up state pairing-dependent depression

Previous experiments were targeted to layer 2/3 of the barrel cortex. To investigate whether the plasticity effect found in layer 2/3 also occurs in other cortical layers, recordings were carried out using a linear electrode probe, which was inserted into a single barrel column and spanned all layers. In addition, this setup was used to pharmacologically investigate whether long-term depression after Up state pairing is dependent on NMDA receptors. Using a linear probe allowed sufficient access to the brain surface for application of the antagonist. This

would have otherwise been difficult to achieve with the previously used 8 x 8 array, since it covered most of the craniotomy.

Linear electrode placement was examined post hoc in coronal sections (Fig. 25). Boundaries between cortical layers were identified by individual differences in cell density, with layer 4 showing characteristic barrel structures which were less cell-dense. The approximate thickness of each layer was then measured. Based on the depth of the probe and a spacing of 50 μm between individual electrode sites, it was possible to align the recording and determine the number of channels for each layer.



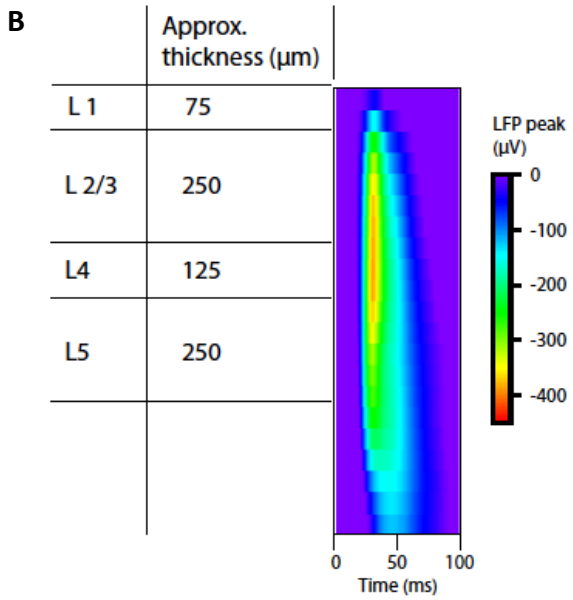


Figure 25. Identification of cortical layers and 32-channel linear probe recording sites. (**A**) Electrode tracts were stained using DiI (red). Cell bodies were stained with DAPI. Layers were identified by their differences in cell density and the presence of barrel structures in layer 4. (**B**) Based on the approximate thickness of each layer and a spacing of 50 µm between recording sites, the number of recording sites per layer was determined.

5.2.7 Effects of the NMDA receptor antagonist AP5 on whisker responses and Up states

To investigate whether plasticity after Up state pairing is dependent on NMDA receptors, the NMDA receptor antagonist AP5 was applied to the surface of the barrel cortex for the duration of the experiment. Within minutes of application of 100 µM D-AP5 to the surface of the cortex, the whisker response was strongly suppressed across layers (Fig. 26). This was particularly pronounced in the evoked spiking response, which was almost completely inhibited in layers 2/3 and

4. Specifically, the normalised STH peak was significantly reduced in layer 2/3 (18.45 ± 10.6 %), layer 4 (19.96 ± 4.15 %), and layer 5 (37.88 ± 13.34 %) after application of AP5 compared to before ($t(3) = -7.69$, $p = 0.005$ in layer 2/3, $t(3) = -19.29$, $p < 0.001$ in layer 4, $t(3) = -4.66$, $p = 0.019$ in layer 5, two-tailed one-sample *t*-test versus 100 %). Similarly, the normalised total spike count was significantly suppressed in layer 2/3 (14.57 ± 9.00 %), layer 4 (8.28 ± 4.14 %), and layer 5 (29.19 ± 10.34) compared to its pre-AP5 baseline ($t(3) = -9.50$, $p = 0.002$ in layer 2/3, $t(3) = -21.17$, $p < 0.001$ in layer 4, $t(3) = -6.85$, $p = 0.006$ in layer 5, two-tailed one-sample *t*-test versus 100 %). The normalised LFP peak amplitude was also significantly decreased, albeit to a lesser extent, in layer 2/3 (56.61 ± 5.78 %), layer 4 (62.54 ± 7.22 %), and layer 5 (63.85 ± 8.48 %) compared to its original value ($t(3) = -7.51$, $p = 0.005$ in layer 2/3, $t(3) = -5.19$, $p = 0.014$ in layer 4, $t(3) = -4.27$, $p = 0.024$ in layer 5, two-tailed one-sample *t*-test versus 100 %).

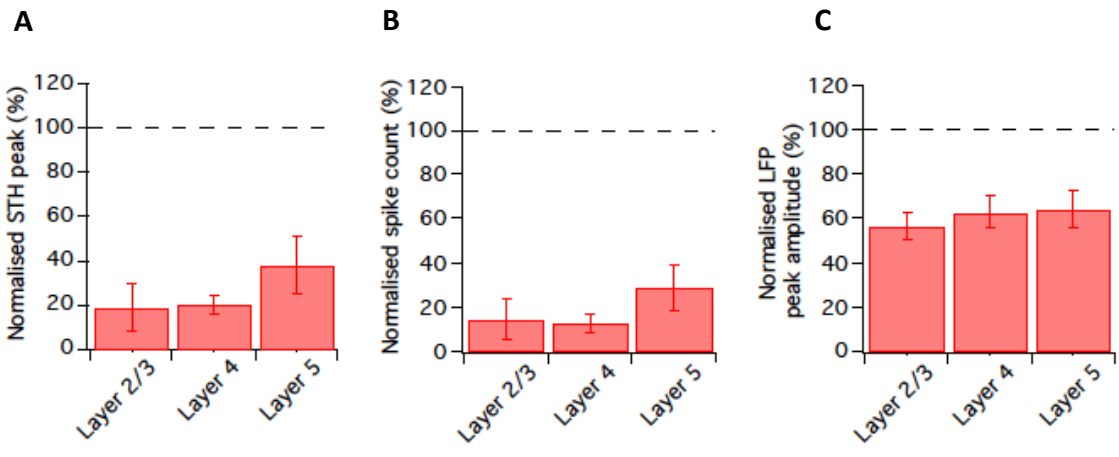


Figure 26. AP5 strongly suppressed responses to whisker deflection in all layers. Baseline responses measured within 20 min after AP5 application were averaged and normalised to baseline responses measured within 20 min before AP5 was applied (*n* =

4). Error bars show SEM. (**A**) Normalised STH peak. (**B**) Normalised spike count. (**C**) Normalised LFP amplitude.

AP5 application did not seem to suppress Up states in the barrel cortex. Up states were still present in the LFP in all layers. Post-hoc measurements revealed a marginal reduction of the Up state duration after AP5 application compared to before (from 1.08 ± 0.02 s to 0.98 ± 0.03 s) and concomitant increase of the Down state duration (from 0.40 ± 0.06 s to 0.48 ± 0.05 s; Fig. 27). However, only the effect on Up states was significant ($t(3) = 6.73$, $p = 0.007$ for Up state duration, $t(3) = -2.48$, $p = 0.089$ for Down state duration).

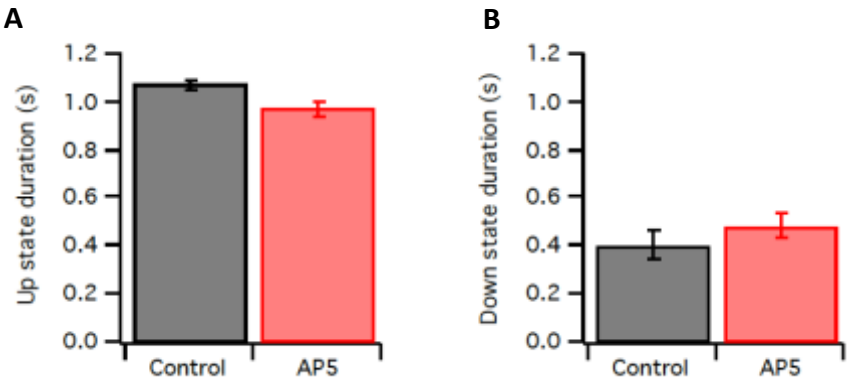


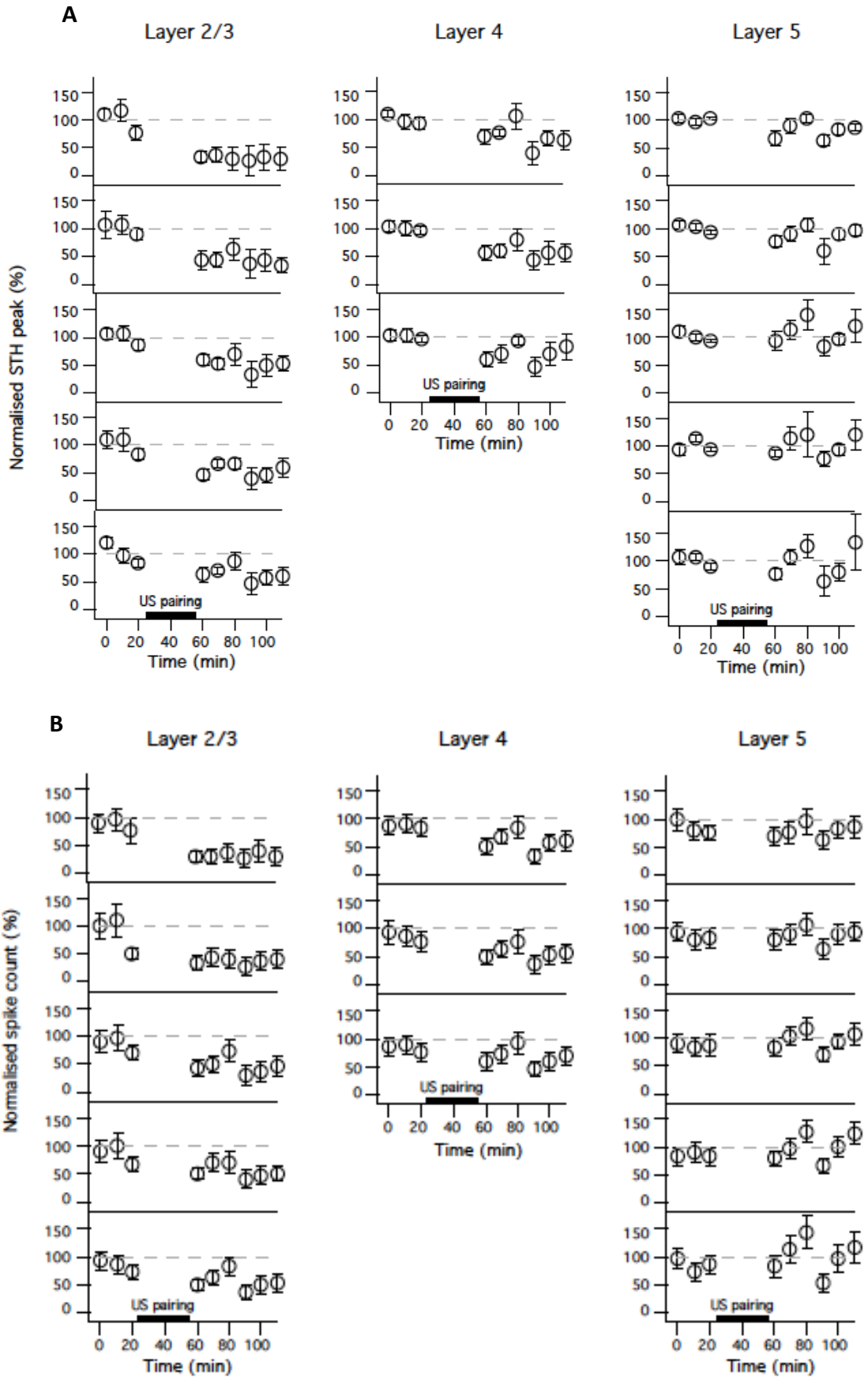
Figure 27. Average Up/Down state duration before and after AP5 application. Measurements were made on 20 min of baseline recording before AP5 application (black) and 20 minutes after AP5 application (red) ($n = 4$). Error bars show SEM. (**A**) Up state duration. (**B**) Down state duration.

Due to the strong suppression of spiking responses to whisker deflection, only the normalised LFP peak was analysed for effects of AP5 on depression after Up state pairing. The normalised LFP peak was analysed in a three-way mixed ANOVA to

compare differences across layers and over time between control and drug conditions. For simplicity of presentation, I will first discuss the laminar profile of LFP and STH data only in controls, before presenting pharmacological effects on the LFP response.

5.2.8 Laminar profile of plasticity in the barrel cortex after Up state pairing

After pairing deflections of a single whisker with Up states, responses to that whisker were depressed more strongly in superficial layers. When average normalised response measurements were plotted for each channel individually, I found that plasticity of the whisker response after pairing gradually decreased from superficial to deep channels. This was true for the normalised STH peak (Fig. 28A) and the normalised spike count (Fig. 28B), as well as the normalised LFP peak (Fig. 28C).


A
Layer 2/3
Layer 4
Layer 5
Normalised STH peak (%)
US pairing
Time (min)
B
Layer 2/3
Layer 4
Layer 5
Normalised spike count (%)
US pairing
Time (min)

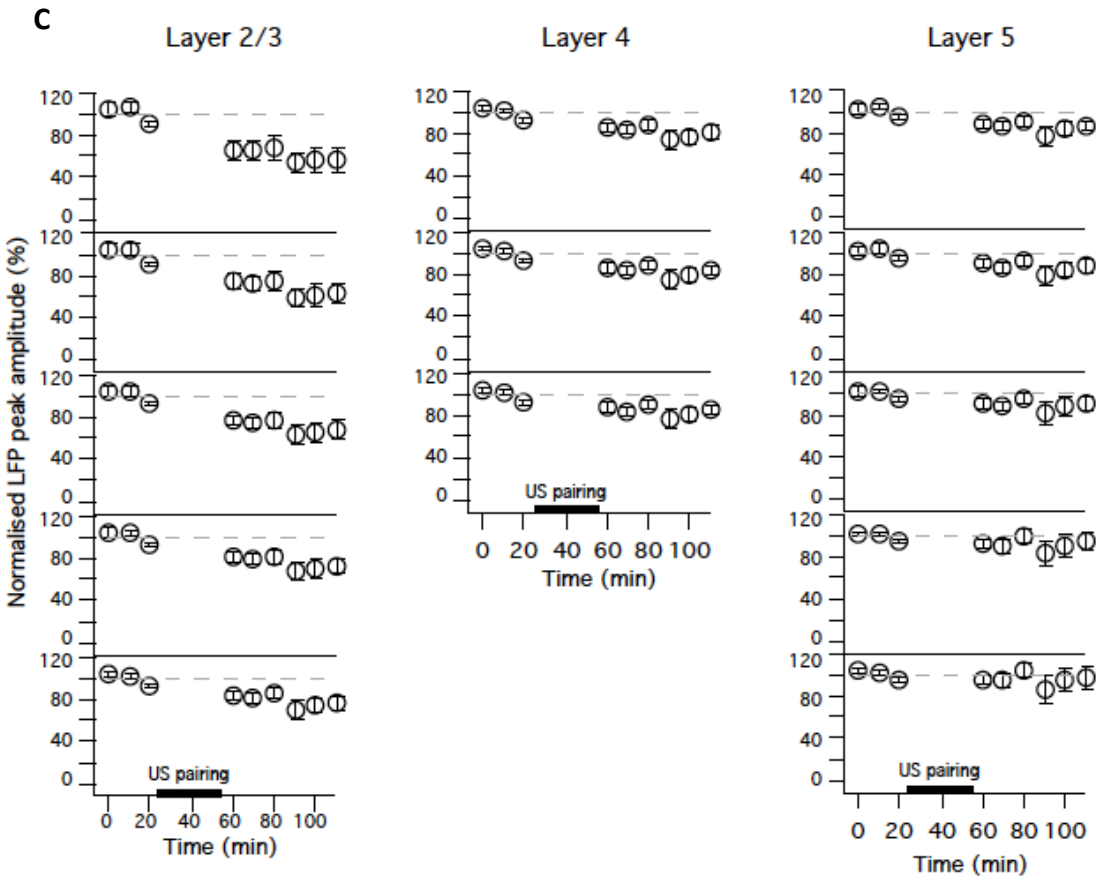


Figure 28. Normalised whisker response measures before and after Up state pairing across layers. Channels are ordered from superficial (top) to deep (bottom) for each layer. Data were normalised to pre-pairing baseline. Depression after pairing was strongest in more superficial layers and gradually declined towards layer 5. Error bars show SEM. (**A**) Normalised STH peak (n = 4). (**B**) Normalised spike count (n = 4). (**C**) Normalised LFP peak (n = 5). One experiment was excluded from the analysis of spiking activity due to insufficient MUA recording quality.

When normalised STH peak responses after Up state pairing were averaged for each layer (Fig. 29), post-pairing depression of whisker-evoked spiking was only present in layer 2/3 (49.09 ± 13.34 %) and layer 4 (65.73 ± 12.95 %), but not in layer 5 (94.72 ± 11.54 %). This was also true for the spike count measure, where normalised responses were depressed in layer 2/3 (51.88 ± 18.68 %) and layer 4

(68.66 ± 18.06 %), but remained stable on average in layer 5 (104.42 ± 12.55 %). The normalised LFP peak showed more modest levels of depression in layer 2/3 (70.92 ± 6.79 %) and layer 4 (82.94 ± 4.42 %), with a minimal amount of depression also present in layer 5 (89.73 ± 6.00 %). Levels of depression in layer 2/3 were comparable with those previously found using an 8 x 8 electrode array (see table 2). The effect of layer on the size of the post-pairing normalised whisker-evoked spiking response over time was analysed using two-way repeated-measures ANOVA. While depression after pairing of both the normalised STH peak and normalised spike count decreased from superficial to deep layers, the main effect of layer was only significant for the normalised spike count ($F(2, 8) = 11.23$, $p = 0.005$), whereas it was not statistically significant for the normalised STH peak ($F(1.0, 4.1) = 7.39$, $p = 0.052$, Greenhouse-Geisser-corrected *dF*). There was no significant main effect of time after pairing on either the normalised STH peak ($F(2.1, 8.3) = 2.81$, $p = 0.116$, Greenhouse-Geisser-corrected *dF*) or the normalised spike count ($F(1.6, 6.4) = 3.51$, $p = 0.098$, Greenhouse-Geisser-corrected *dF*). Moreover, there was no significant interaction between layer and response over time for the normalised STH peak ($F(1.7, 6.7) = 1.37$, $p = 0.310$, Greenhouse-Geisser-corrected *dF*) and the normalised spike count ($F(2.2, 8.9) = 1.09$, $p = 0.383$). Since the normalised LFP peak over time was not only compared between layers, but also between control and drug conditions, results were analysed in a three-way mixed ANOVA. Similar to the normalised spike count, I found a significant main effect of layer on the normalised LFP peak after pairing ($F(1.1, 7.5) = 19.11$, $p = 0.003$, Greenhouse-Geisser-corrected *dF*). Here, Bonferroni post-hoc tests showed a significant difference between layer 2/3 and layer 5 ($p = 0.038$). Again, the main effect of time after pairing was not significant ($F(5, 35) =$

1.05, p = 0.404) and there was no significant interaction between layers and response over time (F(1.6, 11.1) = 3.39, p = 0.079, Greenhouse-Geisser-corrected dF). Taken together, these results suggest that the amount of depression after pairing was different across layers, but did not vary much over time.

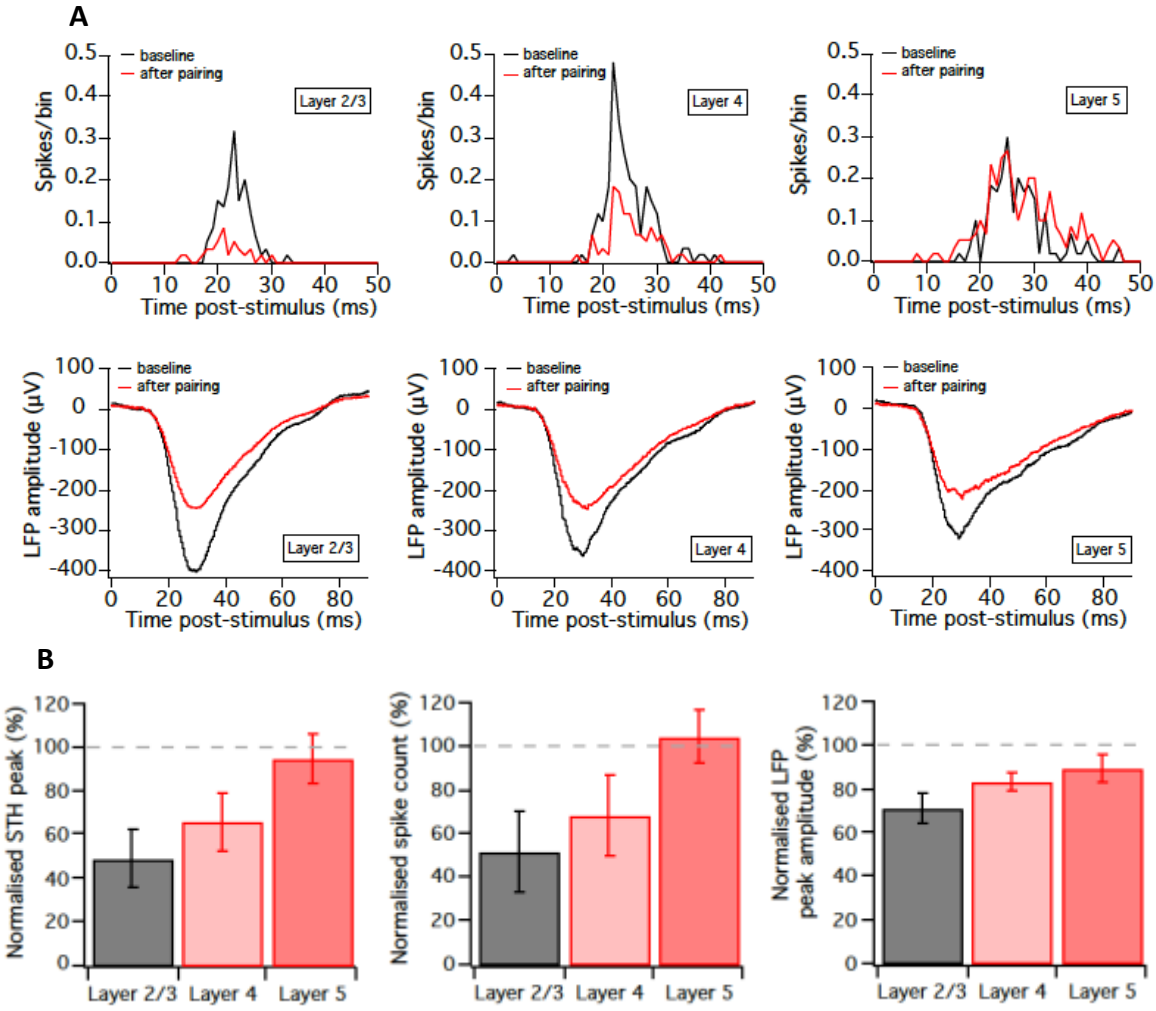
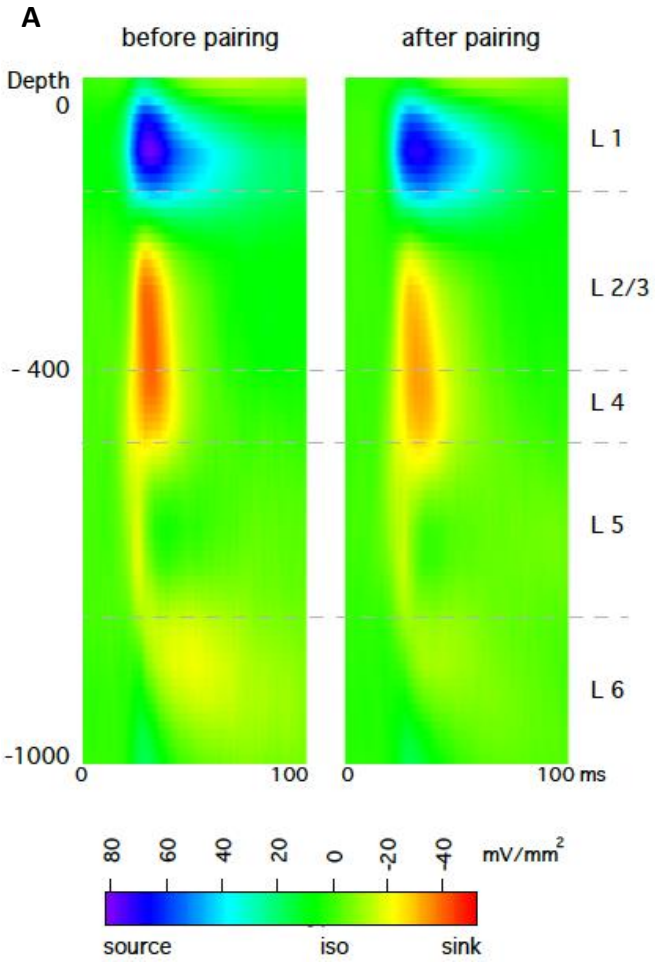


Figure 29. Differences in plasticity between layers. (**A**) Example traces showing the response to whisker deflection before (black) and after Up state pairing (red). STHs and average LFP traces are shown for a single representative channel in each layer. STH bin size is 1 ms. (**B**) Average responses across layers after Up state pairing, normalised to pre-pairing baseline. Error bars are SEM.

Current-source density (CSD) analysis was carried out on the laminar data to localise any current sinks and sources in response to the whisker stimulus which may be altered after pairing with Up states. This was done in an attempt to eliminate any confounding effects of volume conduction on the recorded LFP responses both horizontally and across layers. The activation pattern revealed a large current sink in layer 2/3 and layer 4, coupled with a current source in layer 1 (Fig. 30A). After Up state pairing, the shape of the current sink and source remained largely the same as before pairing. However, a decrease in the peak amplitude of the current sink was observed after pairing in some channels (Fig. 30B).



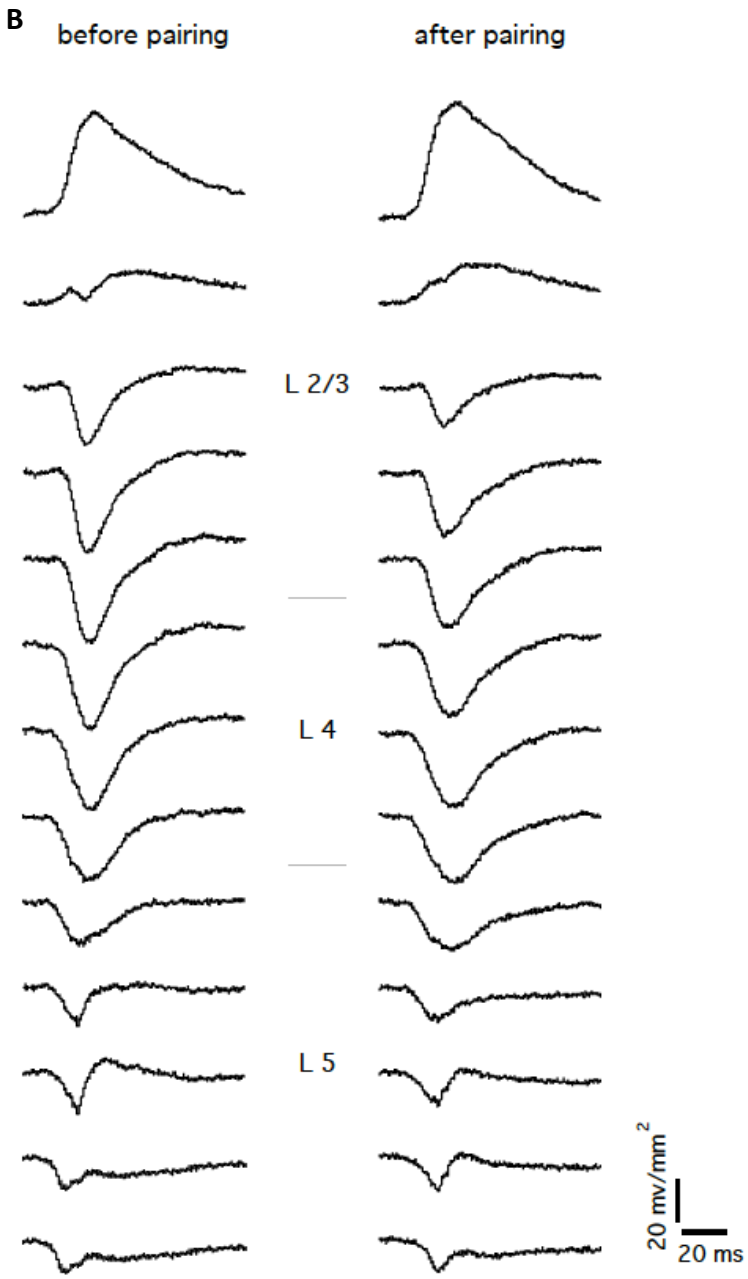


Figure 30. Example CSD profile before and after Up state pairing. (**A**) Contour plots of the CSD profile of the whisker response from 5 min baseline recordings before (left) and after (right) Up state pairing. Contour plots were interpolated from the laminar CSD profile. Current sources are shown in cold colours (blue), current sinks in hot colours (red). (**B**) CSD traces of individual channels along layers 2/3, 4, and 5, ordered from superficial (top) to deep (bottom).

In an attempt to elucidate whether depression is apparent at the earliest, thalamocortical response component or whether it is intracortically-mediated, the peak with the shortest latency in layer 4 was compared to the biggest peak in layer 2/3 (Fig. 31). To determine whether these CSD responses were significantly depressed compared to baseline, normalised peak responses were analysed against 100 % in two-tailed one-sample *t*-tests. Only those experiments were included in the analysis which had CSD profiles with a clear short-latency component in layer 4. Here, I found that the normalised CSD peak of the short-latency response, which presumably resulted from thalamocortical connections to layer 4, was not significantly depressed 0-30 minutes after pairing (93.76 ± 4.84 %; $t(2) = -1.28$, $p = 0.327$) and 30-60 minutes after pairing (87.84 ± 11.71 %; $t(2) = -1.04$, $p = 0.408$). In contrast to this, the peak CSD amplitude in layer 2/3 was significantly depressed 30-60 minutes after pairing (52.59 ± 6.58 %; $t(2) = -7.21$, $p = 0.019$). This effect was not found to be statistically significant 0-30 minutes after pairing (54.47 ± 12.18 %; $t(2) = -3.74$, $p = 0.065$). Taken together, these results are consistent with depression of intracortical, rather than thalamocortical connections.

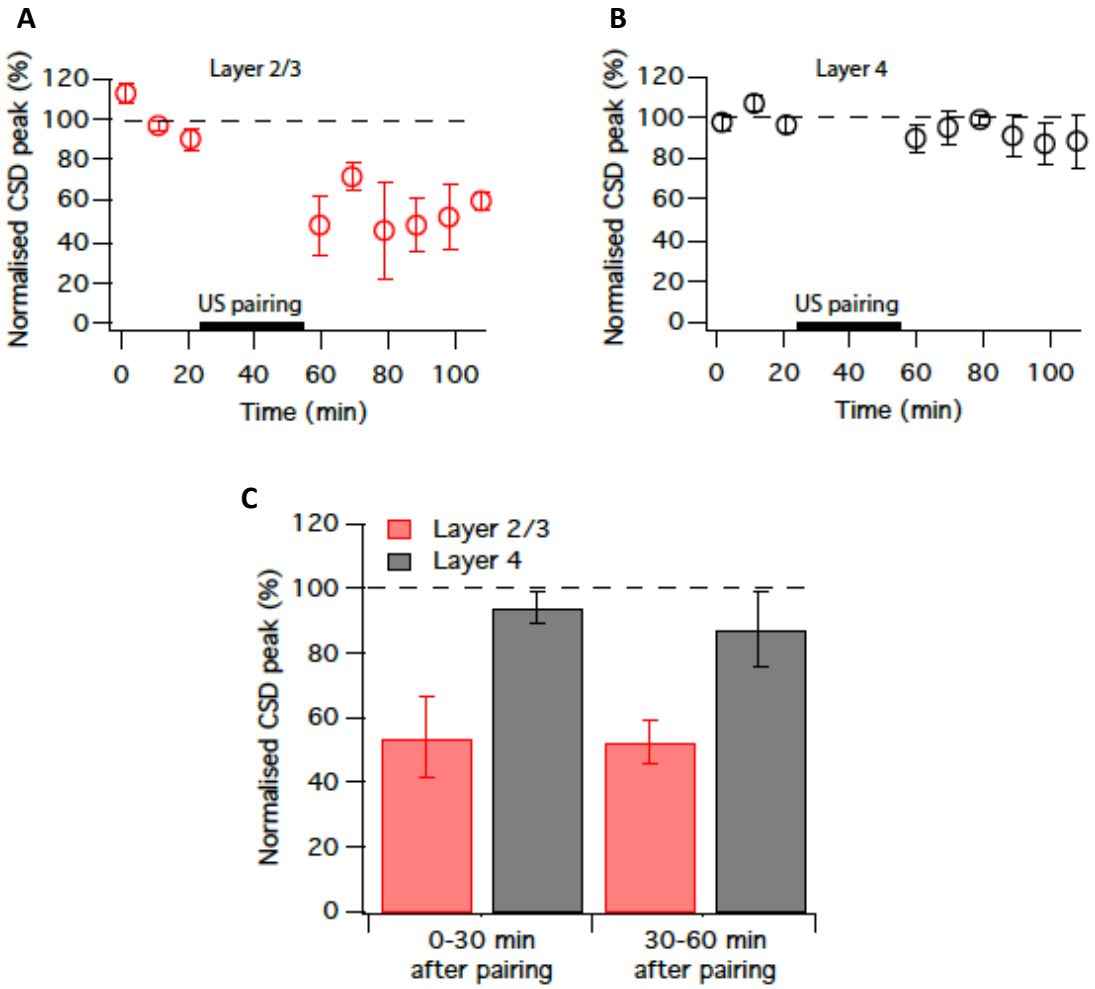
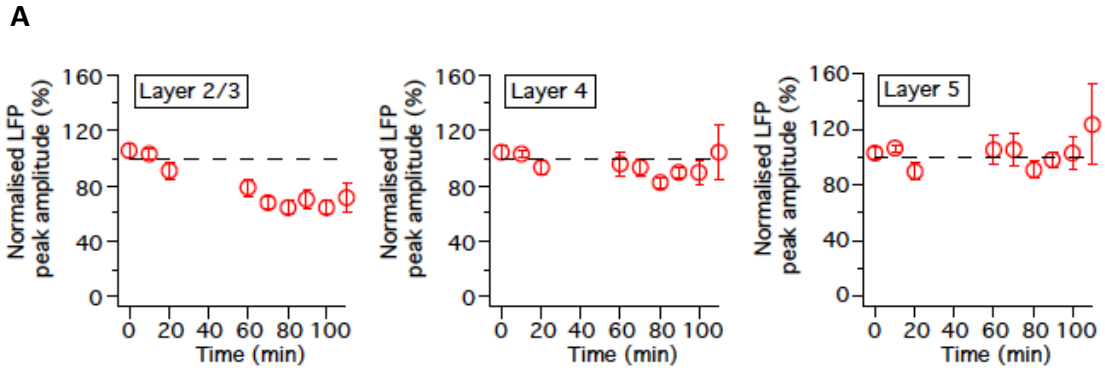


Figure 31. CSD current sink peaks in layer 2/3 and layer 4. (**A**) CSD peak in layer 2/3 over time, normalised to the pre-pairing baseline period and averaged across experiments (*n* = 3). Error bars are SEM. The channel with the biggest response in layer 2/3 was used for the analysis. (**B**) CSD peak in layer 4 over time, normalised to the pre-pairing baseline period and averaged across experiments (*n* = 3). Error bars are SEM. The fastest-responding channel was used for the analysis. (**C**) Normalised CSD peak in layer 2/3 (red) and layer 4 (black), averaged over 0-30 min after pairing and 30-60 min after pairing. Error bars show SEM.

5.2.9 Inhibition of NMDA receptors with AP5 did not significantly affect depression after Up state pairing

As mentioned earlier, effects of AP5 on plasticity were only analysed on the LFP response due to the strong suppression of spiking responses to whisker deflection after application of the drug. The effect of depression on the normalised LFP peak after Up state pairing remained unchanged in layer 2/3 (69.41 ± 5.23 %) and was slightly less in layer 4 (92.47 ± 7.88 %) and layer 5 (104.37 ± 11.60 %) when NMDA receptors were inhibited with AP5 compared to control conditions (Fig. 32). However, there was no significant interaction between drug and layer effects ($F(1.1, 7.5) = 1.75$, $p = 0.227$, mixed ANOVA with Greenhouse-Geisser-corrected *dF*), and between drug and normalised LFP over time after pairing ($F(5, 35) = 1.31$, $p = 0.281$). The interaction between all three variables was also not significant ($F(1.6, 11.1) = 1.54$, $p = 0.252$, Greenhouse-Geisser-corrected *dF*).



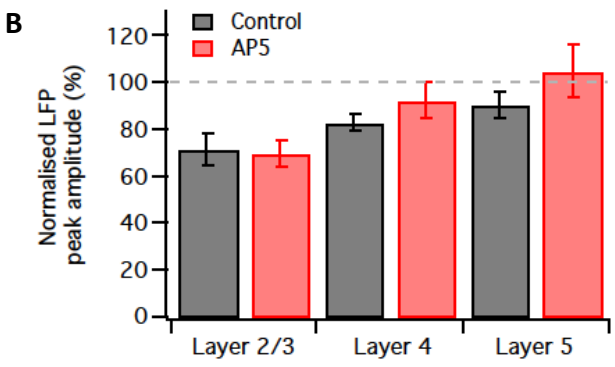


Figure 32. AP5 did not inhibit long-term depression of whisker responses after Up state pairing. (**A**) LFP peak amplitude over time, normalised to pre-pairing baseline and averaged across experiments (n = 4). Error bars show SEM. (**B**) Comparison of the normalised LFP peak amplitude between layers after pairing, with and without AP5. Error bars show SEM. No significant difference was found with AP5 compared to control.

5.3 Discussion

5.3.1 Optogenetic approach to control Up/Down states

I investigated whether it is possible to interfere with Up/Down state activity using optogenetics, as has been suggested in a previous study (Beltramo et al., 2013). I tested this approach by injecting the optogenetic silencer ArchT3 into the barrel cortex, where it was expressed in excitatory pyramidal neurons. I found that, while activating ArchT3 in slices of barrel cortex was sufficient to inhibit evoked Up states *in vitro*, I was unable to achieve any significant silencing of spontaneous Up states in the barrel cortex of anaesthetised mice *in vivo*. There are several possible reasons for this. Firstly, different methods of virus injection were used for *in vitro* and *in vivo* experiments, which may have led to differences in expression and thus the propensity to inhibit network activity. However, this is unlikely to have had a dramatic effect, given that the expression of ArchT3 was confirmed by histology after each experiment. In both cases, I found widespread expression in the barrel cortex across all layers. Small differences may nevertheless exist, as the expression level was not measured quantitatively. Another possibility is that the LED light source used *in vivo* did not emit at an intensity high enough to induce any significant, wide-spread inhibition, particularly in deep layers. Insufficient activation of ArchT3 in layer 5 pyramidal neurons may have prevented the inhibition of Up states, given that there is evidence from previous studies suggesting that Up states are generated in layer 5 of the cortex (Beltramo et al., 2013; Chauvette et al., 2010; Le Bon-Jego and Yuste,

2007; Sanchez-Vives and McCormick, 2000). Within this context, it may be necessary to restrict expression of the optogenetic silencer to layer 5, which is what was attempted by Beltramo et al. to inhibit Up/Down state activity in the barrel cortex *in vivo* (Beltramo et al., 2013). Taken together, any of these reasons does not in itself preclude that Up states can be optogenetically silenced. However, it may also be impossible to achieve complete inhibition of Up states using an optogenetic approach *in vivo*. While electrically-evoked Up states *in vitro* likely result from the recurrent activity of only a subset of interconnected neurons and may therefore be easier to inhibit by light, the Up state-generating network *in vivo* may simply be too extensive to perturb using such a targeted approach.

Optogenetic inhibition of Up states, if successful, could provide a powerful tool to study plasticity *in vivo*, not only during anaesthesia, but also in naturally sleeping mice. Synaptic plasticity in the barrel cortex is thought to underlie experience-dependent plasticity of sensory maps induced by whisker deprivation. Optogenetic inhibition of Up states in the barrel cortex during a period of whisker deprivation could be used to study whether slow oscillations play a role in experience-dependent plasticity. This would further require a feedback system which induces light stimulation upon detection of Up states during slow wave sleep.

5.3.2 Up states and Down states differentially modulate plasticity of whisker responses in the barrel cortex after chronic whisker stimulation

To investigate whether Up states and Down states have different effects on plasticity of paired inputs in the barrel cortex, I used an experimental protocol in which whisker stimuli were paired with spontaneous Up states or Down states. This was done by means of an Arduino-based system to detect Up states and, upon detection, induce a train of whisker deflections. The size of the LFP and STH response to deflection of the paired whisker was compared before and after pairing to infer whether plasticity had occurred. The results obtained here show that Up states and Down states were indeed different in their ability to mediate plasticity in layer 2/3 of the barrel cortex. Pairing with Up states induced long-term depression of the whisker response to approximately 50 % of its original size, which was measured until one hour after pairing. Conversely, pairing with Down states only had short-term effects. While some small amount of depression occurred immediately after pairing, the size of the whisker response recovered to its pre-baseline value within 20-30 minutes. However, given the higher false-positive rate for Down state pairings compared to Up state pairings (see Appendix), it cannot be excluded that the short-term depression was due to the coincidence of some whisker stimuli with Up states, rather than an effect mediated by Down state pairings themselves.

To address the question whether long-term depression is specific to the stimulated whisker pathway, I looked at the effect of Up state pairing on the

response to a second, unpaired whisker in a subset of experiments. I found a significant correlation between paired and unpaired whiskers in all response measures, indicating that the effect of depression after Up state pairing was not specific to the stimulated whisker. As mentioned previously, the cortical area activated by a single whisker spans several barrels due to intracortical connections (Armstrong-James and Callahan, 1991; Fox, 1994; Fox et al., 2003). The whiskers used here, D1 and B2, had significant overlap in their receptive fields in layer 2/3, despite their respective barrels not being directly adjacent to each other in the barrel map. If this overlap involved some of the same neurons, it is possible that depression after Up state pairing also affected responses to surrounding whiskers, albeit to a lesser extent, leading to a decrease in the response to the unpaired whisker.

Further characterisation of the whisker response after Up state pairing suggested that long-term depression in layer 2/3 of the barrel cortex was not restricted to the principal barrel, but occurred across the receptive field of the stimulated whisker. Regression analysis between the amount of depression and the distance to the principal barrel indicated that depression of the spiking response at a particular recording site can be predicted by its distance from the principal barrel. These results also suggest that the spiking response was more depressed the further away the response was recorded from the principal barrel. The most prominent activation pathway in the barrel cortex after deflection of a single whisker consists of an initial response which is restricted to the principal barrel via thalamocortical connections to layer 4, before spreading to other layers and neighbouring barrel columns (Armstrong-James et al., 1992). Activation of

neighbouring barrels does not depend on separate thalamocortical synapses, but is the result of intracortical connections (Armstrong-James and Callahan, 1991; Fox, 1994; Fox et al., 2003). While depression of either the thalamocortical pathway to the principal barrel or intracortical pathways can be expected to lead to depression of the response in neighbouring areas, the significant distance-dependent effect suggests that it may be due to horizontal connections in layer 2/3.

The synaptic homeostasis hypothesis suggests that slow wave sleep is associated with downscaling of synapses (Tononi and Cirelli, 2003, 2006, 2014). My findings are consistent with the idea that Up/Down states are associated with synaptic depression. However, they also suggest that depression is activity-dependent rather than global, since the slow oscillation itself did not appear to affect baseline whisker responses. Recent findings in the entorhinal cortex *in vitro* support the idea that Up states can directly induce depression of simultaneously active synapses (Bartram et al., in review). It is conceivable that a similar process may operate in the barrel cortex to achieve depression of whisker responses during Up states *in vivo*. It should be noted that my findings contrast with a previous study in the barrel cortex, where repeated deflections of a whisker pair led to increased connectivity between the two whisker responses only when the whisker deflections were applied during Up states, but not during Down states (Erchova and Diamond, 2004). However, the pairing protocol used by Erchova and Diamond may have favoured a strengthening of connectivity due to the short delay between spontaneous spikes and whisker stimuli. Conversely, in a situation where the timing between Up state spiking and postsynaptic activity is not controlled for,

spike-timing-dependent mechanisms may be more likely to lead to depression due to the longer time window for t-LTD compared to t-LTP in the barrel cortex (Feldman, 2000). Whether spiking activity during Up states is indeed necessary for plasticity in the barrel cortex remains to be determined.

5.3.3 Laminar profile and locus of plasticity after Up state pairing

The first set of experiments showed that pairing of whisker deflections with Up states led to depression of responses to the paired whisker in layer 2/3. To investigate whether this effect can also be observed in other layers, recordings were made from all layers of a single barrel using a linear electrode probe. I found that depression was not restricted to layer 2/3, but also occurred in layer 4, albeit to a lesser extent. Furthermore, depression after Up state pairing decreased from superficial to deep layers, where the whisker response remained unchanged. This effect was observed both in the LFP and STH. However, this did not resolve the locus of plasticity, as it could have resulted from either depression of thalamocortical or intracortical synapses.

CSD analysis of the whisker response showed an activation pattern like the one originally described in rat barrel cortex after whisker stimulation (Di et al., 1990), starting with a large current sink in layer 4, which extends to layers 2/3 and 5. This is consistent with the idea that the whisker response first arrives in layer 4 via thalamocortical projections, before being relayed from layer 4 to layer 2/3 (Armstrong-James et al., 1992). Interestingly, further analysis of the current sink

in layer 4 and layer 2/3 before and after Up state pairing revealed that, while there was significant depression of the layer 2/3 peak after pairing, no significant depression was found in the peak of the earliest responding channel in layer 4. This result is consistent with depression of intracortical, rather than thalamocortical synapses. Indeed, findings from other studies indicate that thalamocortical synapses in the barrel cortex are much less plastic, with a critical period ending with the first postnatal week (Crair and Malenka, 1995; Feldman et al., 1998; Fox, 1995). The age used here was 6-8 weeks and therefore past this critical period. In contrast to thalamocortical synapses, connections to layer 2/3 have been shown to undergo plasticity much more readily, without being restricted to a certain developmental period (Fox, 1992). For instance, experience-dependent depression after whisker deprivation has been demonstrated in layer 2/3 without being present in layer 4 of the same barrel column after the critical period for thalamocortical plasticity (Glazewski and Fox, 1996). In addition, LTP and LTD can be readily induced *in vitro* in the pathway from layer 4 to layer 2/3 in barrel cortex slices (Allen et al., 2003; Feldman, 2000). Taken together, layer-specific results, together with the observation that plasticity was distance-dependent and not pathway-specific, suggest that depression after Up state pairing occurred at connections in layer 2/3. This could be further investigated in the future by using the optogenetic activator Channelrhodopsin-2 (ChR2) localised to specific layers to monitor the effect of Up state pairing on optically-evoked responses in vertical and horizontal connections.

5.3.4 Potential mechanism of long-term depression after Up state pairing

There are various studies linking LTD to the action of NMDA receptors in different brain areas (Malenka and Bear, 2004), including layer 2/3 of the barrel cortex (Banerjee et al., 2014; Rodríguez-Moreno and Paulsen, 2008). I investigated whether such a mechanism may be responsible for plasticity of whisker responses after Up state pairing by applying the NMDA receptor antagonist AP5. However, I found no significant difference in the amount of depression of the LFP peak after pairing when AP5 was applied to the surface of the brain throughout the experiment, suggesting that this type of plasticity may not be dependent on NMDA receptors. The drug significantly affected whisker responses in all layers, with spiking responses being almost completely suppressed in layers 2/3 and 4, making it impossible to analyse STHs before and after pairing. This is consistent with the notion that postsynaptic NMDA receptors play a role in normal synaptic transmission in the barrel cortex *in vivo* (Armstrong-James et al., 1993). It also indicates that the drug was effective at inhibiting NMDA receptors in the experiments described here and that it reached layer 4 upon application to the brain surface. Interestingly, due to the suppressive effect of NMDA receptor antagonists on sensory responses, there is only little evidence directly implicating NMDA receptors in experience-dependent plasticity after whisker trimming *in vivo*. One study suggests that AP5 only partially inhibits experience-dependent plasticity in the barrel cortex (Rema et al., 1998). This inconsistency may be due to confounding effects of NMDA receptor antagonists on normal synaptic transmission. Other studies have instead concentrated on potential downstream

targets of NMDA receptors, whose inhibition does not interfere with normal synaptic transmission, also making it a possible strategy for Up state pairing experiments. For instance, it was found that CamKII plays a role in experience-dependent plasticity in the barrel cortex (Glazewski et al., 1996, 2000) and that depression is dependent on the AMPA receptor subunit GluR1 in layers 2/3 and 4 (Wright et al., 2008). AMPA receptor conductance can be regulated by CamKII via phosphorylation of the GluR1 subunit (Derkach et al., 1999). In addition, it was found that PKA activity plays a role in LTD *in vitro* and in experience-dependent depression in the barrel cortex *in vivo* (Hardingham et al., 2008). However, plasticity can also be regulated by other pathways which do not depend on NMDA receptors, such as via mGluRs (Kubota et al., 2016; Malenka and Bear, 2004) or presynaptic LTD resulting from cannabinoid release by postsynaptic neurons (Bender et al., 2006). In contrast to mechanisms involving a depression of excitatory pathways, plasticity may also be due to an increase in inhibition. This has been suggested to occur in adult barrel cortex after 24 hours of chronic whisker stimulation (Quairiaux et al., 2007). However, this conclusion seemed to be mainly based on structural evidence of an increased density of GABAergic synapses (Knott et al., 2002). Taken together, there is scope for future experiments to investigate the mechanism underlying plasticity after Up state pairing using pharmacological methods or knockout mice.

6 General discussion

6.1 Summary of findings

I investigated whether Up states can facilitate plasticity of paired inputs, and whether Up states and Down states differ in this respect. The mouse barrel cortex was used as a model system for experiments *in vitro* in acute slice preparations and *in vivo* in anaesthetised mice.

By recording from pyramidal neurons in layer 2/3 *in vitro*, I found that neurons in coronal slices of barrel cortex were generally in a Down state and only very rarely displayed any spontaneous activity. However, I also demonstrated that, in this preparation, a single Up state can be evoked by applying a brief electrical pulse to layer 4. Electrical stimulation was most effective at producing Up states when the concentration of extracellular Ca^{2+} was lowered to 1.2 mM and least effective at a concentration of 2 mM. At an intermediate Ca^{2+}-concentration of 1.6 mM, Up states could be evoked in the majority of slices, but at a lower probability compared to 1.2 mM. Consistent with previous studies, I found that application of an NMDA receptor antagonist completely inhibited electrically-evoked Up states in my preparation (Sanchez-Vives and McCormick, 2000; Shu et al., 2003). On the other hand, inhibition of mGluRs may only subtly influence Up state dynamics, since application of an antagonist did not have any significant effects under conditions used here. However, results from pharmacological studies are only preliminary.

Using this model system, I then went on to investigate the effect of electrically-evoked Up states on paired inputs. To achieve this, perforated patch-clamp recordings were made from layer 2/3 pyramidal neurons, while EPSPs were evoked by electrical stimulation in layer 2/3 near the patched cell. During each pairing session, EPSPs were paired with either Up states or Down states. In a subset of experiments, brief current pulses were injected into the cell during pairing to make it spike shortly after each EPSP. This was to investigate the effect of Up states on suprathreshold inputs. In my experiments, I found that pairing a train of EPSPs with Up states induced LTD when EPSPs were applied at 10, 20, or 40 Hz. However, the effect was relatively small and, moreover, no difference was found in the size of the EPSP after pairing with Up states or Down states. In contrast, pairing of suprathreshold inputs with evoked Up states induced LTP. Again, no significant difference was found between Up state and Down state pairings. These results suggest that, in the model system used here, there was no difference between Up states and Down states in their propensity to affect synaptic plasticity. This is somewhat surprising, since data obtained in slices of entorhinal cortex revealed that pairing of subthreshold inputs with Up states, but not Down states, results in synaptic depression (Bartram et al., in review). Another study conducted in the barrel cortex *in vitro* suggests that pairing single spikes with spontaneous Up states results in LTP, indicating that there may be differences between evoked and spontaneous network activity in promoting plasticity. Other potential reasons for the lack of state-dependent plasticity in my barrel cortex preparation include the increased sparseness of evoked Up state activity over time and possibly reduced plasticity in neocortical circuits, which is difficult to overcome by simply increasing the number of pairings during patch-

clamp recordings. There are other ways which could conceivably circumvent these issues. For instance, plasticity could be studied *in vitro* using LFP recordings from barrel cortex slices kept in an interface recording chamber, in which it is easier to induce network activity. It may also be possible to achieve a higher probability and amplitude of evoked Up states by further manipulating the ionic composition of the extracellular solution. Instead, I decided to study plasticity during Up/Down states *in vivo*, where Up states occur spontaneously under anaesthesia and simple sensory stimuli can be applied by deflection of a whisker. While pairing such stimuli with Up states is somewhat less straightforward due to the lack of temporal control over the timing of network activity, this system has the advantage that plasticity can be studied long-term in the intact brain using extracellular recordings, which also allow for more long-term pairings.

In vivo, I investigated whether pairing deflections of a single whisker with Up states over a period can lead to plasticity in the response to that whisker. In a way that was analogous to *in vitro* experiments, 10 Hz whisker deflections were paired with either Up states or Down states. As alluded to above, applying stimuli during Up states under anaesthesia required control over the timing of spontaneous activity. To achieve this, Up/Down states were detected in real time by a mechanism involving the LFP crossing a set voltage threshold during an Up state. I found that pairing of whisker stimuli with Up states led to long-term depression of responses in layer 2/3 of the barrel cortex, whereas pairing with Down states did not have any long-term effects. This was true for principal and surrounding barrels. Specifically, spiking responses after Up state pairing were suppressed more strongly in surrounding barrels. Furthermore, Up state-pairing experiments

in which the response to a second, unpaired whisker was monitored, imply that plasticity was not specific to the stimulated pathway. Laminar analysis showed that depression after Up state pairing was strongest in layer 2/3 and decreased towards layer 5. In addition, CSD analysis of the whisker response indicates that depression occurred at intracortical connections, as no significant depression was found in the earliest (thalamocortical) response component. This, together with the observation that plasticity was distance-dependent and not pathway-specific, suggests that plasticity may occur at horizontal connections in layer 2/3. Lastly, inhibition of NMDA receptors in the barrel cortex by superficial application of the antagonist AP5 did not significantly inhibit depression of whisker responses after Up state pairing.

6.2 Feasibility of the mouse barrel cortex as a model system for evoked Up states and associated plasticity *in vitro*

Synaptic plasticity has been extensively studied in vitro in acute slices of different brain areas, including the barrel cortex. In the barrel cortex, LTP and LTD can be induced in synapses onto layer 2/3 pyramidal neurons by stimulating vertical or horizontal pathways (for example: Allen et al., 2003; Banerjee et al., 2014; Hardingham et al., 2008), although it should be noted that the exact pathway cannot be distinguished when electrical stimulation is used. While these experiments are typically carried out using high extracellular Ca^{2+} concentrations of 2 mM, I found that evoking Up states by electrical stimulation is much more reliable at lower Ca^{2+} concentrations, which may alter the propensity of synapses to undergo plasticity. Nevertheless, my experiments have shown that it is possible

to both induce plasticity and evoke Up states at an intermediate concentration of 1.6 mM. Being able to generate Up states by brief electrical pulses has the advantage that onset timing can be tightly controlled with respect to paired inputs. Furthermore, using such a reduced system makes it possible to study the effect of network activity in the absence of other factors such as neuromodulators. However, evoked Up states under conditions used here were almost always subthreshold, which is different to *in vivo* observations. Interestingly, it was not possible to obtain stable whole-cell recordings in my experiments, making it necessary to establish long-lasting perforated patch-clamp recordings. This recording configuration makes it impossible to carry out pharmacological studies by drug application via the patch pipette, a technique often used to elucidate the molecular mechanism of plasticity (for example: Bender et al., 2006; Hardingham et al., 2008; Rodríguez-Moreno et al., 2011).

6.3 Feasibility of the mouse barrel cortex as a model system for plasticity during spontaneous network activity under anaesthesia *in vivo*

The barrel cortex has the advantage that plasticity can also be studied in the whole organism *in vivo*, including under anaesthesia. Under anaesthesia, a simple stimulus can be applied by deflection of a whisker, which results in a discrete response that can be measured in the barrel cortex using extracellular electrodes. Pairing inputs with Up states or Down states *in vivo*, where slow oscillations occur spontaneously during anaesthesia, requires control over the timing of stimuli and ongoing spontaneous activity. While this may be difficult to achieve by

optogenetically forcing the network into a Down state, I have demonstrated that it is feasible to pair inputs with spontaneous activity by using a feedback system to detect Up states and apply whisker deflections. The obvious disadvantage of studying plasticity *in vivo* is the difficulty associated with pharmacological studies. For example, application of NMDA receptor antagonists has a suppressive effect on whisker responses, since NMDA receptors contribute to synaptic transmission *in vivo*. Interestingly, my observation that AP5 did not affect plasticity of whisker responses after Up state pairing is somewhat consistent with findings from experience-dependent plasticity, which was only partially inhibited after AP5 application (Rema et al., 1998).

6.4 Comparison between *in vitro* and *in vivo* findings

There seems to be some discrepancy between *in vitro* and *in vivo* data in terms of the effect of Up state and Down state pairings on plasticity. While I found no difference in the amount of depression after both pairings *in vitro*, long-term depression *in vivo* only occurred when inputs were paired with Up states. There are many differences between experimental setups *in vitro* and *in vivo* which could account for the discrepancies between results. Firstly, there may have been differences between properties of evoked Up states *in vitro* and spontaneous Up states *in vivo*. For example, I found that NMDA receptor antagonists had different effects *in vitro*, where evoked Up states were inhibited, and *in vivo*, where spontaneous Up states were still present after continued drug application. This may indicate differences in network state between the two systems, although it cannot be excluded that the lack of an effect *in vivo* was due to insufficient cortical

penetration of the drug. While the suppression of whisker responses suggests that AP5 reached deep layers, the concentration may not have been enough to affect network activity. Irrespective of this, there may have been differences between Up/Down states *in vitro* and *in vivo* in terms of their propensity to mediate plasticity of coincident inputs. As mentioned above, spontaneous Up states under anaesthesia were accompanied by spiking activity, whereas evoked Up states in slices were almost always subthreshold. If Up states mediate depression by spike-timing-based mechanisms, as it has been suggested elsewhere, it is conceivable that there was insufficient spiking activity to produce a significant effect *in vitro*. It is also possible that there are differences between pathways within the barrel cortex in their ability to undergo synaptic depression, and that synapses activated by stimulation protocols *in vitro* were less plastic. However, it should also be kept in mind that a much higher number of pairings was applied *in vivo*, something which would not be possible *in vitro*. It is conceivable that the number of Up state pairings *in vitro* was simply not enough to produce a significant difference, even though the underlying circuitry had the capacity to undergo plasticity. Another difference between *in vitro* and *in vivo* models is the potential action of neuromodulators, which are absent in slices. However, for neuromodulators to mediate the effect observed here, they would themselves have to undergo fluctuations consistent with Up/Down state activity. While neurons have been observed in various subcortical structures which display Up/Down state-correlated firing (Détári et al., 1997; Eschenko et al., 2012; Manns et al., 2000; Schweimer et al., 2011), it is unclear whether this impacts cortical activity. Finally, even though adolescent mice were used in both types of experiment, it cannot be ruled out that discrepancies between findings were due to developmental

differences in plasticity. If this was the case, one might expect circuits to be more plastic in younger animals (Fox, 2002). However, this seems to somewhat contradict my observations, because mice used for *in vivo* experiments were approximately four weeks older than mice used for *in vitro* experiments.

6.5 Conclusions and future directions

Taken together, observations *in vivo*, but not *in vitro* agree with earlier findings obtained from slices of entorhinal cortex (Bartram et al., in review) and provide support for synaptic depression during cortical slow oscillations. While long-term depression is generally consistent with the SHY (Tononi and Cirelli, 2003, 2006, 2014), data obtained here points towards an activity-dependent mechanism, rather than global synaptic downscaling. In addition, *in vivo* results suggest that Up states can directly facilitate long-term depression. In the future, it will be interesting to elucidate the pathway and mechanism underlying this type of plasticity. For instance, the underlying circuitry could be investigated by pairing Up states with light-evoked responses in mice with layer-specific expression of ChR2. In addition, the molecular mechanism of plasticity could be studied *in vivo* in knockout mice or by applying antagonists to the surface of the barrel cortex. For example, the AMPA receptor subunit GluR1, as well as mGluRs, have previously been implicated in certain types of plasticity in the barrel cortex (Bender et al., 2006; Kubota et al., 2016; Wright et al., 2008). In addition to this, it would be interesting to determine the role of Up state spiking in mediating synaptic depression. *In vivo*, this would require suppressing spiking activity during Up states, which may be possible using optogenetic methods. Finally, it would be

particularly valuable to investigate whether Up states play a role in experience-dependent plasticity in naturally sleeping mice.

7 Appendix

7.1 General properties of *in vitro* plasticity experiments

Up state duration and probability was measured after each experiment. All baseline recording sweeps were used except during pairing periods.

Experiment ID	Paired with	Pairing frequency (Hz)	US probability (%)	US duration (s)
10US1	Up state	10	85.29	0.89
10US2	Up state	10	84.52	1.30
10US3	Up state	10	30.17	1.38
10US4	Up state	10	69.61	1.15
10US5	Up state	10	23.53	1.74
10US6	Up state	10	48.62	1.31
		Average	**56.96**	**1.30**

Table 5. Properties of Up state pairing experiments with EPSPs at a frequency of 10 Hz.

Experiment ID	Paired with	Pairing frequency (Hz)	US probability (%)	US duration (s)
10DS1	Down state	10	12.90	1.75
10DS2	Down state	10	39.39	1.54
10DS3	Down state	10	33.33	1.33
10DS4	Down state	10	65.09	1.48
10DS5	Down state	10	10.55	2.51
		Average	**32.25**	**1.72**

Table 6. Properties of Down state pairing experiments with EPSPs at a frequency of 10 Hz.

Experi-ment ID	Paired with	Pairing frequency (Hz)	US probability (%)	US duration (s)
20US1	Up state	20	81.76	1.01
20US2	Up state	20	69.93	1.44
20US3	Up state	20	94.58	1.31
20US4	Up state	20	77.78	1.27
20US5	Up state	20	58.78	1.54
		Average	**76.57**	**1.32**

Table 7. Properties of Up state pairing experiments with EPSPs at a frequency of 20 Hz.

Experiment ID	Paired with	Pairing frequency (Hz)	US probability (%)	US duration (s)
20DS1	Down state	20	43.25	2.10
20DS2	Down state	20	45.87	1.88
20DS3	Down state	20	7.33	3.42
20DS4	Down state	20	13.89	1.82
20DS5	Down state	20	18.45	2.02
		Average	**25.76**	**2.25**

Table 8. Properties of Down state pairing experiments with EPSPs at a frequency of 20 Hz.

Experi-ment ID	Paired with	Pairing frequency (Hz)	US probability (%)	US duration (s)
40US1	Up state	40	34.54	1.56
40US2	Up state	40	82.63	1.21
40US3	Up state	40	59.89	1.44
40US4	Up state	40	43.52	1.10
40US5	Up state	40	26.25	2.04
		Average	**49.37**	**1.47**

Table 9. Properties of Up state pairing experiments with EPSPs at a frequency of 40 Hz.

Experiment ID	Paired with	Pairing frequency (Hz)	US probability (%)	US duration (s)
40DS1	Down state	40	41.81	1.76
40DS2	Down state	40	43.04	1.72
40DS3	Down state	40	16.87	0.99
40DS4	Down state	40	23.30	1.82
40DS5	Down state	40	80.00	1.04
		Average	**41.00**	**1.47**

Table 10. Properties of Down state pairing experiments with EPSPs at a frequency of 40 Hz.

Experiment ID	Paired with	Pairing frequency (Hz)	US probability (%)	US duration (s)
S20US1	Up state	20	71.66	1.38
S20US2	Up state	20	65.21	1.39
S20US3	Up state	20	93.82	1.83
S20US4	Up state	20	87.97	1.20
S20US5	Up state	20	65.54	1.34
		Average	**76.84**	**1.43**

Table 11. Properties of Up state pairing experiments with suprathreshold inputs. It was not possible to accurately count the number of successful pairings, since suprathreshold trains frequently masked the end of an Up state.

Experiment ID	Paired with	Pairing frequency (Hz)	US probability (%)	US duration (s)
S20DS1	Down state	20	16.86	0.89
S20DS2	Down state	20	34.87	1.40
S20DS3	Down state	20	50.90	1.12
S20DS4	Down state	20	35.95	0.95
S20DS5	Down state	20	0.68	1.28
		Average	**27.85**	**1.13**

Table 12. Properties of Down state pairing experiments with suprathreshold inputs.

7.2 General properties of *in vivo* plasticity experiments

Up/Down state parameters were measured using a 5 min sham pairing period without whisker stimulation which was recorded before the start of each experiment. This was done to ensure accurate measurement of false positive rates for Up/Down state pairings, without interference by whisker responses which may otherwise be falsely detected as Up states by the Up state detection algorithm.

Exper-iment ID	Paired with	No. of pairings	False positive (%)	Up state duration (s)	Down state duration (s)	Up state frequency (Hz)
US1	Up state	5124	6.46	0.63	0.67	0.78
US2	Up state	3520	11.71	1.08	0.33	0.71
US3	Up state	6269	7.65	0.95	0.32	0.84
US4	Up state	4889	3.35	1.12	1.07	0.46
US5	Up state	6376	5.45	1.00	0.57	0.64
US6	Up state	9191	16.35	0.81	0.49	0.78
	Average	**5895**	**8.50**	**0.93**	**0.58**	**0.70**

Table 13. Properties of Up state pairing experiments using the 64-channel electrode array.

Experiment ID	Paired with	No. of pairings	False positive (%)	Up state duration (s)	Down state duration (s)	Up state frequency (Hz)
DS1	Down state	3547	31.52	0.88	0.36	0.81
DS2	Down state	6469				
DS3	Down state	7063	36.41	0.92	0.66	0.64
DS4	Down state	6807	30.19	1.00	0.69	0.60
DS5	Down state	2983	34.63	1.05	0.96	0.50
	Average	**5374**	**33.19**	**0.96**	**0.67**	**0.64**

Table 14. Properties of Down state pairing experiments using the 64-channel electrode array. The missing entries for DS2 are due to lack of the control recording period of Down state pairings without whisker stimulation. Because the Down state pairing paradigm was otherwise robust (with very similar false positive rates across experiments), DS2 was still included in the analysis.

Experiment ID	Paired with	No. of pairings	False positive (%)	Up state duration (s)	Down state duration (s)	Up state frequency (Hz)
USL1	Up state	5809	14.41	1.11	0.91	0.5
USL2	Up state	8444	3.83	1.12	0.57	0.60
USL3	Up state	8369	3.03	0.80	1.67	0.41
USL4	Up state	7994	1.50	0.94	0.51	0.70
USL5	Up state	5013	0.21	0.95	0.60	0.66
	Average	**7126**	**4.60**	**0.98**	**0.85**	**0.57**

Table 15. Properties of Up state pairing experiments using the 32-channel linear electrode probe. Only control experiments (without drug application) are included in this table.

Exper-iment ID	Paired with	No. of pairings	False positive (%)	Up state duration (s)	Down state duration (s)	Up state frequency (Hz)
USL9	Up state	7494	1.92	1.02	0.42	0.69
USL10	Up state	6192	0.46	0.92	0.53	0.69
USL11	Up state	8149	1.62	1.02	0.39	0.71
USL12	Up state	5794	0.26	1.20	0.75	0.52
	Average	**6907**	**1.07**	**1.04**	**0.52**	**0.65**

Table 16. Properties of Up state pairing experiments using the 32-channel linear electrode probe. Only AP5 experiments are included in this table.

8 References

Abraham, W.C., and Williams, J.M. (2003). Properties and Mechanisms of LTP Maintenance. The Neuroscientist *9*, 463–474.

Achermann, P., and Borbély, A.A. (1997). Low-frequency (<1 Hz) oscillations in the human sleep electroencephalogram. Neuroscience *81*, 213–222.

Allen, C.B., Celikel, T., and Feldman, D.E. (2003). Long-term depression induced by sensory deprivation during cortical map plasticity in vivo. Nat. Neurosci. *6*, 291–299.

Amzica, F., and Steriade, M. (1995). Short- and long-range neuronal synchronization of the slow (< 1 Hz) cortical oscillation. J. Neurophysiol. *73*, 20–38.

Anderson, J., Lampl, I., Reichova, I., Carandini, M., and Ferster, D. (2000). Stimulus dependence of two-state fluctuations of membrane potential in cat visual cortex. Nat. Neurosci. *3*, 617–621.

Anwyl, R. (2009). Metabotropic glutamate receptor-dependent long-term potentiation. Neuropharmacology *56*, 735–740.

Armstrong-James, M., and Callahan, C.A. (1991). Thalamo-cortical processing of vibrissal information in the rat. II. Spatiotemporal convergence in the thalamic ventroposterior medial nucleus (VPm) and its relevance to generation of receptive fields of S1 cortical “Barrel” neurones. J. Comp. Neurol. *303*, 211–224.

Armstrong-James, M., and Fox, K. (1987). Spatiotemporal convergence and divergence in the rat S1 “Barrel” cortex. J. Comp. Neurol. *263*, 265–281.

Armstrong-James, M., and George, M.J. (1988). Influence of anesthesia on spontaneous activity and receptive field size of single units in rat Sm1 neocortex. Exp. Neurol. *99*, 369–387.

Armstrong-James, M., Callahan, C.A., and Friedman, M.A. (1991). Thalamo-cortical processing of vibrissal information in the rat. I. Intracortical origins of surround but not centre-receptive fields of layer IV neurones in the rat S1 barrel field cortex. J. Comp. Neurol. *303*, 193–210.

Armstrong-James, M., Fox, K., and Das-Gupta, A. (1992). Flow of excitation within rat barrel cortex on striking a single vibrissa. J. Neurophysiol. *68*, 1345–1358.

Armstrong-James, M., Welker, E., and Callahan, C.A. (1993). The contribution of NMDA and non-NMDA receptors to fast and slow transmission of sensory information in the rat SI barrel cortex. J. Neurosci. *13*, 2149–2160.

Aroniadou-Anderjaska, V., and Keller, A. (1995). LTP in the barrel cortex of adult rats. Neuroreport *6*, 2297–2300.

Artola, A., and Singer, W. (1987). Long-term potentiation and NMDA receptors in rat visual cortex. Nature *330*, 649–652.

Artola, A., Bröcher, S., and Singer, W. (1990). Different voltage-dependent thresholds for inducing long-term depression and long-term potentiation in slices of rat visual cortex. Nature *347*, 69–72.

Banerjee, A., González-Rueda, A., Sampaio-Baptista, C., Paulsen, O., and Rodríguez-Moreno, A. (2014). Distinct mechanisms of spike timing-dependent LTD at vertical and horizontal inputs onto L2/3 pyramidal neurons in mouse barrel cortex. Physiol. Rep. *2*, e00271.

Barrionuevo, G., Schottler, F., and Lynch, G. (1980). The effects of repetitive low frequency stimulation on control and "potentiated" synaptic responses in the hippocampus. Life Sci. *27*, 2385–2391.

Bartram, J., Kahn, M.C., Tuohy, S., Paulsen, O., Wilson, T., and Mann, E.O. (in review). Selective weakening of subthreshold synaptic inputs during cortical slow waves. Nat. Commun.

Bellone, C., Lüscher, C., and Mameli, M. (2008). Mechanisms of synaptic depression triggered by metabotropic glutamate receptors. Cell. Mol. Life Sci. *65*, 2913–2923.

Beltramo, R., D'Urso, G., Dal Maschio, M., Farisello, P., Bovetti, S., Clovis, Y., Lassi, G., Tucci, V., De Pietri Tonelli, D., and Fellin, T. (2013). Layer-specific excitatory circuits differentially control recurrent network dynamics in the neocortex. Nat. Neurosci. *16*, 227–234.

Bender, V.A., Bender, K.J., Brasier, D.J., and Feldman, D.E. (2006). Two Coincidence Detectors for Spike Timing-Dependent Plasticity in Somatosensory Cortex. J. Neurosci. *26*, 4166–4177.

Benke, T.A., Lüthi, A., Isaac, J.T.R., and Collingridge, G.L. (1998). Modulation of AMPA receptor unitary conductance by synaptic activity. Nature *393*, 793–797.

Benshalom, G., and White, E.L. (1986). Quantification of thalamocortical synapses with spiny stellate neurons in layer IV of mouse somatosensory cortex. J. Comp. Neurol. *253*, 303–314.

Berger, T., Borgdorff, A., Crochet, S., Neubauer, F.B., Lefort, S., Fauvet, B., Ferezou, I., Carleton, A., Lüscher, H.-R., and Petersen, C.C.H. (2007). Combined Voltage and Calcium Epifluorescence Imaging In Vitro and In Vivo Reveals Subthreshold and Suprathreshold Dynamics of Mouse Barrel Cortex. J. Neurophysiol. *97*, 3751–3762.

Bermudez Contreras, E.J., Schjetnan, A.G.P., Muhammad, A., Bartho, P., McNaughton, B.L., Kolb, B., Gruber, A.J., and Luczak, A. (2013). Formation and Reverberation of Sequential Neural Activity Patterns Evoked by Sensory Stimulation Are Enhanced during Cortical Desynchronization. Neuron *79*, 555–566.

Bernardo, K.L., and Woolsey, T.A. (1987). Axonal trajectories between mouse somatosensory thalamus and cortex. J. Comp. Neurol. *258*, 542–564.

Bernardo, K.L., McCasland, J.S., Woolsey, T.A., and Strominger, R.N. (1990). Local intra- and interlaminar connections in mouse barrel cortex. J. Comp. Neurol. *291*, 231–255.

Bindman, L.J., Murphy, K.P., and Pockett, S. (1988). Postsynaptic control of the induction of long-term changes in efficacy of transmission at neocortical synapses in slices of rat brain. J. Neurophysiol. *60*, 1053–1065.

Bliss, T.V.P., and Collingridge, G.L. (1993). A synaptic model of memory: long-term potentiation in the hippocampus. Nature *361*, 31–39.

Bliss, T.V.P., and Lømo, T. (1973). Long-lasting potentiation of synaptic transmission in the dentate area of the anaesthetized rabbit following stimulation of the perforant path. J. Physiol. *232*, 331–356.

Blitzer, R.D., Connor, J.H., Brown, G.P., Wong, T., Shenolikar, S., Iyengar, R., and Landau, E.M. (1998). Gating of CaMKII by cAMP-Regulated Protein Phosphatase Activity During LTP. Science *280*, 1940–1943.

Borbély, A.A. (2001). From slow waves to sleep homeostasis: new perspectives. Arch. Ital. Biol. *139*, 53–61.

Bramham, C.R., and Srebro, B. (1987). Induction of long-term depression and potentiation by low- and high-frequency stimulation in the dentate area of the anesthetized rat: magnitude, time course and EEG. Brain Res. *405*, 100–107.

Brecht, M., Roth, A., and Sakmann, B. (2003). Dynamic Receptive Fields of Reconstructed Pyramidal Cells in Layers 3 and 2 of Rat Somatosensory Barrel Cortex. J. Physiol. *553*, 243–265.

Bröcher, S., Artola, A., and Singer, W. (1992). Agonists of cholinergic and noradrenergic receptors facilitate synergistically the induction of long-term potentiation in slices of rat visual cortex. Brain Res. *573*, 27–36.

Bruno, R.M., and Sakmann, B. (2006). Cortex Is Driven by Weak but Synchronously Active Thalamocortical Synapses. Science *312*, 1622–1627.

Bushey, D., Tononi, G., and Cirelli, C. (2011). Sleep and Synaptic Homeostasis: Structural Evidence in Drosophila. Science *332*, 1576–1581.

Carter, B.C., and Jahr, C.E. (2016). Postsynaptic, not presynaptic NMDA receptors are required for spike-timing-dependent LTD induction. Nat. Neurosci. *19*, 1218–1224.

Castillo, P.E. (2012). Presynaptic LTP and LTD of Excitatory and Inhibitory Synapses. Cold Spring Harb. Perspect. Biol. *4*, a005728.

Castro-Alamancos, M.A., Donoghue, J.P., and Connors, B.W. (1995a). Different forms of synaptic plasticity in somatosensory and motor areas of the neocortex. J. Neurosci. *15*, 5324–5333.

Castro-Alamancos, M.A., Donoghue, J.P., and Connors, B.W. (1995b). Different forms of synaptic plasticity in somatosensory and motor areas of the neocortex. J. Neurosci. *15*, 5324–5333.

Chauvette, S., Volgushev, M., and Timofeev, I. (2010). Origin of Active States in Local Neocortical Networks during Slow Sleep Oscillation. Cereb. Cortex N. Y. NY *20*, 2660–2674.

Chauvette, S., Crochet, S., Volgushev, M., and Timofeev, I. (2011). Properties of Slow Oscillation during Slow-Wave Sleep and Anesthesia in Cats. J. Neurosci. *31*, 14998–15008.

Chen, J.-Y., Chauvette, S., Skorheim, S., Timofeev, I., and Bazhenov, M. (2012). Interneuron-mediated inhibition synchronizes neuronal activity during slow oscillation. J. Physiol. *590*, 3987–4010.

Chiaia, N.L., Rhoades, R.W., Bennett-Clarke, C.A., Fish, S.E., and Killackey, H.P. (1991). Thalamic processing of vibrissal information in the rat. I. Afferent input to the medial ventral posterior and posterior nuclei. J. Comp. Neurol. *314*, 201–216.

Compte, A., Sanchez-Vives, M.V., McCormick, D.A., and Wang, X.-J. (2003). Cellular and Network Mechanisms of Slow Oscillatory Activity (<1 Hz) and Wave Propagations in a Cortical Network Model. J. Neurophysiol. *89*, 2707–2725.

Compte, A., Reig, R., Descalzo, V.F., Harvey, M.A., Puccini, G.D., and Sanchez-Vives, M.V. (2008). Spontaneous High-Frequency (10–80 Hz) Oscillations during Up States in the Cerebral Cortex In Vitro. J. Neurosci. *28*, 13828–13844.

Contreras, D., Timofeev, I., and Steriade, M. (1996). Mechanisms of long-lasting hyperpolarizations underlying slow sleep oscillations in cat corticothalamic networks. J. Physiol. *494*, 251–264.

Crair, M.C., and Malenka, R.C. (1995). A critical period for long-term potentiation at thalamocortical synapses. Nature *375*, 325–328.

Crunelli, V., and Hughes, S.W. (2010). The slow (<1 Hz) rhythm of non-REM sleep: a dialogue between three cardinal oscillators. Nat. Neurosci. *13*, 9–17.

Czarnecki, A., Birtoli, B., and Ulrich, D. (2007). Cellular mechanisms of burst firing-mediated long-term depression in rat neocortical pyramidal cells. J. Physiol. *578*, 471–479.

Davidson, T.J., Kloosterman, F., and Wilson, M.A. (2009). Hippocampal Replay of Extended Experience. Neuron *63*, 497–507.

De Kock, C.P.J., Bruno, R.M., Spors, H., and Sakmann, B. (2007). Layer- and cell-type-specific suprathreshold stimulus representation in rat primary somatosensory cortex. J. Physiol. *581*, 139–154.

Derkach, V., Barria, A., and Soderling, T.R. (1999). Ca2+/calmodulin-kinase II enhances channel conductance of α-amino-3-hydroxy-5-methyl-4-isoxazolepropionate type glutamate receptors. Proc. Natl. Acad. Sci. *96*, 3269–3274.

Desîlets-Roy, B., Varga, C., Lavallée, P., and Deschênes, M. (2002). Substrate for Cross-Talk Inhibition between Thalamic Barreloids. J. Neurosci. *22*, RC218-RC218.

Détári, L., Rasmusson, D.D., and Semba, K. (1997). Phasic relationship between the activity of basal forebrain neurons and cortical EEG in urethane-anesthetized rat. Brain Res. *759*, 112–121.

Di, S., Baumgartner, C., and Barth, D.S. (1990). Laminar analysis of extracellular field potentials in rat vibrissa/barrel cortex. J. Neurophysiol. *63*, 832–840.

Diamond, M.E., Armstrong-James, M., and Ebner, F.F. (1992). Somatic sensory responses in the rostral sector of the posterior group (POm) and in the ventral posterior medial nucleus (VPM) of the rat thalamus. J. Comp. Neurol. *318*, 462–476.

Diamond, M.E., Armstrong-James, M., and Ebner, F.F. (1993). Experience-dependent plasticity in adult rat barrel cortex. Proc. Natl. Acad. Sci. U. S. A. *90*, 2082–2086.

Diba, K., and Buzsáki, G. (2007). Forward and reverse hippocampal place-cell sequences during ripples. Nat. Neurosci. *10*, 1241–1242.

Diekelmann, S., and Born, J. (2010). The memory function of sleep. Nat. Rev. Neurosci. *11*, 114–126.

Diering, G.H., Nirujogi, R.S., Roth, R.H., Worley, P.F., Pandey, A., and Huganir, R.L. (2017). Homer1a drives homeostatic scaling-down of excitatory synapses during sleep. Science *355*, 511–515.

Donlea, J.M., Ramanan, N., and Shaw, P.J. (2009). Use-Dependent Plasticity in Clock Neurons Regulates Sleep Need in Drosophila. Science *324*, 105–108.

Dringenberg, H.C., Hamze, B., Wilson, A., Speechley, W., and Kuo, M.-C. (2007). Heterosynaptic Facilitation of In Vivo Thalamocortical Long-Term Potentiation in the Adult Rat Visual Cortex by Acetylcholine. Cereb. Cortex *17*, 839–848.

Dumoulin Bridi, M.C., Aton, S.J., Seibt, J., Renouard, L., Coleman, T., and Frank, M.G. (2015). Rapid eye movement sleep promotes cortical plasticity in the developing brain. Sci. Adv. *1*.

Ebara, S., Kumamoto, K., Matsuura, T., Mazurkiewicz, J.E., and Rice, F.L. (2002). Similarities and differences in the innervation of mystacial vibrissal follicle–sinus complexes in the rat and cat: A confocal microscopic study. J. Comp. Neurol. *449*, 103–119.

Erchova, I.A., and Diamond, M.E. (2004). Rapid fluctuations in rat barrel cortex plasticity. J. Neurosci. Off. J. Soc. Neurosci. *24*, 5931–5941.

Erchova, I.A., Lebedev, M.A., and Diamond, M.E. (2002). Somatosensory cortical neuronal population activity across states of anaesthesia. Eur. J. Neurosci. *15*, 744–752.

Eschenko, O., Magri, C., Panzeri, S., and Sara, S.J. (2012). Noradrenergic Neurons of the Locus Coeruleus Are Phase Locked to Cortical Up-Down States during Sleep. Cereb. Cortex *22*, 426–435.

Euston, D.R., Tatsuno, M., and McNaughton, B.L. (2007). Fast-Forward Playback of Recent Memory Sequences in Prefrontal Cortex During Sleep. Science *318*, 1147–1150.

Faul, F., Erdfelder, E., Lang, A.-G., and Buchner, A. (2007). G*Power 3: a flexible statistical power analysis program for the social, behavioral, and biomedical sciences. Behav. Res. Methods *39*, 175–191.

Faul, F., Erdfelder, E., Buchner, A., and Lang, A.-G. (2009). Statistical power analyses using G*Power 3.1: tests for correlation and regression analyses. Behav. Res. Methods *41*, 1149–1160.

Feldman, D.E. (2000). Timing-Based LTP and LTD at Vertical Inputs to Layer II/III Pyramidal Cells in Rat Barrel Cortex. Neuron *27*, 45–56.

Feldman, D.E., Nicoll, R.A., Malenka, R.C., and Isaac, J.T.R. (1998). Long-Term Depression at Thalamocortical Synapses in Developing Rat Somatosensory Cortex. Neuron *21*, 347–357.

Feldmeyer, D. (2012). Excitatory neuronal connectivity in the barrel cortex. Front. Neuroanat. *6*.

Feldmeyer, D., Egger, V., Lübke, J., and Sakmann, B. (1999). Reliable synaptic connections between pairs of excitatory layer 4 neurones within a single “barrel” of developing rat somatosensory cortex. J. Physiol. *521*, 169–190.

Feldmeyer, D., Lübke, J., Silver, R.A., and Sakmann, B. (2002). Synaptic connections between layer 4 spiny neurone- layer 2/3 pyramidal cell pairs in juvenile rat barrel cortex: physiology and anatomy of interlaminar signalling within a cortical column. J. Physiol. *538*, 803–822.

Feldmeyer, D., Roth, A., and Sakmann, B. (2005). Monosynaptic Connections between Pairs of Spiny Stellate Cells in Layer 4 and Pyramidal Cells in Layer 5A Indicate That Lemniscal and Paralemniscal Afferent Pathways Converge in the Infragranular Somatosensory Cortex. J. Neurosci. *25*, 3423–3431.

Feldmeyer, D., Brecht, M., Helmchen, F., Petersen, C.C.H., Poulet, J.F.A., Staiger, J.F., Luhmann, H.J., and Schwarz, C. (2013). Barrel cortex function. Prog. Neurobiol. *103*, 3–27.

Ferezou, I., Bolea, S., and Petersen, C.C.H. (2006). Visualizing the Cortical Representation of Whisker Touch: Voltage-Sensitive Dye Imaging in Freely Moving Mice. Neuron *50*, 617–629.

Foster, D.J., and Wilson, M.A. (2006). Reverse replay of behavioural sequences in hippocampal place cells during the awake state. Nature *440*, 680–683.

Fox, K. (1992). A critical period for experience-dependent synaptic plasticity in rat barrel cortex. J. Neurosci. *12*, 1826–1838.

Fox, K. (1994). The cortical component of experience-dependent synaptic plasticity in the rat barrel cortex. J. Neurosci. *14*, 7665–7679.

Fox, K. (1995). The critical period for long-term potentiation in primary sensory cortex. Neuron *15*, 485–488.

Fox, K. (2002). Anatomical pathways and molecular mechanisms for plasticity in the barrel cortex. Neuroscience *111*, 799–814.

Fox, K. (2008). Barrel Cortex (Cambridge University Press).

Fox, K., Wright, N., Wallace, H., and Glazewski, S. (2003). The Origin of Cortical Surround Receptive Fields Studied in the Barrel Cortex. J. Neurosci. *23*, 8380–8391.

Frank, M.G. (2012). Erasing Synapses in Sleep: Is It Time to Be SHY? Neural Plast. *2012*, e264378.

Frankenhaeuser, B., and Hodgkin, A.L. (1957). The action of calcium on the electrical properties of squid axons. J. Physiol. *137*, 218–244.

Frankland, P.W., and Bontempi, B. (2005). The organization of recent and remote memories. Nat. Rev. Neurosci. *6*, 119–130.

Friedberg, M.H., Lee, S.M., and Ebner, F.F. (1999). Modulation of Receptive Field Properties of Thalamic Somatosensory Neurons by the Depth of Anesthesia. J. Neurophysiol. *81*, 2243–2252.

Gais, S., Lucas, B., and Born, J. (2006). Sleep after learning aids memory recall. Learn. Mem. *13*, 259–262.

Gambino, F., Pagès, S., Kehayas, V., Baptista, D., Tatti, R., Carleton, A., and Holtmaat, A. (2014). Sensory-evoked LTP driven by dendritic plateau potentials in vivo. Nature *515*, 116–119.

Garside, P., Arizpe, J., Lau, C.-I., Goh, C., and Walsh, V. (2015). Cross-hemispheric Alternating Current Stimulation During a Nap Disrupts Slow Wave Activity and Associated Memory Consolidation. Brain Stimulat. *8*, 520–527.

Gerdeman, G.L., Ronesi, J., and Lovinger, D.M. (2002). Postsynaptic endocannabinoid release is critical to long-term depression in the striatum. Nat. Neurosci. *5*, 446–451.

Gilestro, G.F., Tononi, G., and Cirelli, C. (2009). Widespread Changes in Synaptic Markers as a Function of Sleep and Wakefulness in Drosophila. Science *324*, 109–112.

Glazewski, S. (1998). Experience-dependent changes in vibrissae evoked responses in the rodent barrel cortex. Acta Neurobiol. Exp. (Warsz.) *58*, 309–320.

Glazewski, S., and Fox, K. (1996). Time course of experience-dependent synaptic potentiation and depression in barrel cortex of adolescent rats. J. Neurophysiol. *75*, 1714–1729.

Glazewski, S., Chen, C.-M., Silva, A., and Fox, K. (1996). Requirement for α-CaMKII in Experience-Dependent Plasticity of the Barrel Cortex. Science *272*, 421–423.

Glazewski, S., Herman, C., McKenna, M., Chapman, P.F., and Fox, K. (1998a). Long-term potentiation in vivo in layers II/III of rat barrel cortex. Neuropharmacology *37*, 581–592.

Glazewski, S., McKenna, M., Jacquin, M., and Fox, K. (1998b). Experience-dependent depression of vibrissae responses in adolescent rat barrel cortex. Eur. J. Neurosci. *10*, 2107–2116.

Glazewski, S., Giese, K.P., Silva, A., and Fox, K. (2000). The role of α-CaMKII autophosphorylation in neocortical experience-dependent plasticity. Nat. Neurosci. *3*, 911–918.

Golmayo, L., Nuñez, A., and Zaborszky, L. (2003). Electrophysiological evidence for the existence of a posterior cortical–prefrontal–basal forebrain circuitry in modulating sensory responses in visual and somatosensory rat cortical areas. Neuroscience *119*, 597–609.

Gottlieb, J.P., and Keller, A. (1997). Intrinsic circuitry and physiological properties of pyramidal neurons in rat barrel cortex. Exp. Brain Res. *115*, 47–60.

Haider, B., Duque, A., Hasenstaub, A.R., Yu, Y., and McCormick, D.A. (2007). Enhancement of Visual Responsiveness by Spontaneous Local Network Activity In Vivo. J. Neurophysiol. *97*, 4186–4202.

Han, Y., Huang, M.-D., Sun, M.-L., Duan, S., and Yu, Y.-Q. (2015). Long-Term Synaptic Plasticity in Rat Barrel Cortex. Cereb. Cortex *25*, 2741–2751.

Hardingham, N., and Fox, K. (2006). The Role of Nitric Oxide and GluR1 in Presynaptic and Postsynaptic Components of Neocortical Potentiation. J. Neurosci. *26*, 7395–7404.

Hardingham, N., Glazewski, S., Pakhotin, P., Mizuno, K., Chapman, P.F., Giese, K.P., and Fox, K. (2003). Neocortical Long-Term Potentiation and Experience-Dependent Synaptic Plasticity Require α-Calcium/Calmodulin-Dependent Protein Kinase II Autophosphorylation. J. Neurosci. *23*, 4428–4436.

Hardingham, N., Wright, N., Dachtler, J., and Fox, K. (2008). Sensory Deprivation Unmasks a PKA-Dependent Synaptic Plasticity Mechanism that Operates in Parallel with CaMKII. Neuron *60*, 861–874.

Hartings, J.A., Temereanca, S., and Simons, D.J. (2000). High Responsiveness and Direction Sensitivity of Neurons in the Rat Thalamic Reticular Nucleus to Vibrissa Deflections. J. Neurophysiol. *83*, 2791–2801.

Hasenstaub, A., Sachdev, R.N.S., and McCormick, D.A. (2007). State Changes Rapidly Modulate Cortical Neuronal Responsiveness. J. Neurosci. *27*, 9607–9622.

Hayashi, Y., Shi, S.-H., Esteban, J.A., Piccini, A., Poncer, J.-C., and Malinow, R. (2000). Driving AMPA Receptors into Synapses by LTP and CaMKII: Requirement for GluR1 and PDZ Domain Interaction. Science *287*, 2262–2267.

Hays, S.A., Huber, K.M., and Gibson, J.R. (2011). Altered Neocortical Rhythmic Activity States in Fmr1 KO Mice Are Due to Enhanced mGluR5 Signaling and Involve Changes in Excitatory Circuitry. J. Neurosci. *31*, 14223–14234.

Hill, S., Tononi, G., and Ghilardi, M.F. (2008). Sleep improves the variability of motor performance. Brain Res. Bull. *76*, 605–611.

Hinard, V., Mikhail, C., Pradervand, S., Curie, T., Houtkooper, R.H., Auwerx, J., Franken, P., and Tafti, M. (2012). Key Electrophysiological, Molecular, and Metabolic Signatures of Sleep and Wakefulness Revealed in Primary Cortical Cultures. J. Neurosci. *32*, 12506–12517.

Hubel, D.H., and Wiesel, T.N. (1970). The period of susceptibility to the physiological effects of unilateral eye closure in kittens. J. Physiol. *206*, 419–436.

Huber, R., Mäki, H., Rosanova, M., Casarotto, S., Canali, P., Casali, A.G., Tononi, G., and Massimini, M. (2013). Human Cortical Excitability Increases with Time Awake. Cereb. Cortex *23*, 1–7.

Isaac, J.T.R., Crair, M.C., Nicoll, R.A., and Malenka, R.C. (1997). Silent Synapses during Development of Thalamocortical Inputs. Neuron *18*, 269–280.

Ismailov, I., Kalikulov, D., Inoue, T., and Friedlander, M.J. (2004). The Kinetic Profile of Intracellular Calcium Predicts Long-Term Potentiation and Long-Term Depression. J. Neurosci. *24*, 9847–9861.

Ito, M. (1985). Processing of vibrissa sensory information within the rat neocortex. J. Neurophysiol. *54*, 479–490.

Jacquin, M.F., Barcia, M., and Rhoades, R.W. (1989). Structure-function relationships in rat brainstem subnucleus interpolaris: IV. Projection neurons. J. Comp. Neurol. *282*, 45–62.

Jasper, H.H., and Tessier, J. (1971). Acetylcholine Liberation from Cerebral Cortex during Paradoxical (REM) Sleep. Science *172*, 601–602.

Ji, D., and Wilson, M.A. (2007). Coordinated memory replay in the visual cortex and hippocampus during sleep. Nat. Neurosci. *10*, 100–107.

Johnson, L.A., Euston, D.R., Tatsuno, M., and McNaughton, B.L. (2010). Stored-Trace Reactivation in Rat Prefrontal Cortex Is Correlated with Down-to-Up State Fluctuation Density. J. Neurosci. *30*, 2650–2661.

Karlsson, M.P., and Frank, L.M. (2009). Awake replay of remote experiences in the hippocampus. Nat. Neurosci. *12*, 913–918.

Knott, G.W., Quairiaux, C., Genoud, C., and Welker, E. (2002). Formation of Dendritic Spines with GABAergic Synapses Induced by Whisker Stimulation in Adult Mice. Neuron *34*, 265–273.

Kojic, L., Gu, Q., Douglas, R.M., and Cynader, M.S. (2001). Laminar distribution of cholinergic- and serotonergic-dependent plasticity within kitten visual cortex. Dev. Brain Res. *126*, 157–162.

Kossut, M., and Hand, P. (1984). Early development of changes in cortical representation of C3 vibrissa following neonatal denervation of surrounding vibrissa receptors: A 2-deoxyglucose study in the rat. Neurosci. Lett. *46*, 7–12.

Krupa, D.J., Wiest, M.C., Shuler, M.G., Laubach, M., and Nicolelis, M.A.L. (2004). Layer-Specific Somatosensory Cortical Activation During Active Tactile Discrimination. Science *304*, 1989–1992.

Kruskal, P.B., Li, L., and MacLean, J.N. (2013). Circuit reactivation dynamically regulates synaptic plasticity in neocortex. Nat. Commun. *4*, 2574.

Kubota, J., Mikami, Y., Kanemaru, K., Sekiya, H., Okubo, Y., and Iino, M. (2016). Whisker experience-dependent mGluR signaling maintains synaptic strength in the mouse adolescent cortex. Eur. J. Neurosci. *44*, 2004–2014.

Kudrimoti, H.S., Barnes, C.A., and McNaughton, B.L. (1999). Reactivation of Hippocampal Cell Assemblies: Effects of Behavioral State, Experience, and EEG Dynamics. J. Neurosci. *19*, 4090–4101.

Lanté, F., Toledo-Salas, J.-C., Ondrejcak, T., Rowan, M.J., and Ulrich, D. (2011). Removal of Synaptic Ca2+-Permeable AMPA Receptors during Sleep. J. Neurosci. *31*, 3953–3961.

Larson, J., Wong, D., and Lynch, G. (1986). Patterned stimulation at the theta frequency is optimal for the induction of hippocampal long-term potentiation. Brain Res. *368*, 347–350.

Lavzin, M., Rapoport, S., Polsky, A., Garion, L., and Schiller, J. (2012). Nonlinear dendritic processing determines angular tuning of barrel cortex neurons in vivo. Nature *490*, 397–401.

Le Bon-Jego, M., and Yuste, R. (2007). Persistently active, pacemaker-like neurons in neocortex. Front. Neurosci. *1*.

Lee, A.K., and Wilson, M.A. (2002). Memory of Sequential Experience in the Hippocampus during Slow Wave Sleep. Neuron *36*, 1183–1194.

Lee, L.-J., and Erzurumlu, R.S. (2005). Altered parcellation of neocortical somatosensory maps in N-methyl-D-aspartate receptor-deficient mice. J. Comp. Neurol. *485*, 57–63.

Lee, H.-K., Barbarosie, M., Kameyama, K., Bear, M.F., and Huganir, R.L. (2000). Regulation of distinct AMPA receptor phosphorylation sites during bidirectional synaptic plasticity. Nature *405*, 955–959.

Li, W., Ma, L., Yang, G., and Gan, W.-B. (2017). REM sleep selectively prunes and maintains new synapses in development and learning. Nat. Neurosci. *20*, 427–437.

Linden, D.J., and Routtenberg, A. (1989). The role of protein kinase C in long-term potentiation: a testable model. Brain Res. Rev. *14*, 279–296.

Lisman, J. (1989). A mechanism for the Hebb and the anti-Hebb processes underlying learning and memory. Proc. Natl. Acad. Sci. U. S. A. *86*, 9574–9578.

Lisman, J., Schulman, H., and Cline, H. (2002). The molecular basis of CaMKII function in synaptic and behavioural memory. Nat. Rev. Neurosci. *3*, 175–190.

Liu, Z.-W., Faraguna, U., Cirelli, C., Tononi, G., and Gao, X.-B. (2010). Direct Evidence for Wake-Related Increases and Sleep-Related Decreases in Synaptic Strength in Rodent Cortex. J. Neurosci. *30*, 8671–8675.

Lorincz, M.L., Gunner, D., Bao, Y., Connelly, W.M., Isaac, J.T.R., Hughes, S.W., and Crunelli, V. (2015). A distinct class of slow (0.2–2 Hz) intrinsically bursting layer 5 pyramidal neurons determines UP/DOWN state dynamics in the neocortex. J. Neurosci. *35*, 5442–5458.

Lu, S.-M., and Lin, R.C.-S. (1993). Thalamic Afferents of the Rat Barrel Cortex: A Light-and Electron-Microscopic Study Using Phaseolus vulgaris Leucoagglutinin as an Anterograde Tracer. Somatosens. Mot. Res. *10*, 1–16.

Lübke, J., Egger, V., Sakmann, B., and Feldmeyer, D. (2000). Columnar Organization of Dendrites and Axons of Single and Synaptically Coupled Excitatory Spiny Neurons in Layer 4 of the Rat Barrel Cortex. J. Neurosci. *20*, 5300–5311.

Lynch, G., Larson, J., Kelso, S., Barrionuevo, G., and Schottler, F. (1983). Intracellular injections of EGTA block induction of hippocampal long-term potentiation. Nature *305*, 719–721.

Ma, P.M., and Woolsey, T.A. (1984). Cytoarchitectonic correlates of the vibrissae in the medullary trigeminal complex of the mouse. Brain Res. *306*, 374–379.

MacLean, J.N., Watson, B.O., Aaron, G.B., and Yuste, R. (2005). Internal Dynamics Determine the Cortical Response to Thalamic Stimulation. Neuron *48*, 811–823.

Malenka, R.C., and Bear, M.F. (2004). LTP and LTD: An Embarrassment of Riches. Neuron *44*, 5–21.

Malenka, R.C., and Nicoll, and R.A. (1999). Long-Term Potentiation--A Decade of Progress? Science *285*, 1870–1874.

Malenka, R.C., and Nicoll, R.A. (1993). NMDA-receptor-dependent synaptic plasticity: multiple forms and mechanisms. Trends Neurosci. *16*, 521–527.

Malenka, R.C., Kauer, J.A., Zucker, R.S., and Nicoll, R.A. (1988). Postsynaptic calcium is sufficient for potentiation of hippocampal synaptic transmission. Science *242*, 81–84.

Malinow, R., and Malenka, R.C. (2002). Ampa Receptor Trafficking and Synaptic Plasticity. Annu. Rev. Neurosci. *25*, 103–126.

Mann, E.O., Kohl, M.M., and Paulsen, O. (2009). Distinct Roles of GABAA and GABAB Receptors in Balancing and Terminating Persistent Cortical Activity. J. Neurosci. *29*, 7513–7518.

Manns, I.D., Alonso, A., and Jones, B.E. (2000). Discharge Properties of Juxtacellularly Labeled and Immunohistochemically Identified Cholinergic Basal

Forebrain Neurons Recorded in Association with the Electroencephalogram in Anesthetized Rats. J. Neurosci. *20*, 1505–1518.

Maret, S., Faraguna, U., Nelson, A.B., Cirelli, C., and Tononi, G. (2011). Sleep and waking modulate spine turnover in the adolescent mouse cortex. Nat. Neurosci. *14*, 1418–1420.

Markram, H., Lübke, J., Frotscher, M., and Sakmann, B. (1997). Regulation of Synaptic Efficacy by Coincidence of Postsynaptic APs and EPSPs. Science *275*, 213–215.

Markram, H., Gerstner, W., and Sjöström, P.J. (2011). A History of Spike-Timing-Dependent Plasticity. Front. Synaptic Neurosci. *3*.

Marrosu, F., Portas, C., Mascia, M.S., Casu, M.A., Fà, M., Giagheddu, M., Imperato, A., and Gessa, G.L. (1995). Microdialysis measurement of cortical and hippocampal acetylcholine release during sleep-wake cycle in freely moving cats. Brain Res. *671*, 329–332.

Marshall, L., Helgadóttir, H., Mölle, M., and Born, J. (2006). Boosting slow oscillations during sleep potentiates memory. Nature *444*, 610–613.

Mednick, S., Nakayama, K., and Stickgold, R. (2003). Sleep-dependent learning: a nap is as good as a night. Nat. Neurosci. *6*, 697–698.

Mégevand, P., Troncoso, E., Quairiaux, C., Muller, D., Michel, C.M., and Kiss, J.Z. (2009). Long-term plasticity in mouse sensorimotor circuits after rhythmic whisker stimulation. J. Neurosci. Off. J. Soc. Neurosci. *29*, 5326–5335.

Miller, S.G., Patton, B.L., and Kennedy, M.B. (1988). Sequences of autophosphorylation sites in neuronal type II CaM kinase that control Ca2+-independent activity. Neuron *1*, 593–604.

Min, R., and Nevian, T. (2012). Astrocyte signaling controls spike timing-dependent depression at neocortical synapses. Nat. Neurosci. *15*, 746–753.

Mitzdorf, U. (1985). Current source-density method and application in cat cerebral cortex: investigation of evoked potentials and EEG phenomena. Physiol. Rev. *65*, 37–100.

Moore, C.I., and Nelson, S.B. (1998). Spatio-Temporal Subthreshold Receptive Fields in the Vibrissa Representation of Rat Primary Somatosensory Cortex. J. Neurophysiol. *80*, 2882–2892.

Mountcastle, V.B. (1997). The columnar organization of the neocortex. Brain *120*, 701–722.

Mulkey, R.M., and Malenka, R.C. (1992). Mechanisms underlying induction of homosynaptic long-term depression in area CA1 of the hippocampus. Neuron *9*, 967–975.

Nádasdy, Z., Hirase, H., Czurkó, A., Csicsvari, J., and Buzsáki, G. (1999). Replay and Time Compression of Recurring Spike Sequences in the Hippocampus. J. Neurosci. *19*, 9497–9507.

Narayanan, R.T., Egger, R., Johnson, A.S., Mansvelder, H.D., Sakmann, B., de Kock, C.P.J., and Oberlaender, M. (2015). Beyond Columnar Organization: Cell Type- and Target Layer-Specific Principles of Horizontal Axon Projection Patterns in Rat Vibrissal Cortex. Cereb. Cortex N. Y. NY *25*, 4450–4468.

Nelson, A.B., Faraguna, U., Zoltan, J.T., Tononi, G., and Cirelli, C. (2013). Sleep Patterns and Homeostatic Mechanisms in Adolescent Mice. Brain Sci. *3*, 318–343.

Nere, A.T., Hashmi, A., Cirelli, C., and Tononi, G. (2013). Sleep-Dependent Synaptic Down-Selection (I): Modeling the Benefits of Sleep on Memory Consolidation and Integration. Front. Neurol. *4*.

Neske, G.T. (2016). The Slow Oscillation in Cortical and Thalamic Networks: Mechanisms and Functions. Front. Neural Circuits *9*.

Nevian, T., and Sakmann, B. (2006). Spine Ca2+ Signaling in Spike-Timing-Dependent Plasticity. J. Neurosci. *26*, 11001–11013.

Nicholson, C., and Freeman, J.A. (1975). Theory of current source-density analysis and determination of conductivity tensor for anuran cerebellum. J. Neurophysiol. *38*, 356–368.

Nicolelis, M.A., and Chapin, J.K. (1994). Spatiotemporal structure of somatosensory responses of many-neuron ensembles in the rat ventral posterior medial nucleus of the thalamus. J. Neurosci. *14*, 3511–3532.

Ohno, S., Kuramoto, E., Furuta, T., Hioki, H., Tanaka, Y.R., Fujiyama, F., Sonomura, T., Uemura, M., Sugiyama, K., and Kaneko, T. (2012). A Morphological Analysis of Thalamocortical Axon Fibers of Rat Posterior Thalamic Nuclei: A Single Neuron Tracing Study with Viral Vectors. Cereb. Cortex *22*, 2840–2857.

Olcese, U., Esser, S.K., and Tononi, G. (2010). Sleep and Synaptic Renormalization: A Computational Study. J. Neurophysiol. *104*, 3476–3493.

Petersen, C.C.H. (2007). The Functional Organization of the Barrel Cortex. Neuron *56*, 339–355.

Petersen, R.S., and Diamond, M.E. (2000). Spatial–Temporal Distribution of Whisker-Evoked Activity in Rat Somatosensory Cortex and the Coding of Stimulus Location. J. Neurosci. *20*, 6135–6143.

Petersen, C.C.H., Hahn, T.T.G., Mehta, M., Grinvald, A., and Sakmann, B. (2003a). Interaction of sensory responses with spontaneous depolarization in layer 2/3 barrel cortex. Proc. Natl. Acad. Sci. *100*, 13638–13643.

Petersen, C.C.H., Grinvald, A., and Sakmann, B. (2003b). Spatiotemporal Dynamics of Sensory Responses in Layer 2/3 of Rat Barrel Cortex Measured In Vivo by Voltage-Sensitive Dye Imaging Combined with Whole-Cell Voltage Recordings and Neuron Reconstructions. J. Neurosci. *23*, 1298–1309.

Petersen, C.C.H., Hahn, T.T.G., Mehta, M., Grinvald, A., and Sakmann, B. (2003c). Interaction of sensory responses with spontaneous depolarization in layer 2/3 barrel cortex. Proc. Natl. Acad. Sci. *100*, 13638–13643.

Pierret, T., Lavallée, P., and Deschênes, M. (2000). Parallel Streams for the Relay of Vibrissal Information through Thalamic Barreloids. J. Neurosci. *20*, 7455–7462.

Pinto, D.J., Hartings, J.A., Brumberg, J.C., and Simons, D.J. (2003). Cortical Damping: Analysis of Thalamocortical Response Transformations in Rodent Barrel Cortex. Cereb. Cortex *13*, 33–44.

Porter, J.T., Johnson, C.K., and Agmon, A. (2001). Diverse Types of Interneurons Generate Thalamus-Evoked Feedforward Inhibition in the Mouse Barrel Cortex. J. Neurosci. *21*, 2699–2710.

Quairiaux, C., Armstrong-James, M., and Welker, E. (2007). Modified Sensory Processing in the Barrel Cortex of the Adult Mouse After Chronic Whisker Stimulation. J. Neurophysiol. *97*, 2130–2147.

Rasch, B., and Born, J. (2007). Maintaining memories by reactivation. Curr. Opin. Neurobiol. *17*, 698–703.

Rasch, B., and Born, J. (2013). About Sleep's Role in Memory. Physiol. Rev. *93*, 681–766.

Rasch, B., Pommer, J., Diekelmann, S., and Born, J. (2009). Pharmacological REM sleep suppression paradoxically improves rather than impairs skill memory. Nat. Neurosci. *12*, 396–397.

Rasmusson, D.. (2000a). The role of acetylcholine in cortical synaptic plasticity. Behav. Brain Res. *115*, 205–218.

Rasmusson, D.D. (2000b). The role of acetylcholine in cortical synaptic plasticity. Behav. Brain Res. *115*, 205–218.

Rema, V., Armstrong-James, M., and Ebner, F.F. (1998). Experience-Dependent Plasticity of Adult Rat S1 Cortex Requires Local NMDA Receptor Activation. J. Neurosci. *18*, 10196–10206.

Rema, V., Armstrong-James, M., Jenkinson, N., and Ebner, F.F. (2006). Short exposure to an enriched environment accelerates plasticity in the barrel cortex of adult rats. Neuroscience *140*, 659–672.

Ribeiro, S., Mello, C.V., Velho, T., Gardner, T.J., Jarvis, E.D., and Pavlides, C. (2002). Induction of Hippocampal Long-Term Potentiation during Waking Leads to Increased Extrahippocampal zif-268 Expression during Ensuing Rapid-Eye-Movement Sleep. J. Neurosci. *22*, 10914–10923.

Ribeiro, S., Shi, X., Engelhard, M., Zhou, Y., Zhang, H., Gervasoni, D., Lin, S.-C., Wada, K., Lemos, N.A.M., and Nicolelis, M.A.L. (2007). Novel experience induces persistent sleep-dependent plasticity in the cortex but not in the hippocampus. Front. Neurosci. *1*.

Riedner, B.A., Vyazovskiy, V.V., Huber, R., Massimini, M., Esser, S., Murphy, M., and Tononi, G. (2007). Sleep Homeostasis and Cortical Synchronization: III. A High-Density EEG Study of Sleep Slow Waves in Humans. Sleep *30*, 1643–1657.

Rigas, P., and Castro-Alamancos, M.A. (2007). Thalamocortical Up states: differential effects of intrinsic and extrinsic cortical inputs on persistent activity. J. Neurosci. Off. J. Soc. Neurosci. *27*, 4261–4272.

Rodriguez, A.V., Funk, C.M., Vyazovskiy, V.V., Nir, Y., Tononi, G., and Cirelli, C. (2016). Why Does Sleep Slow-Wave Activity Increase After Extended Wake? Assessing the Effects of Increased Cortical Firing During Wake and Sleep. J. Neurosci. *36*, 12436–12447.

Rodríguez-Moreno, A., and Paulsen, O. (2008). Spike timing–dependent long-term depression requires presynaptic NMDA receptors. Nat. Neurosci. *11*, 744–745.

Rodríguez-Moreno, A., Kohl, M.M., Reeve, J.E., Eaton, T.R., Collins, H.A., Anderson, H.L., and Paulsen, O. (2011). Presynaptic Induction and Expression of Timing-Dependent Long-Term Depression Demonstrated by Compartment-Specific Photorelease of a Use-Dependent NMDA Receptor Antagonist. J. Neurosci. *31*, 8564–8569.

Sachdev, R.N.S., Ebner, F.F., and Wilson, C.J. (2004). Effect of Subthreshold Up and Down States on the Whisker-Evoked Response in Somatosensory Cortex. J. Neurophysiol. *92*, 3511–3521.

Sadowski, J.H.L.P., Jones, M.W., and Mellor, J.R. (2016). Sharp-Wave Ripples Orchestrate the Induction of Synaptic Plasticity during Reactivation of Place Cell Firing Patterns in the Hippocampus. Cell Rep. *14*, 1916–1929.

Sanchez-Vives, M.V., and McCormick, D.A. (2000). Cellular and network mechanisms of rhythmic recurrent activity in neocortex. Nat. Neurosci. *3*, 1027–1034.

Sanchez-Vives, M.V., Mattia, M., Compte, A., Perez-Zabalza, M., Winograd, M., Descalzo, V.F., and Reig, R. (2010). Inhibitory Modulation of Cortical Up States. J. Neurophysiol. *104*, 1314–1324.

Schlaggar, B.L., and O'Leary, D.D.M. (1994). Early development of the somatotopic map and barrel patterning in rat somatosensory cortex. J. Comp. Neurol. *346*, 80–96.

Schubert, D., Staiger, J.F., Cho, N., Kötter, R., Zilles, K., and Luhmann, H.J. (2001). Layer-Specific Intracolumnar and Transcolumnar Functional Connectivity of Layer V Pyramidal Cells in Rat Barrel Cortex. J. Neurosci. *21*, 3580–3592.

Schubert, D., Kötter, R., Zilles, K., Luhmann, H.J., and Staiger, J.F. (2003). Cell Type-Specific Circuits of Cortical Layer IV Spiny Neurons. J. Neurosci. *23*, 2961–2970.

Schubert, D., Kötter, R., and Staiger, J.F. (2007). Mapping functional connectivity in barrel-related columns reveals layer- and cell type-specific microcircuits. Brain Struct. Funct. *212*, 107–119.

Schweimer, J.V., Mallet, N., Sharp, T., and Ungless, M.A. (2011). Spike-timing relationship of neurochemically-identified dorsal raphe neurons during cortical slow oscillations. Neuroscience *196*, 115–123.

Seol, G.H., Ziburkus, J., Huang, S., Song, L., Kim, I.T., Takamiya, K., Huganir, R.L., Lee, H.-K., and Kirkwood, A. (2007). Neuromodulators Control the Polarity of Spike-Timing-Dependent Synaptic Plasticity. Neuron *55*, 919–929.

Sheroziya, M.G., Halbach, O. von B. und, Unsicker, K., and Egorov, A.V. (2009). Spontaneous Bursting Activity in the Developing Entorhinal Cortex. J. Neurosci. *29*, 12131–12144.

Shu, Y., Hasenstaub, A., and McCormick, D.A. (2003). Turning on and off recurrent balanced cortical activity. Nature *423*, 288–293.

Siegel, J.M. (2001). The REM Sleep-Memory Consolidation Hypothesis. Science *294*, 1058–1063.

Simons, D.J., and Carvell, G.E. (1989). Thalamocortical response transformation in the rat vibrissa/barrel system. J. Neurophysiol. *61*, 311–330.

Sjöström, P.J., and Häusser, M. (2006). A Cooperative Switch Determines the Sign of Synaptic Plasticity in Distal Dendrites of Neocortical Pyramidal Neurons. Neuron *51*, 227–238.

Sjöström, P.J., Turrigiano, G.G., and Nelson, S.B. (2001). Rate, Timing, and Cooperativity Jointly Determine Cortical Synaptic Plasticity. Neuron *32*, 1149–1164.

Sjöström, P.J., Turrigiano, G.G., and Nelson, S.B. (2003). Neocortical LTD via Coincident Activation of Presynaptic NMDA and Cannabinoid Receptors. Neuron *39*, 641–654.

Sjöström, P.J., Turrigiano, G.G., and Nelson, S.B. (2004). Endocannabinoid-Dependent Neocortical Layer-5 LTD in the Absence of Postsynaptic Spiking. J. Neurophysiol. *92*, 3338–3343.

Skaggs, W.E., and McNaughton, B.L. (1996). Replay of Neuronal Firing Sequences in Rat Hippocampus During Sleep Following Spatial Experience. Science *271*, 1870–1873.

Smith, C. (2001). Sleep states and memory processes in humans: procedural versus declarative memory systems. Sleep Med. Rev. *5*, 491–506.

Steriade, M. (2004). Acetylcholine systems and rhythmic activities during the waking–sleep cycle. B.-P. in B. Research, ed. (Elsevier), pp. 179–196.

Steriade, M. (2006). Grouping of brain rhythms in corticothalamic systems. Neuroscience *137*, 1087–1106.

Steriade, M., Nunez, A., and Amzica, F. (1993a). A novel slow (< 1 Hz) oscillation of neocortical neurons in vivo: depolarizing and hyperpolarizing components. J. Neurosci. *13*, 3252–3265.

Steriade, M., McCormick, D.A., and Sejnowski, T.J. (1993b). Thalamocortical oscillations in the sleeping and aroused brain. Science *262*, 679–685.

Steriade, M., Nunez, A., and Amzica, F. (1993c). Intracellular analysis of relations between the slow (< 1 Hz) neocortical oscillation and other sleep rhythms of the electroencephalogram. J. Neurosci. *13*, 3266–3283.

Steriade, M., Amzica, F., and Nunez, A. (1993d). Cholinergic and noradrenergic modulation of the slow (approximately 0.3 Hz) oscillation in neocortical cells. J. Neurophysiol. *70*, 1385–1400.

Steriade, M., Timofeev, I., and Grenier, F. (2001). Natural Waking and Sleep States: A View From Inside Neocortical Neurons. J. Neurophysiol. *85*, 1969–1985.

Takahashi, N., Oertner, T.G., Hegemann, P., and Larkum, M.E. (2016). Active cortical dendrites modulate perception. Science *354*, 1587–1590.

Timofeev, I., Grenier, F., Bazhenov, M., Sejnowski, T.J., and Steriade, M. (2000). Origin of Slow Cortical Oscillations in Deafferented Cortical Slabs. Cereb. Cortex *10*, 1185–1199.

Timofeev, I., Grenier, F., and Steriade, M. (2001). Disfacilitation and active inhibition in the neocortex during the natural sleep-wake cycle: An intracellular study. Proc. Natl. Acad. Sci. *98*, 1924–1929.

Tononi, G., and Cirelli, C. (2003). Sleep and synaptic homeostasis: a hypothesis. Brain Res. Bull. *62*, 143–150.

Tononi, G., and Cirelli, C. (2006). Sleep function and synaptic homeostasis. Sleep Med. Rev. *10*, 49–62.

Tononi, G., and Cirelli, C. (2014). Sleep and the Price of Plasticity: From Synaptic and Cellular Homeostasis to Memory Consolidation and Integration. Neuron *81*, 12–34.

Trachtenberg, J.T., Chen, B.E., Knott, G.W., Feng, G., Sanes, J.R., Welker, E., and Svoboda, K. (2002). Long-term in vivo imaging of experience-dependent synaptic plasticity in adult cortex. Nature *420*, 788–794.

Trageser, J.C., Burke, K.A., Masri, R., Li, Y., Sellers, L., and Keller, A. (2006). State-Dependent Gating of Sensory Inputs by Zona Incerta. J. Neurophysiol. *96*, 1456–1463.

Van Der Loos, H. (1976). Barreloids in mouse somatosensory thalamus. Neurosci. Lett. *2*, 1–6.

Vivo, L. de, Bellesi, M., Marshall, W., Bushong, E.A., Ellisman, M.H., Tononi, G., and Cirelli, C. (2017). Ultrastructural evidence for synaptic scaling across the wake/sleep cycle. Science *355*, 507–510.

Volgushev, M., Chauvette, S., Mukovski, M., and Timofeev, I. (2006). Precise Long-Range Synchronization of Activity and Silence in Neocortical Neurons during Slow-Wave Sleep. J. Neurosci. *26*, 5665–5672.

Vyazovskiy, V.V., and Faraguna, U. (2014). Sleep and Synaptic Homeostasis. In Sleep, Neuronal Plasticity and Brain Function, P. Meerlo, R.M. Benca, and T. Abel, eds. (Springer Berlin Heidelberg), pp. 91–121.

Vyazovskiy, V., Borbély, A.A., and Tobler, I. (2000). Unilateral vibrissae stimulation during waking induces interhemispheric EEG asymmetry during subsequent sleep in the rat. J. Sleep Res. *9*, 367–371.

Vyazovskiy, V.V., Riedner, B.A., Cirelli, C., and Tononi, G. (2007). Sleep Homeostasis and Cortical Synchronization: II. A Local Field Potential Study of Sleep Slow Waves in the Rat. Sleep *30*, 1631–1642.

Vyazovskiy, V.V., Cirelli, C., Pfister-Genskow, M., Faraguna, U., and Tononi, G. (2008). Molecular and electrophysiological evidence for net synaptic potentiation in wake and depression in sleep. Nat. Neurosci. *11*, 200–208.

Vyazovskiy, V.V., Olcese, U., Lazimy, Y.M., Faraguna, U., Esser, S.K., Williams, J.C., Cirelli, C., and Tononi, G. (2009). Cortical firing and sleep homeostasis. Neuron *63*, 865–878.

Wagner, U., Gais, S., and Born, J. (2001). Emotional Memory Formation Is Enhanced across Sleep Intervals with High Amounts of Rapid Eye Movement Sleep. Learn. Mem. *8*, 112–119.

Wagner, U., Gais, S., Haider, H., Verleger, R., and Born, J. (2004). Sleep inspires insight. Nature *427*, 352–355.

Walker, M.P., Brakefield, T., Morgan, A., Hobson, J.A., and Stickgold, R. (2002). Practice with Sleep Makes Perfect: Sleep-Dependent Motor Skill Learning. Neuron *35*, 205–211.

Wallace, H., and Fox, K. (1999). The effect of vibrissa deprivation pattern on the form of plasticity induced in rat barrel cortex. Somatosens. Mot. Res. *16*, 122–138.

Wallace, H., Glazewski, S., Liming, K., and Fox, K. (2001). The Role of Cortical Activity in Experience-Dependent Potentiation and Depression of Sensory Responses in Rat Barrel Cortex. J. Neurosci. *21*, 3881–3894.

Wei, Y., Krishnan, G.P., and Bazhenov, M. (2016). Synaptic Mechanisms of Memory Consolidation during Sleep Slow Oscillations. J. Neurosci. *36*, 4231–4247.

Welker, C. (1971). Microelectrode delineation of fine grain somatotopic organization of SmI cerebral neocortex in albino rat. Brain Res. *26*, 259–275.

Wilent, W.B., and Contreras, D. (2004). Synaptic Responses to Whisker Deflections in Rat Barrel Cortex as a Function of Cortical Layer and Stimulus Intensity. J. Neurosci. *24*, 3985–3998.

Wilent, W.B., and Contreras, D. (2005). Dynamics of excitation and inhibition underlying stimulus selectivity in rat somatosensory cortex. Nat. Neurosci. *8*, 1364–1370.

Wilson, M.A., and McNaughton, B.L. (1994). Reactivation of hippocampal ensemble memories during sleep. Science *265*, 676–679.

Wimmer, V.C., Bruno, R.M., de Kock, C.P.J., Kuner, T., and Sakmann, B. (2010). Dimensions of a Projection Column and Architecture of VPM and POm Axons in Rat Vibrissal Cortex. Cereb. Cortex N. Y. NY *20*, 2265–2276.

Woolsey, T.A., and Van der Loos, H. (1970). The structural organization of layer IV in the somatosensory region (S I) of mouse cerebral cortex: The description of a cortical field composed of discrete cytoarchitectonic units. Brain Res. *17*, 205–242.

Woolsey, T.A., and Wann, J.R. (1976). Areal changes in mouse cortical barrels following vibrissal damage at different postnatal ages. J. Comp. Neurol. *170*, 53–66.

Woolsey, T.A., Welker, C., and Schwartz, R.H. (1975). Comparative anatomical studies of the Sml face cortex with special reference to the occurrence of “barrels” in layer IV. J. Comp. Neurol. *164*, 79–94.

Wright, N., Glazewski, S., Hardingham, N., Phillips, K., Pervolaraki, E., and Fox, K. (2008). Laminar analysis of the role of GluR1 in experience-dependent and synaptic depression in barrel cortex. Nat. Neurosci. *11*, 1140–1142.

Yang, G., and Gan, W.-B. (2012). Sleep contributes to dendritic spine formation and elimination in the developing mouse somatosensory cortex. Dev. Neurobiol. *72*, 1391–1398.

Yang, G., Lai, C.S.W., Cichon, J., Ma, L., Li, W., and Gan, W.-B. (2014). Sleep promotes branch-specific formation of dendritic spines after learning. Science *344*, 1173–1178.

Yuste, R., and Bonhoeffer, T. (2001). Morphological Changes in Dendritic Spines Associated with Long-Term Synaptic Plasticity. Annu. Rev. Neurosci. *24*, 1071–1089.

Zhang, E., Hansen, A.J., Wieloch, T., and Lauritzen, M. (1990). Influence of MK-801 on Brain Extracellular Calcium and Potassium Activities in Severe Hypoglycemia. J. Cereb. Blood Flow Metab. *10*, 136–139.

Zhu, J.J., and Connors, B.W. (1999). Intrinsic Firing Patterns and Whisker-Evoked Synaptic Responses of Neurons in the Rat Barrel Cortex. J. Neurophysiol. *81*, 1171–1183.